A Particulate Perspective on Soil Mechanics

2015 Géotechnique Lecture

Dr. Catherine O'Sullivan
Dept. Civil and Environmental Engineering
Imperial College London
cath.osullivan@imperial.ac.uk

A Particulate Perspective on Soil Mechanics Can…

- Reveal soil behaviour under stress states that cannot be attained in experiments **(DEM)**
- Explain perplexing soil behaviour **(microCT)**
- Provide scientific rationale for empirical results used in design **(DEM+ microCT)**

Most Cited Contributions Published in Géotechnique

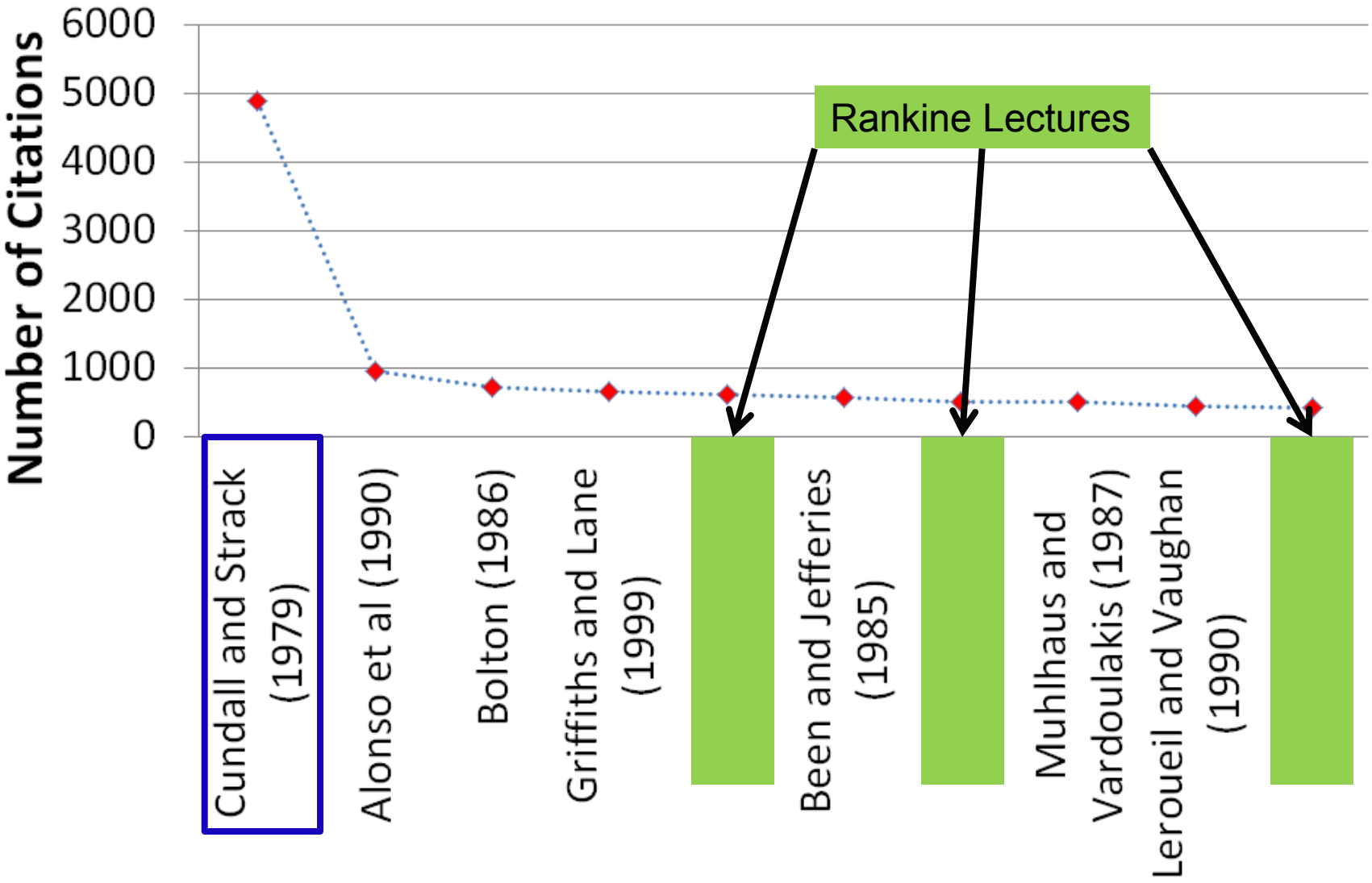

Cundall and Strack (1979)

"A discrete numerical model for granular assemblies"

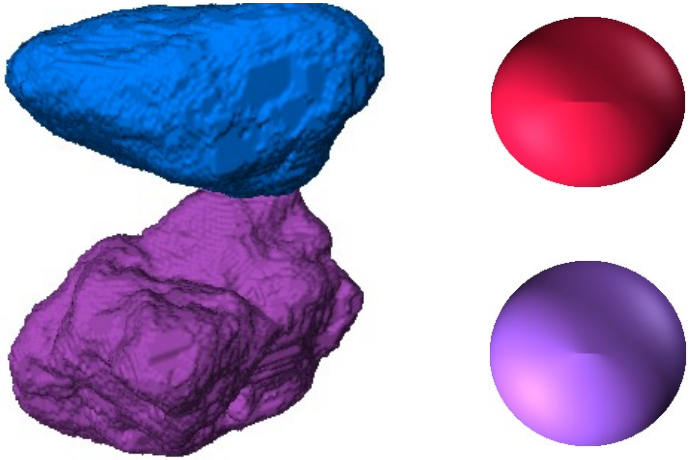

DEM Contact

- Contact force calculated using orthogonal normal and shear springs
- Spring deformation calculated from relative motion of contacting particles
- Sliding governed by Coulomb friction : $T_{max}=\mu F_n$

  μ = coefficient of friction

  F_n = contact normal force

  T_{max}=maximum tangential (shear) force

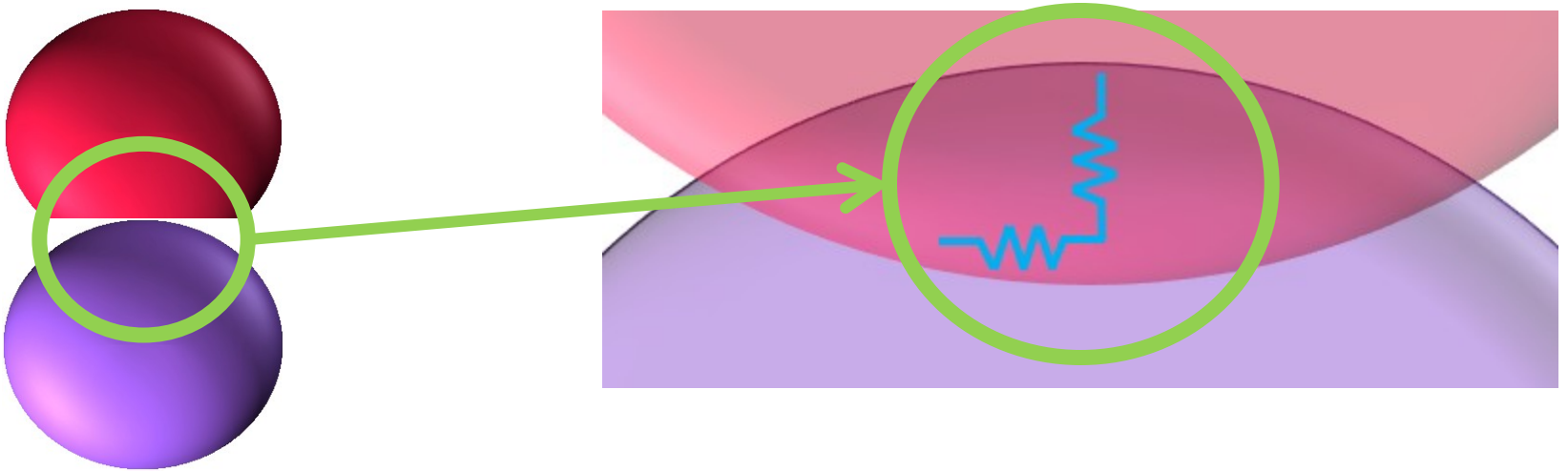

Transient Calculation – In Each Time Step:

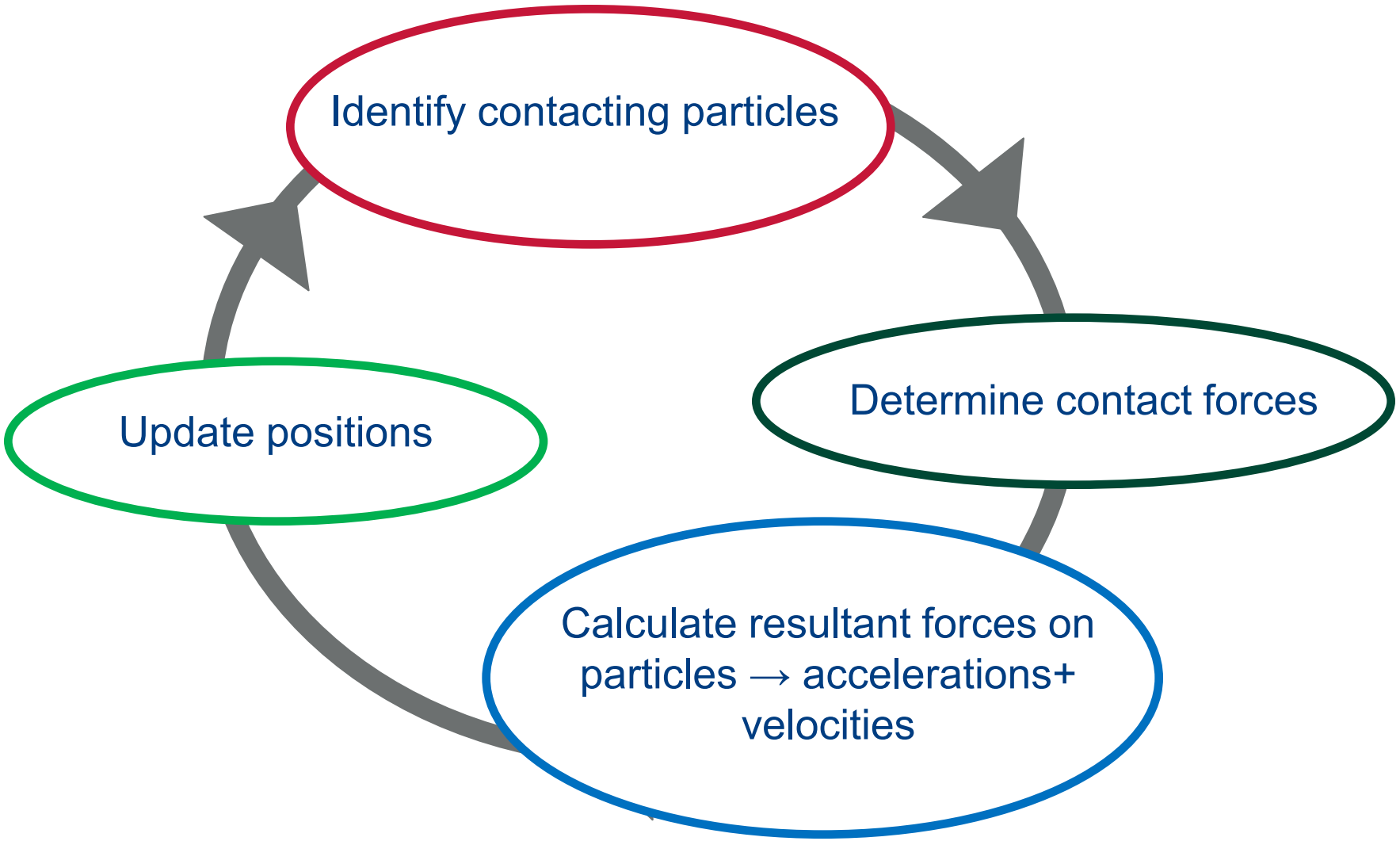

Use of DEM – No of Publications per Year

All Scientific Disciplines

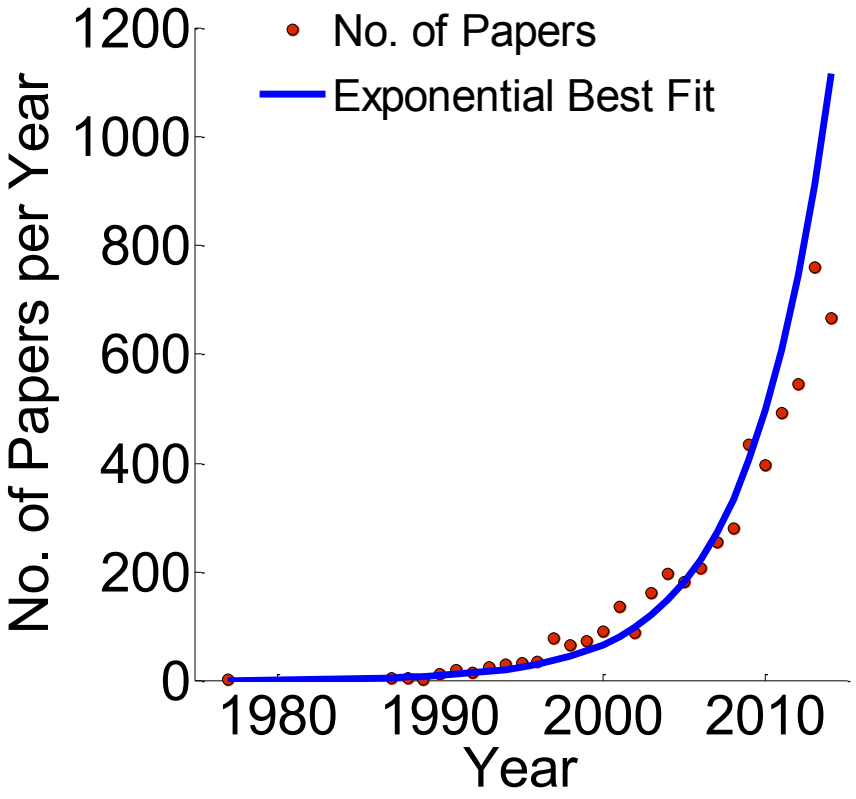

Web of Science (Oct 2015)

chnical journals

DEM simulation of semi-solid metal
Yuan et al (2012)

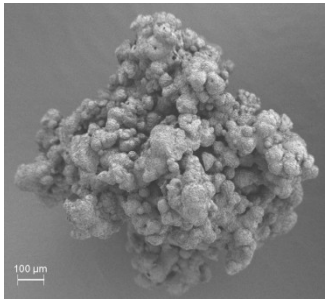

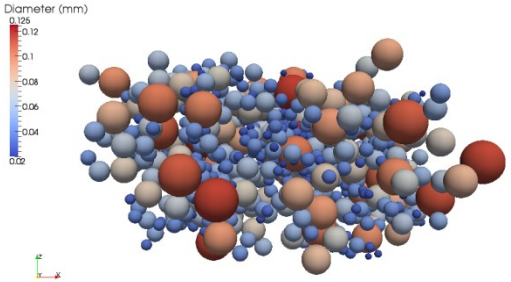

DEM simulation of infant formula
Hanley et al (2012)

Use of DEM – No of Publications per Year

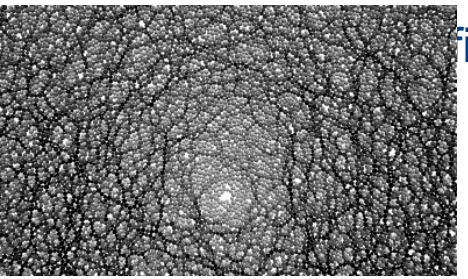

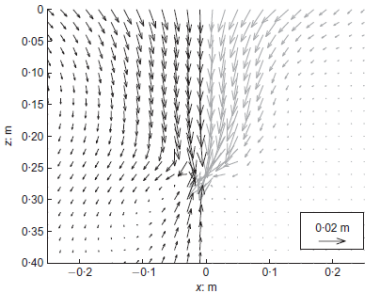

Tunnelling induced displacements
Bym et al. (2013) Géotechnique

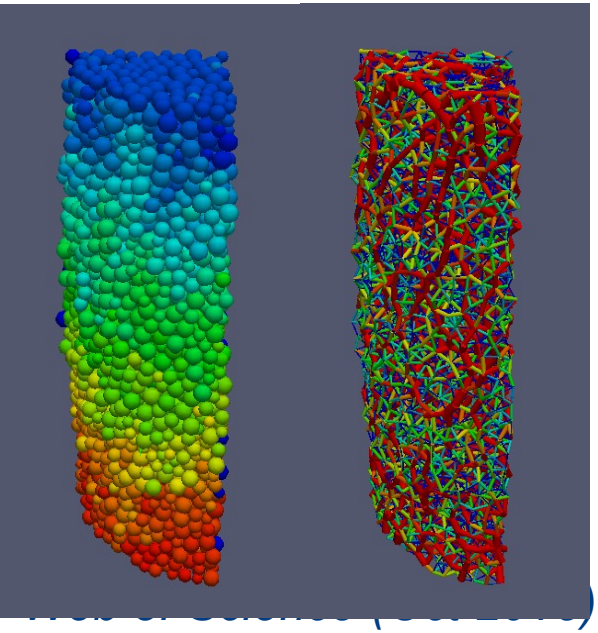

Deformation in triaxial cell
Cui et al. (2007) Géotechnique

Main geotechnical journals

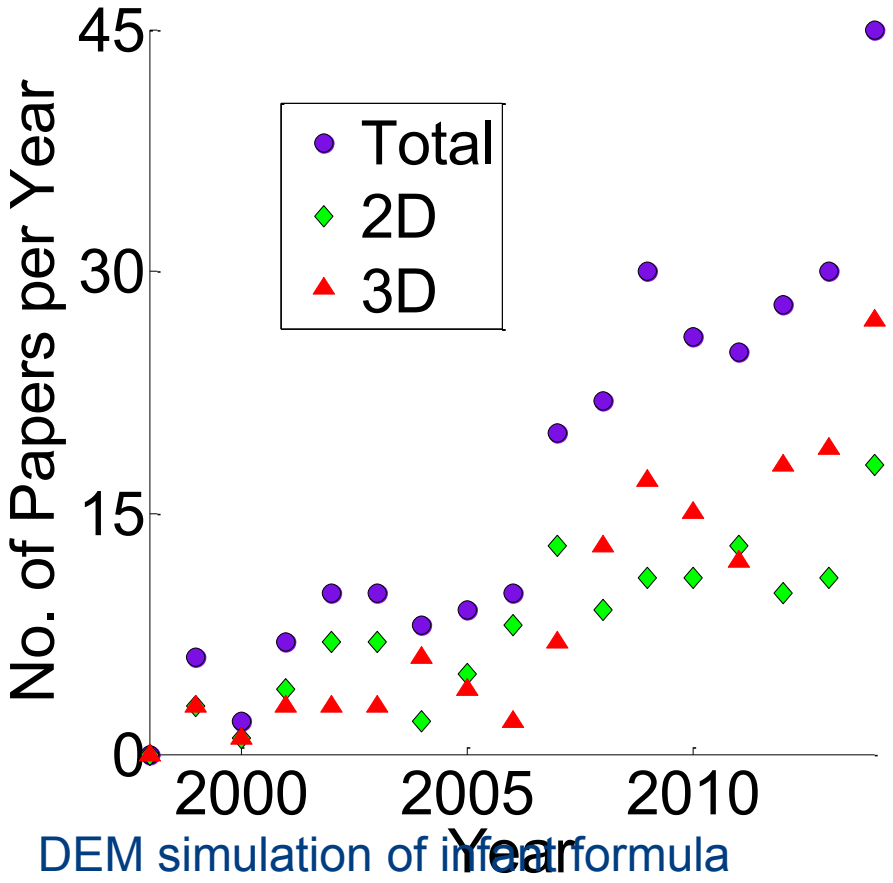

DEM simulation of infiltration formula
Hanley et al (2012)

Direct Shear Test

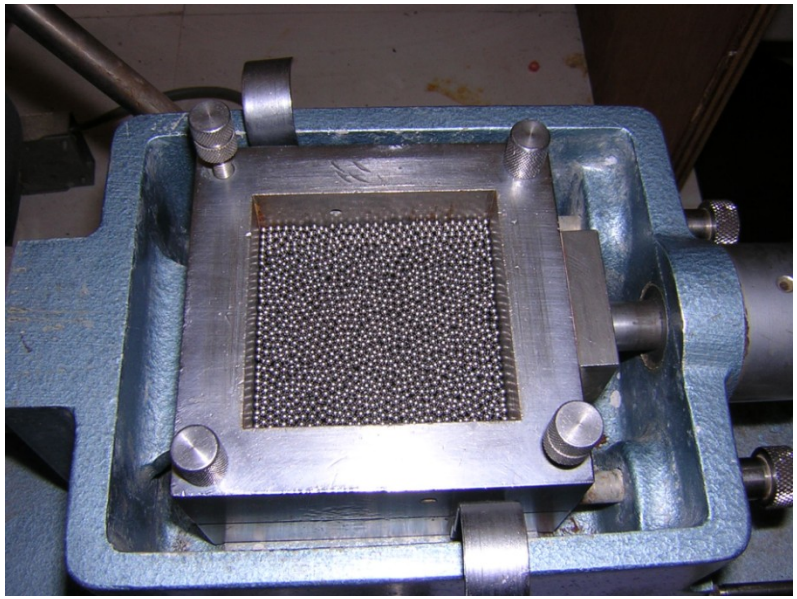

Grade 25 steel precision balls
Diameter 0.992 mm

Cui and O'Sullivan (2006)
Géotechnique

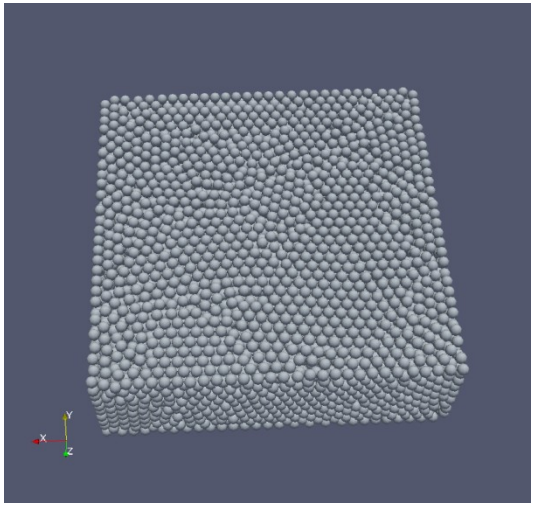

DEM model: 11700 Spheres

Mean $\mu_{surface}$
5.5°

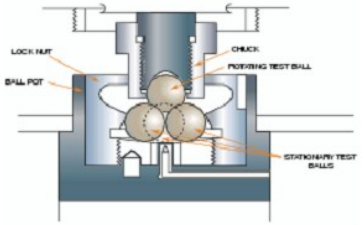

Mean $\mu_{surface}$
5.7°

Direct Shear Test

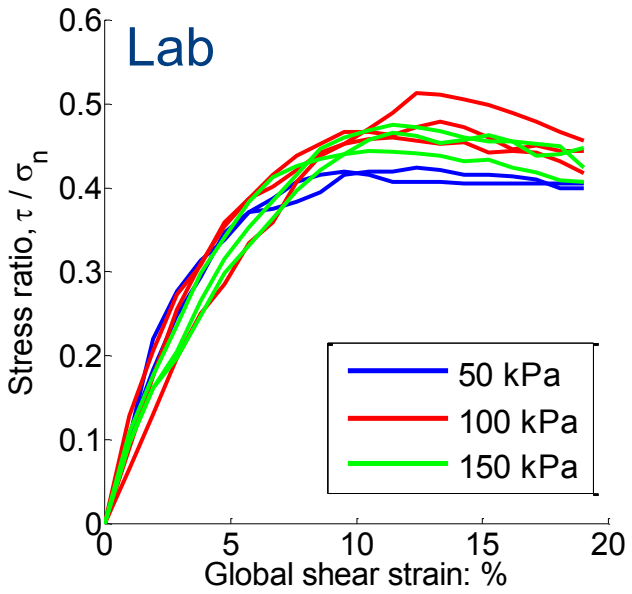

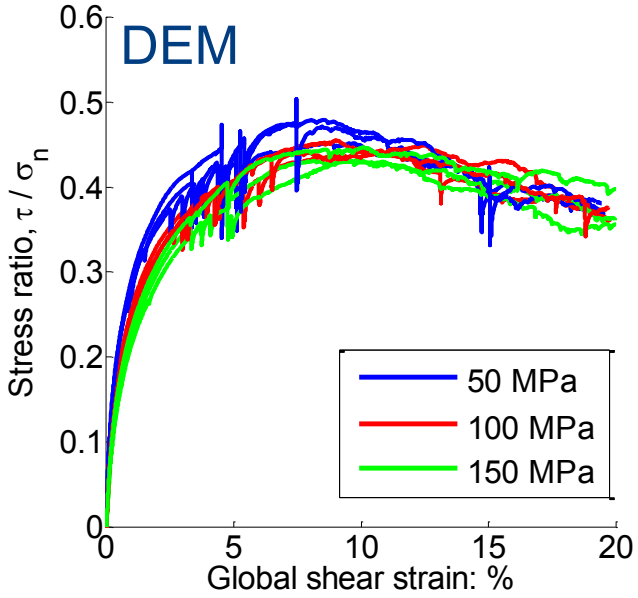

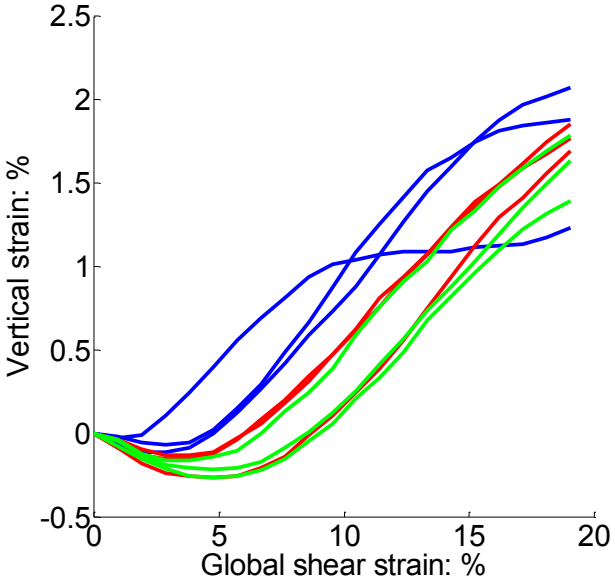

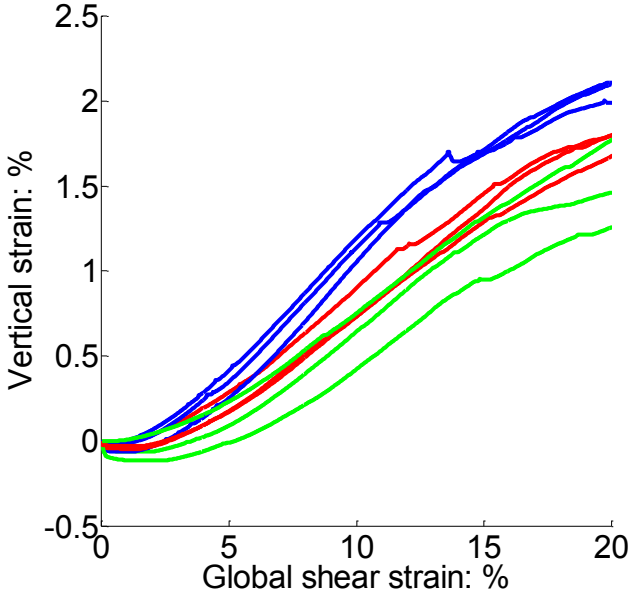

Direct Shear Test

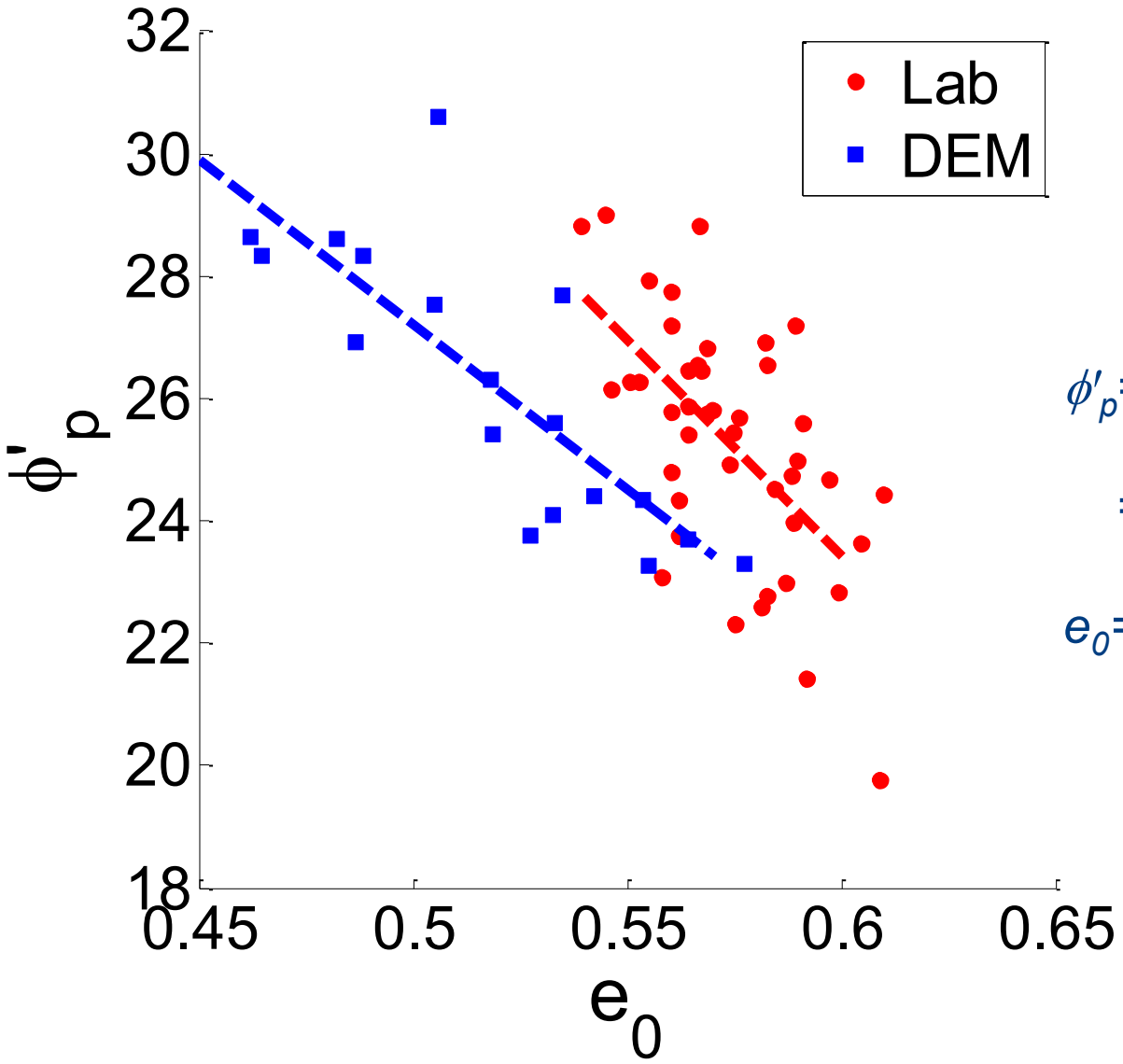

ϕ'_p= peak angle of shearing resistance
= peak "friction" angle

e_0= initial void ratio

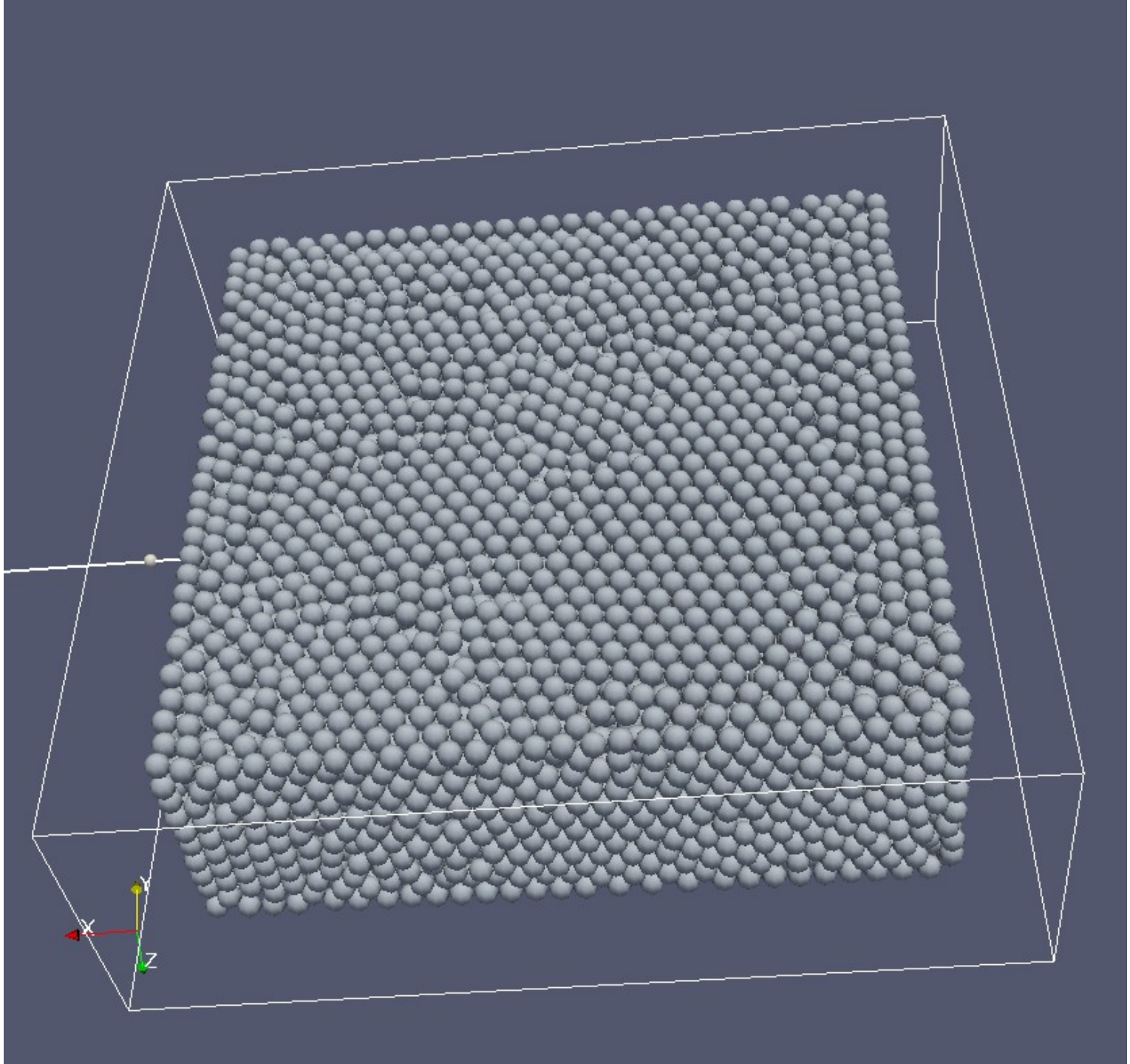
Y
X
Z

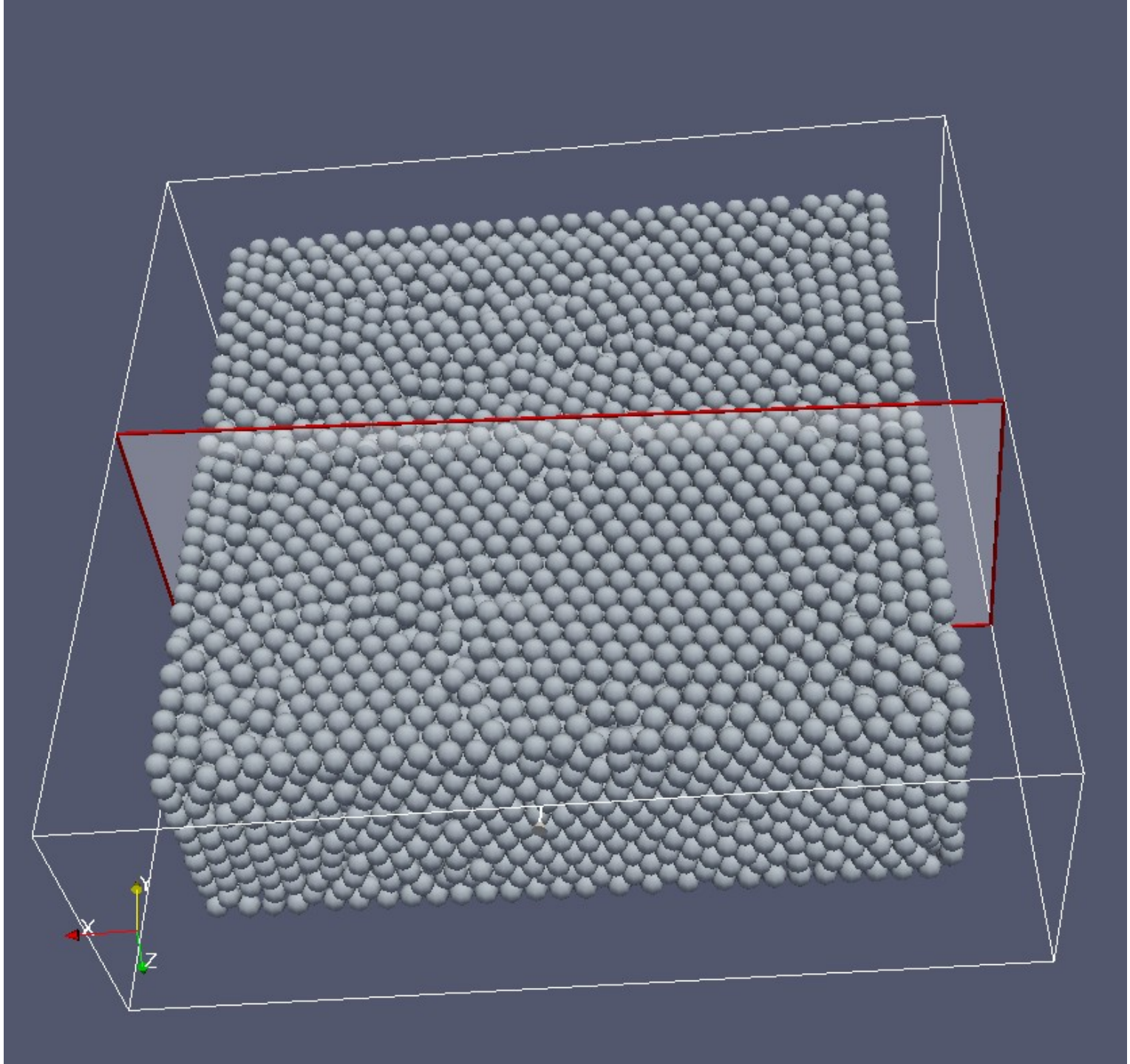
Y
X
Z

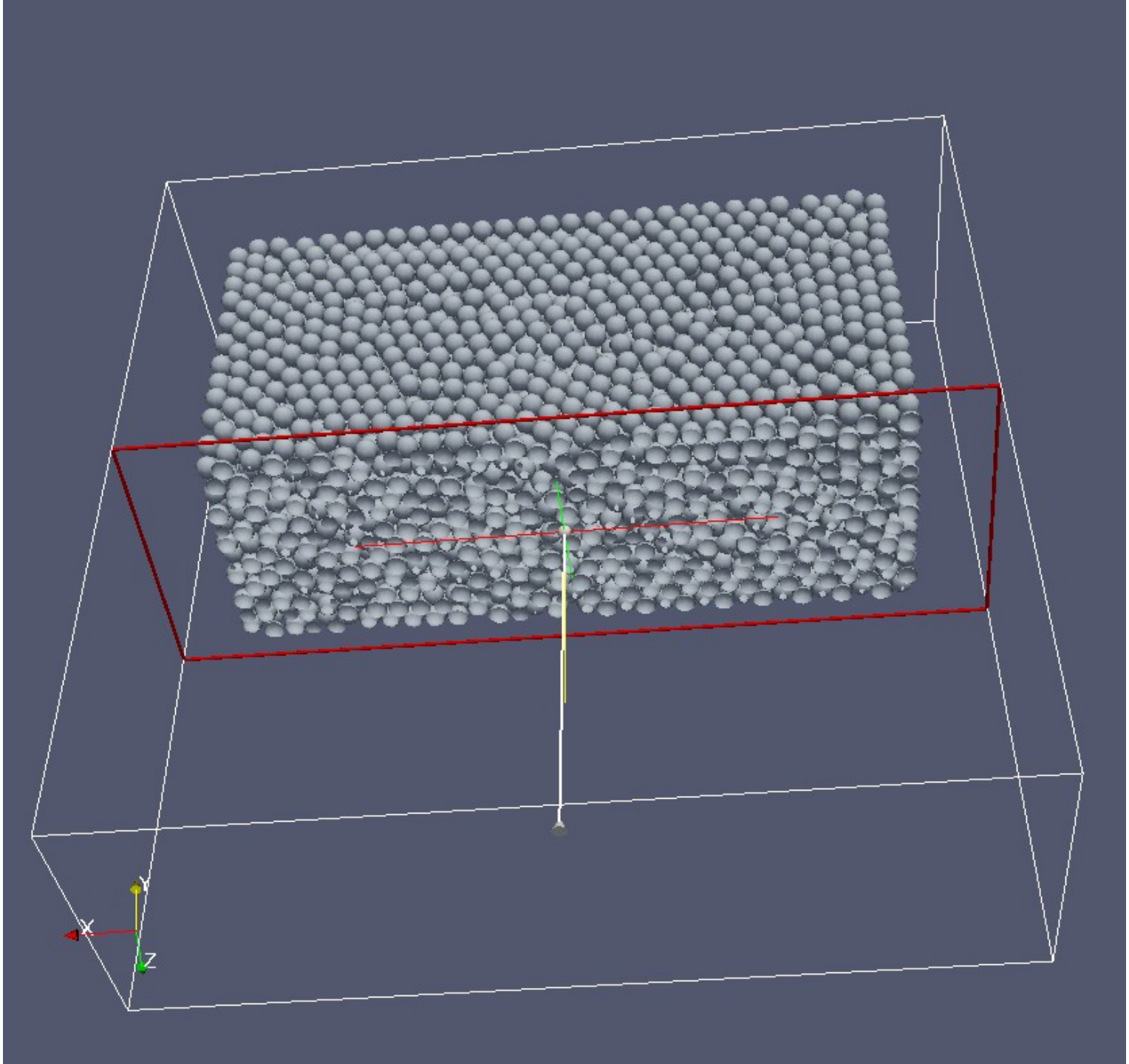
Y
X
Z

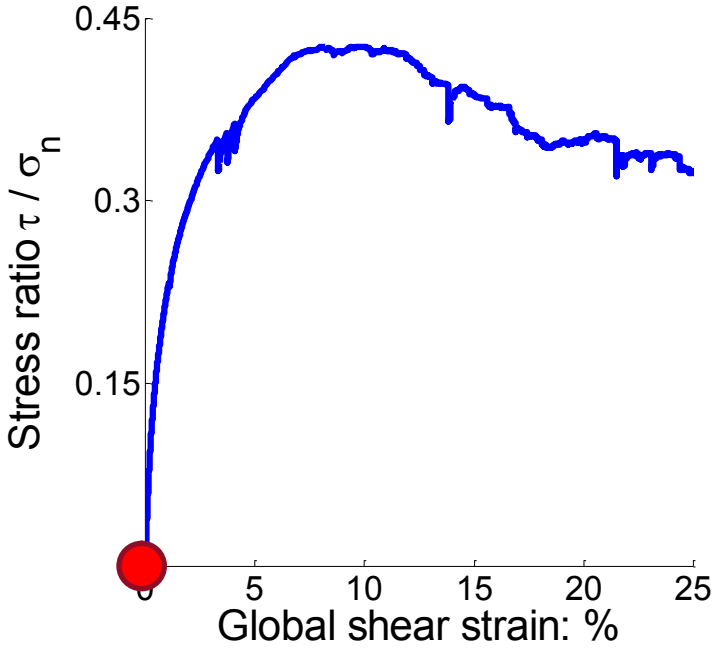
0.45
0.3
0.15
Stress ratio τ / σn
0
5
10
15
20
25
Global shear strain: %

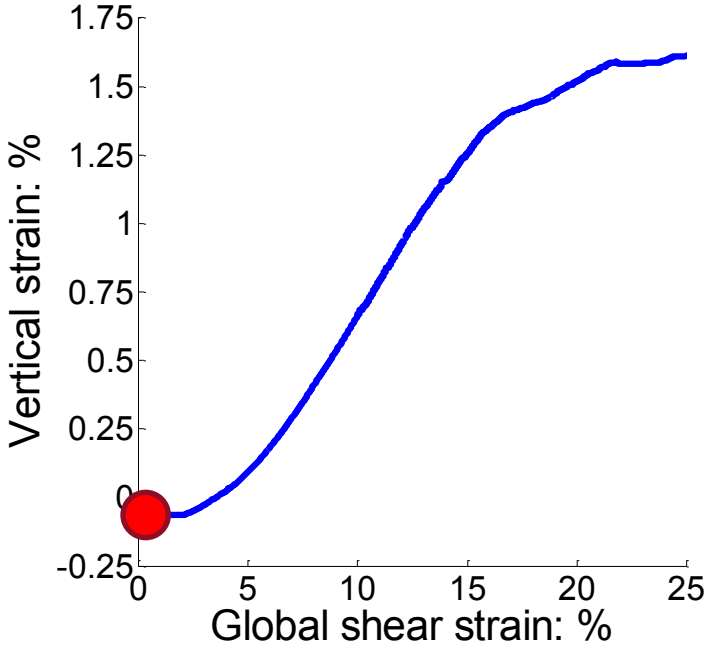
1.75
1.5
1.25
1
0.75
0.5
0.25
0
-0.25
Vertical strain: %
0
5
10
15
20
25
Global shear strain: %

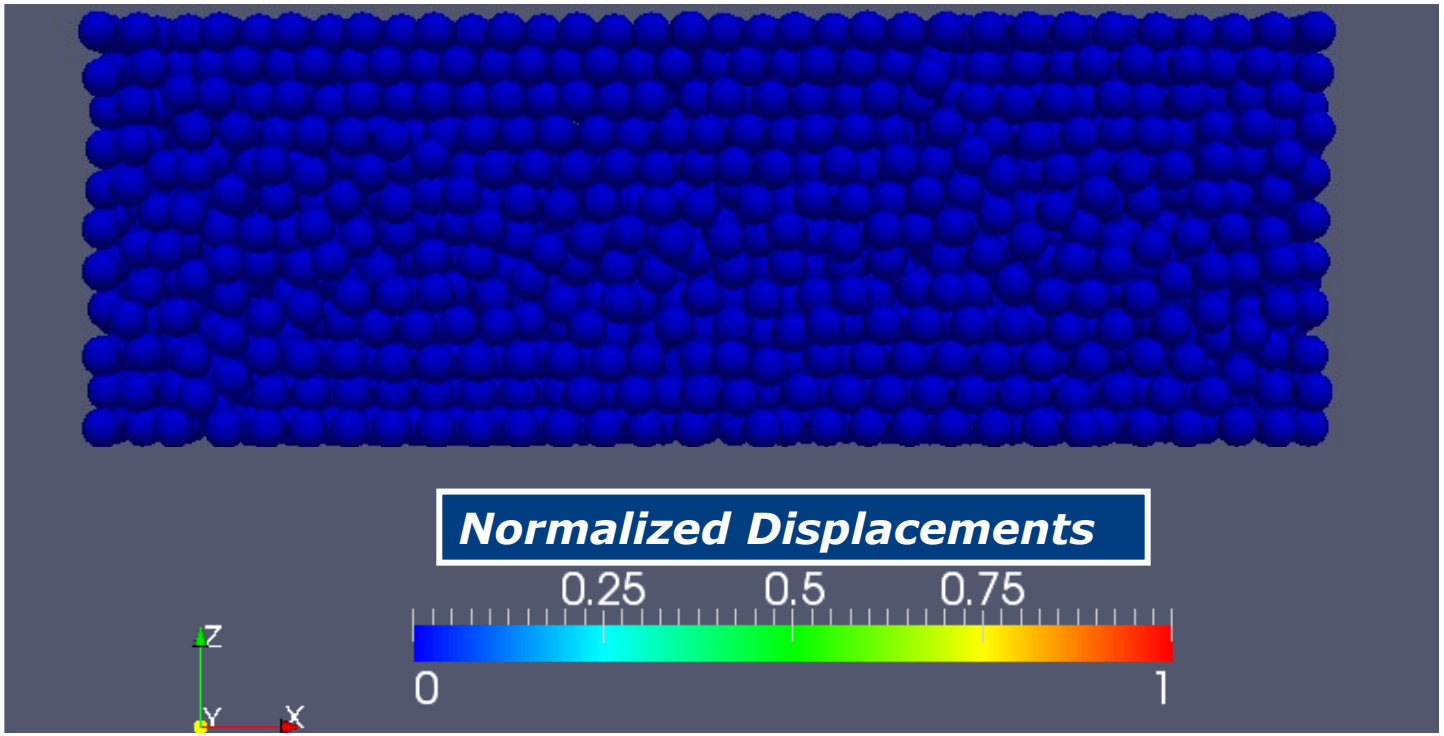
Normalized Displacements
0.25
0.5
0.75
0
1
Z
Y
X

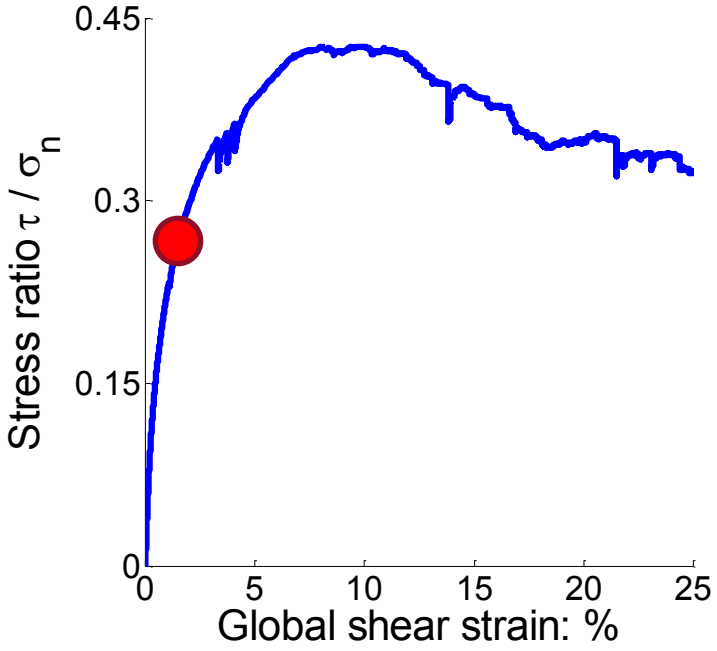
Stress ratio τ / σn
0.45
0.3
0.15
0
0
5
10
15
20
25
Global shear strain: %

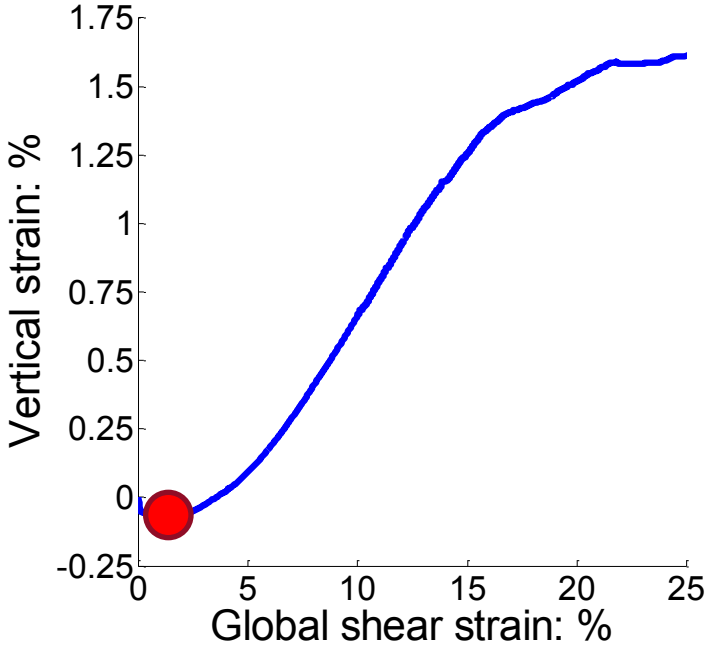
Vertical strain: %
1.75
1.5
1.25
1
0.75
0.5
0.25
0
-0.25
0
5
10
15
20
25
Global shear strain: %

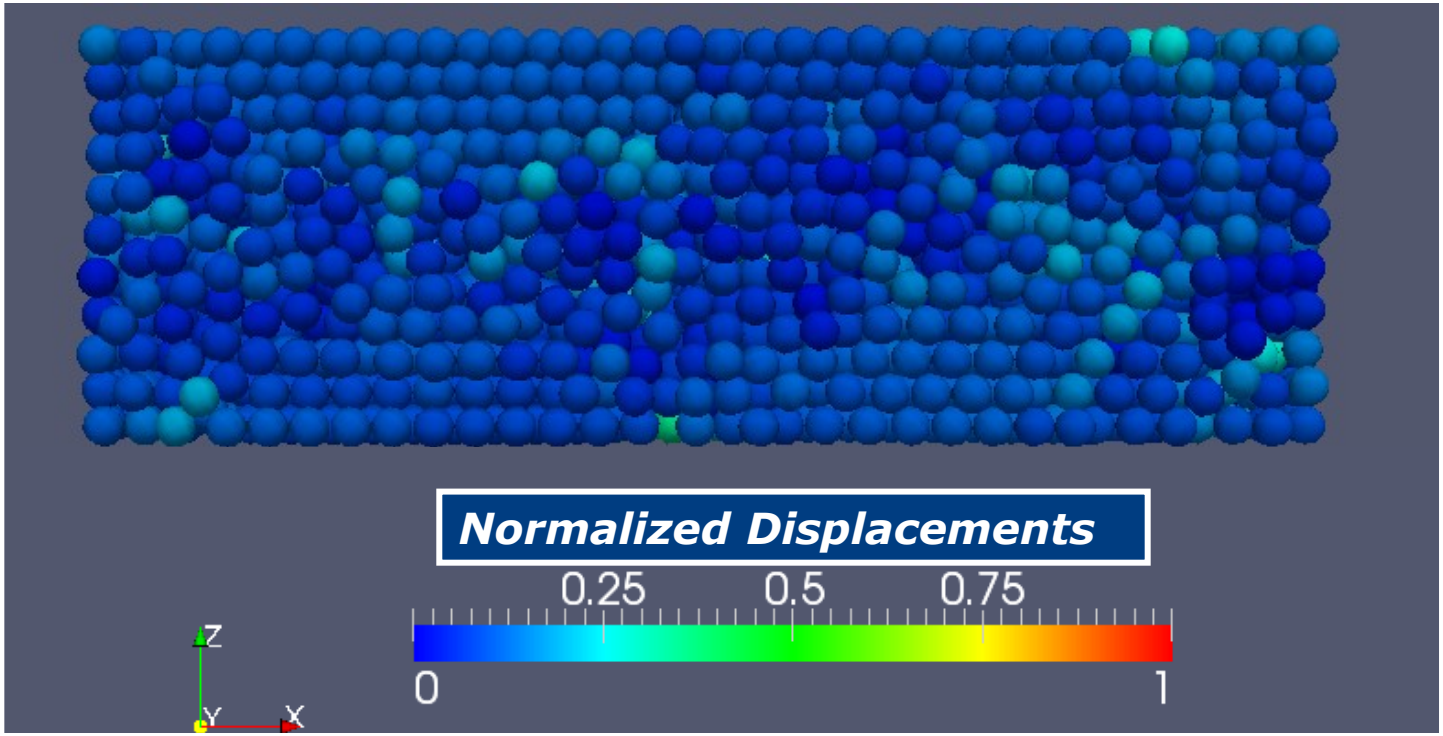
Normalized Displacements
0.25
0.5
0.75
0
1
Z
Y
X

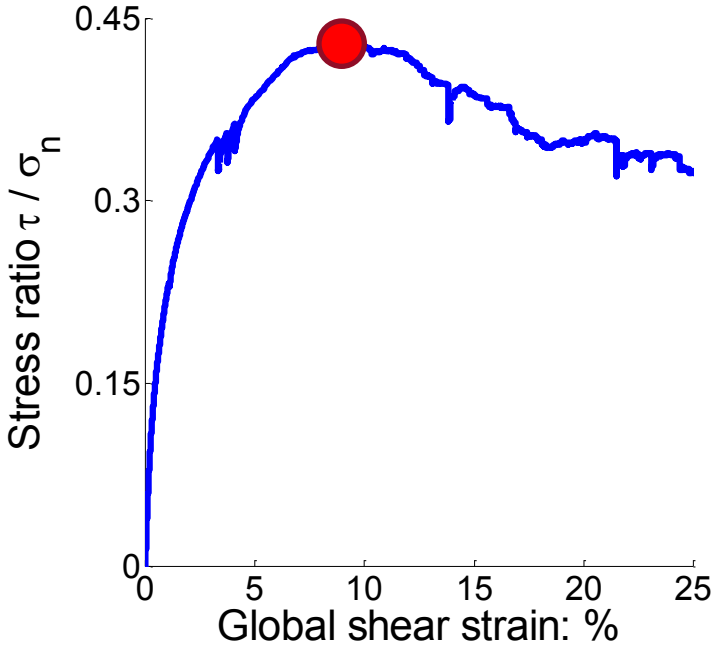
Stress ratio τ / σ_n
0.45
0.3
0.15
0
0
5
10
15
20
25
Global shear strain: %

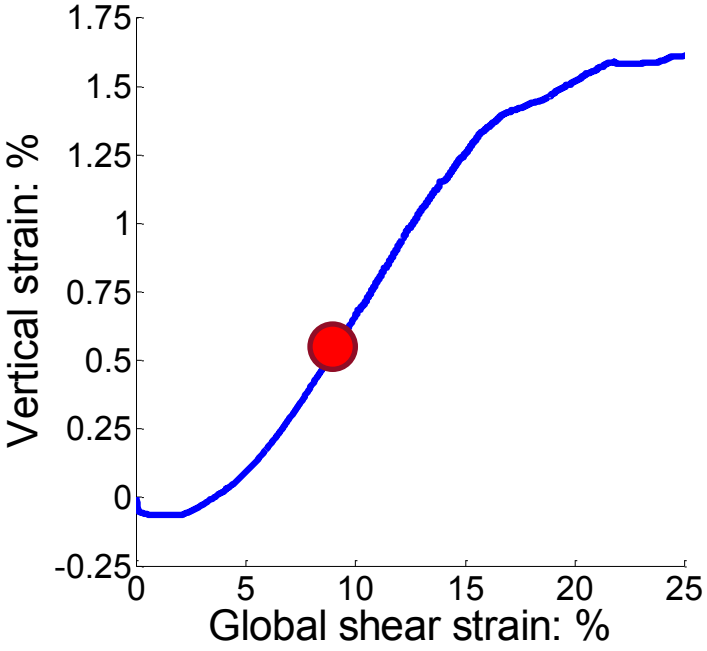
Vertical strain: %
1.75
1.5
1.25
1
0.75
0.5
0.25
0
-0.25
0
5
10
15
20
25
Global shear strain: %

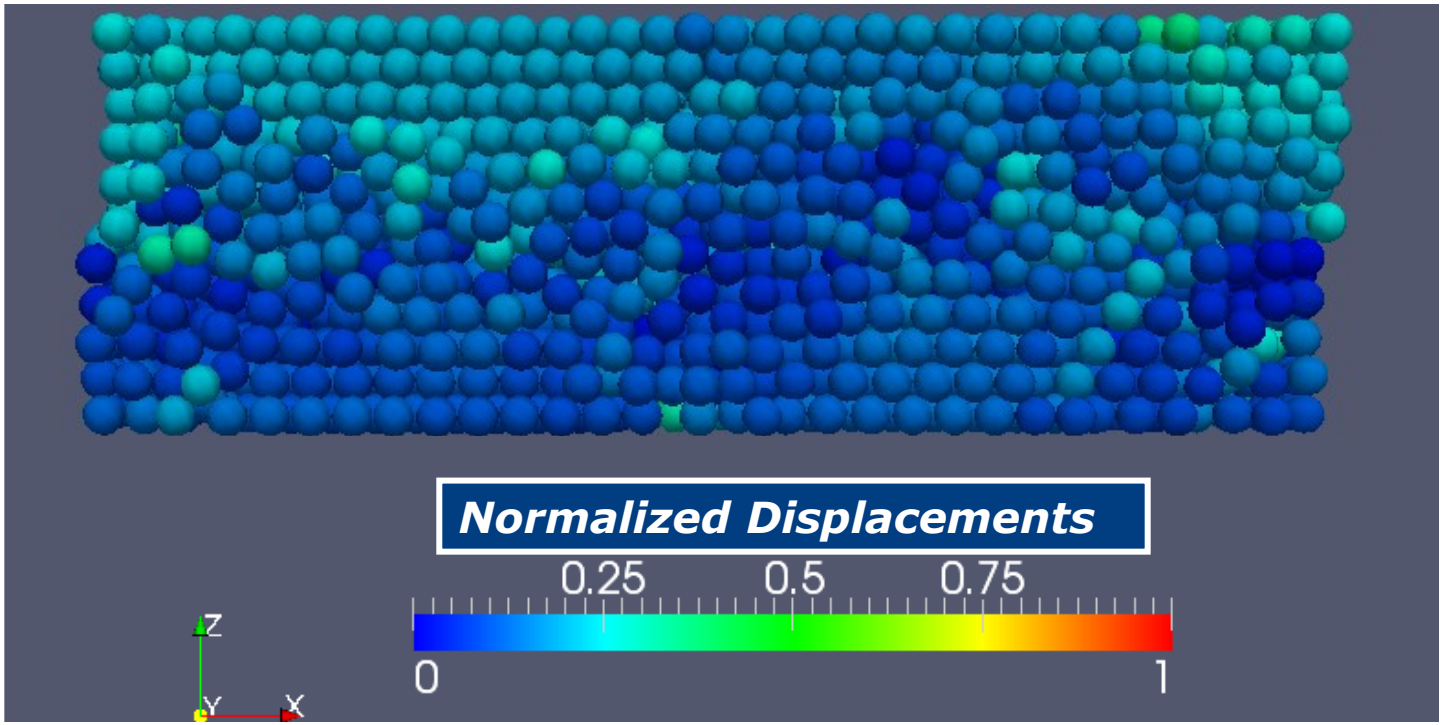
Normalized Displacements
0.25
0.5
0.75
0
1
Z
Y
X

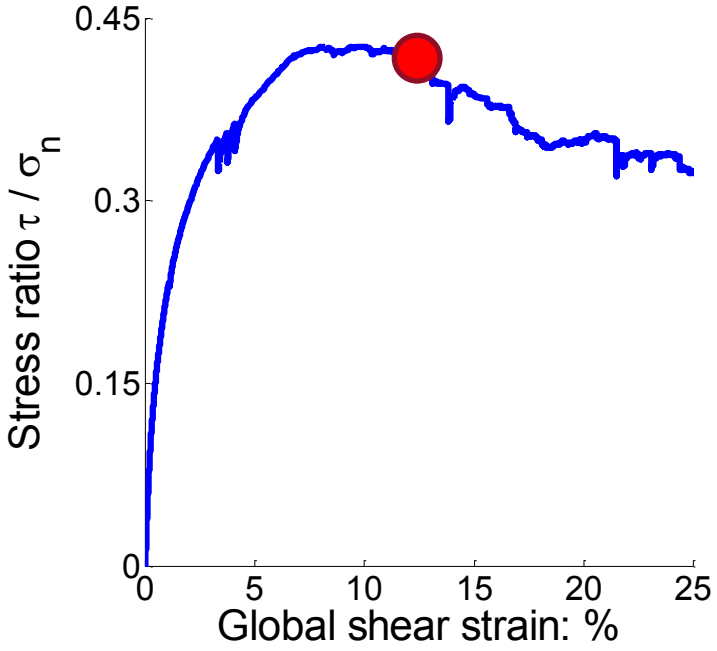
Stress ratio τ / σ_n
0.45
0.3
0.15
0
0
5
10
15
20
25
Global shear strain: %

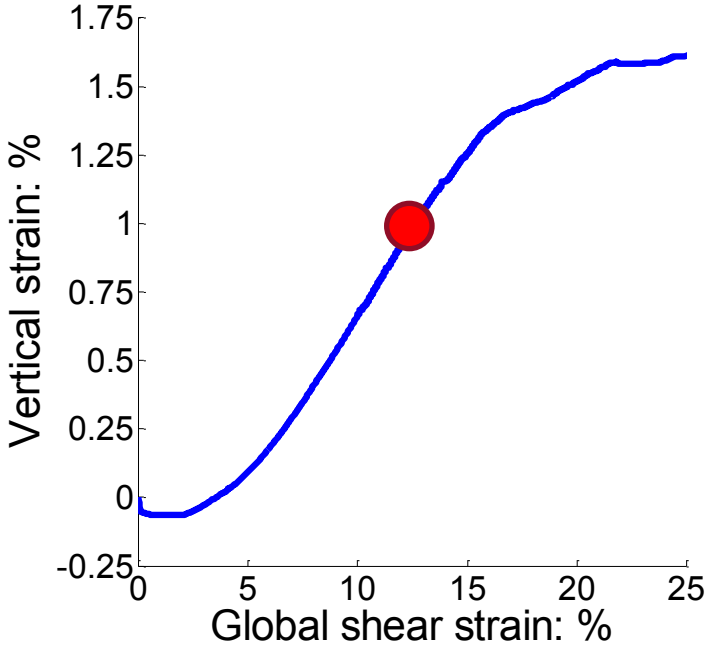
Vertical strain: %
1.75
1.5
1.25
1
0.75
0.5
0.25
0
-0.25
0
5
10
15
20
25
Global shear strain: %

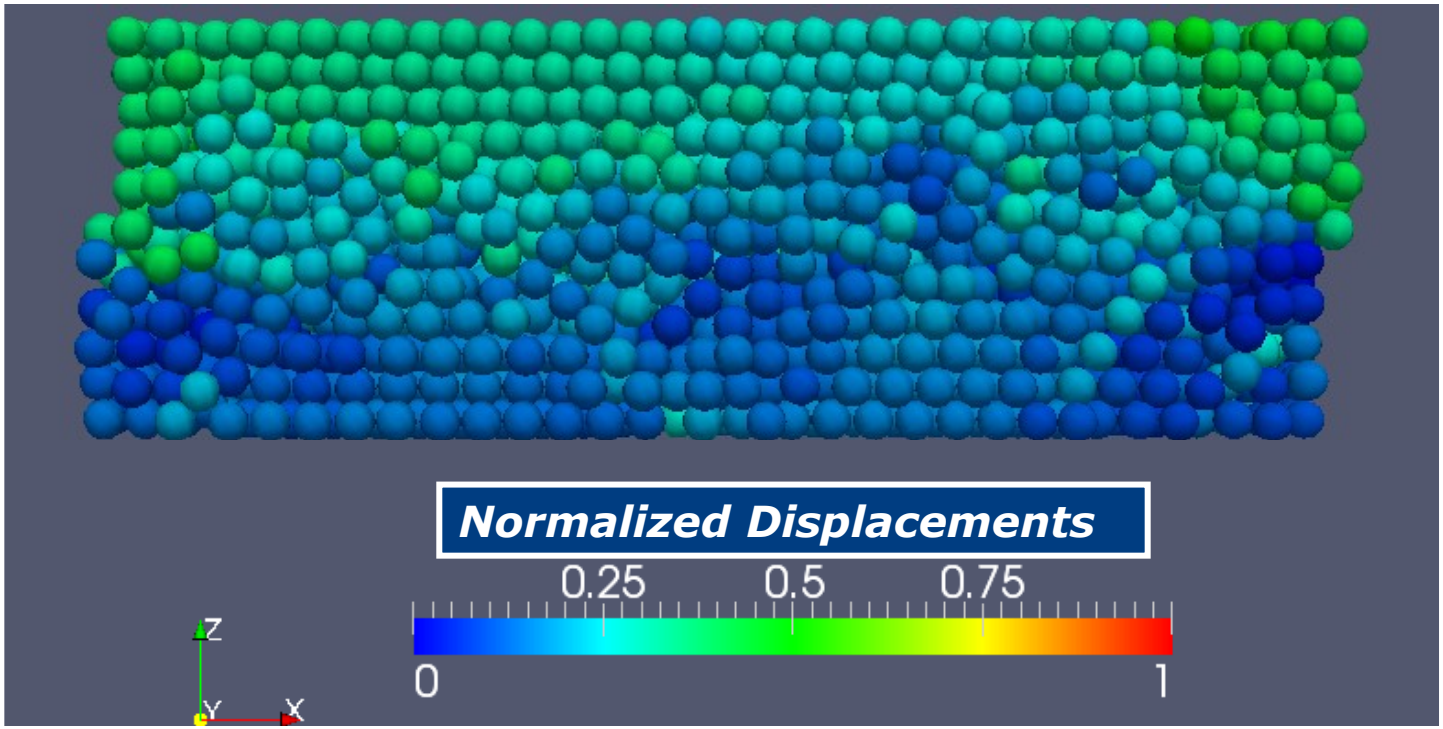
Normalized Displacements
0.25
0.5
0.75
0
1
Z
Y
X

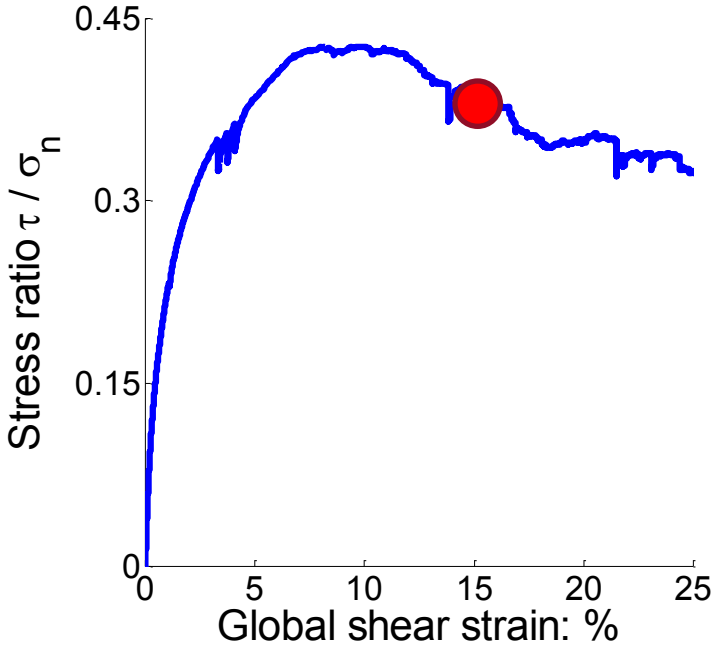
Stress ratio τ / σ_n
0.45
0.3
0.15
0
0
5
10
15
20
25
Global shear strain: %

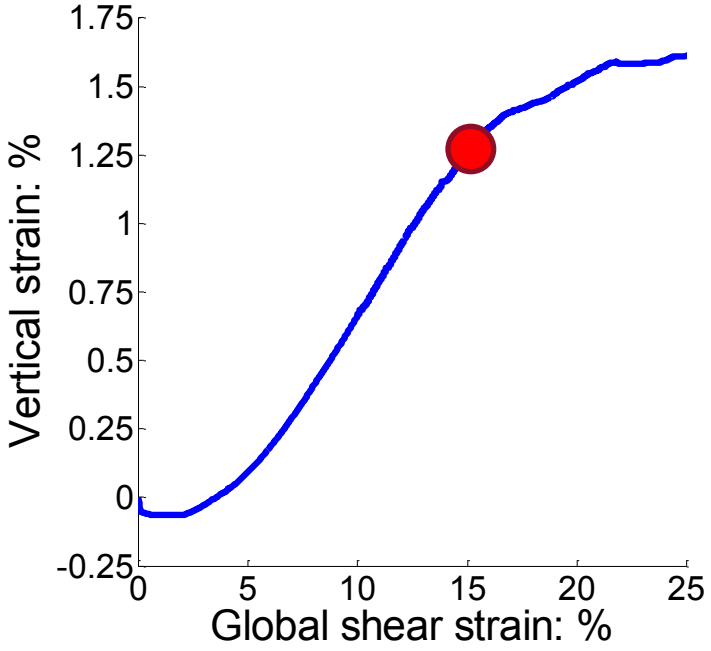
Vertical strain: %
1.75
1.5
1.25
1
0.75
0.5
0.25
0
-0.25
0
5
10
15
20
25
Global shear strain: %

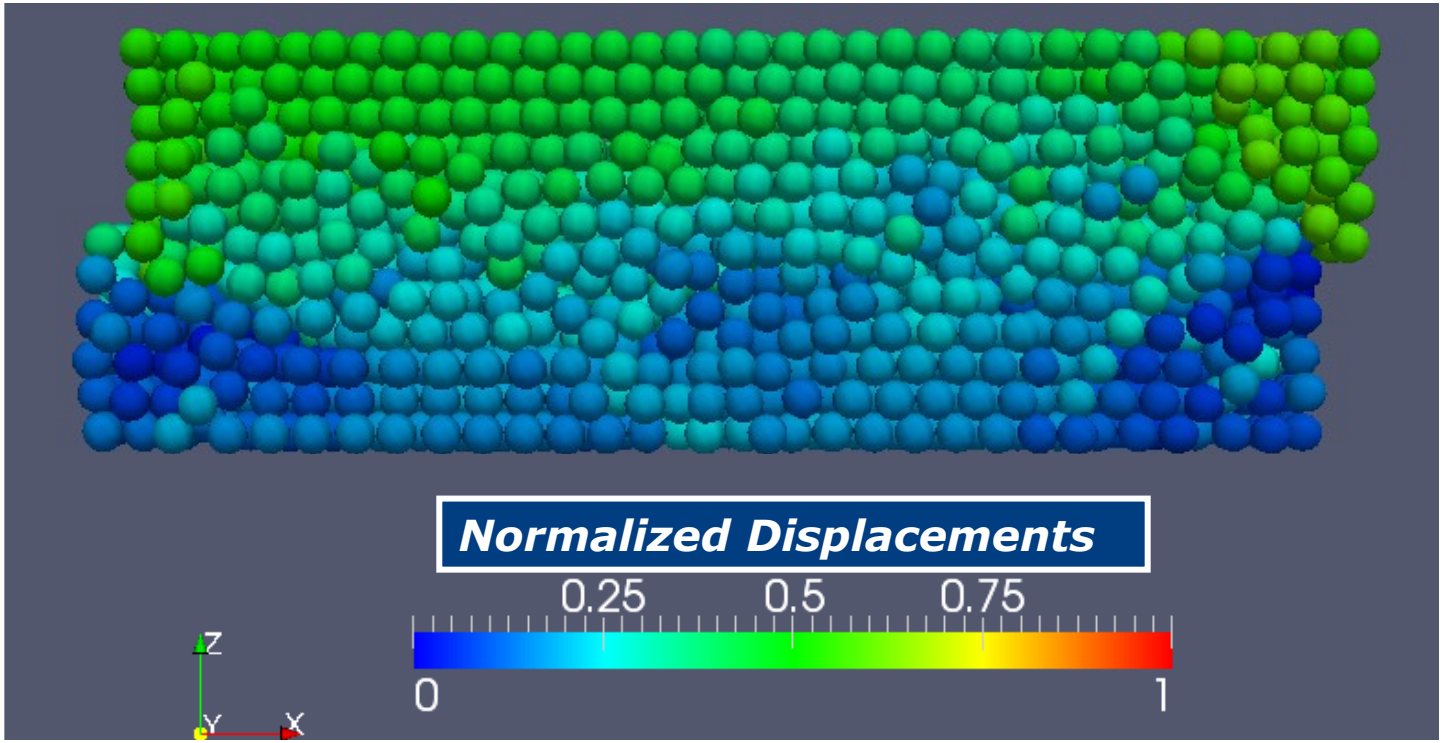
Normalized Displacements
0.25
0.5
0.75
0
1
Z
Y
X

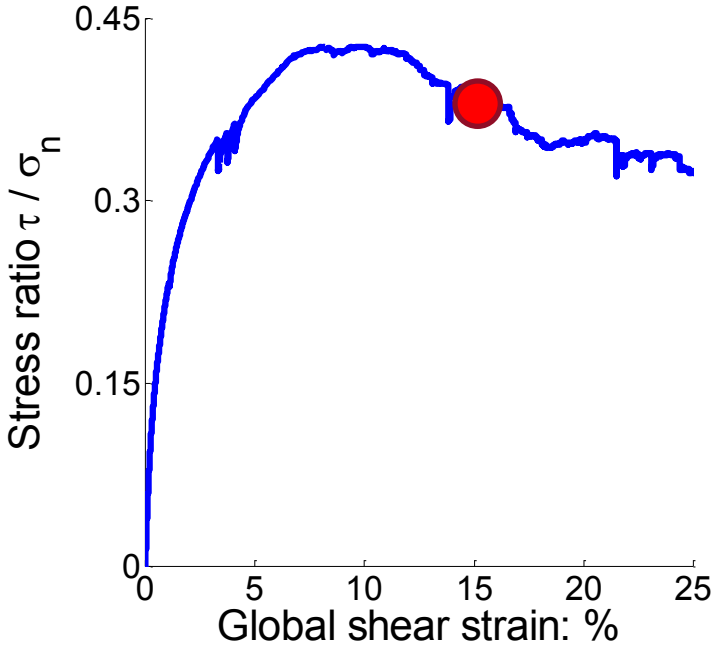
Stress ratio τ / σ_n
0.45
0.3
0.15
0
0
5
10
15
20
25
Global shear strain: %

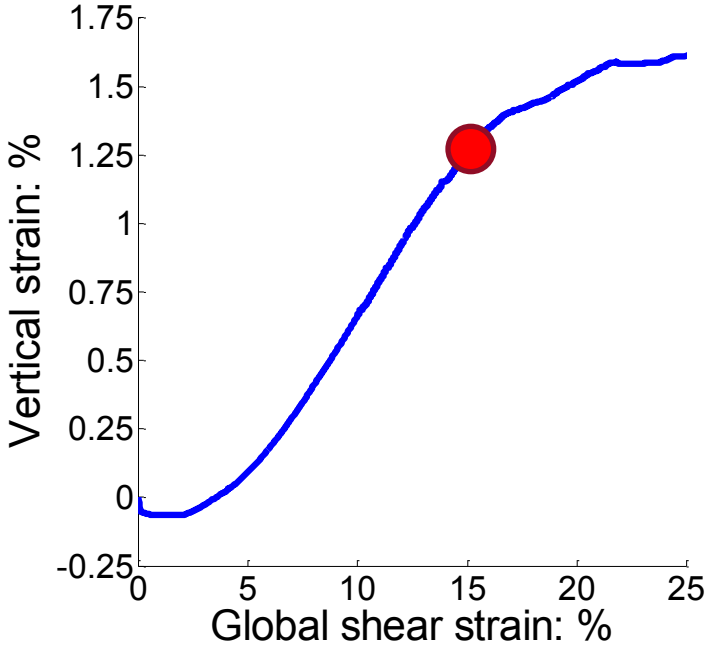
Vertical strain: %
1.75
1.5
1.25
1
0.75
0.5
0.25
0
-0.25
0
5
10
15
20
25
Global shear strain: %

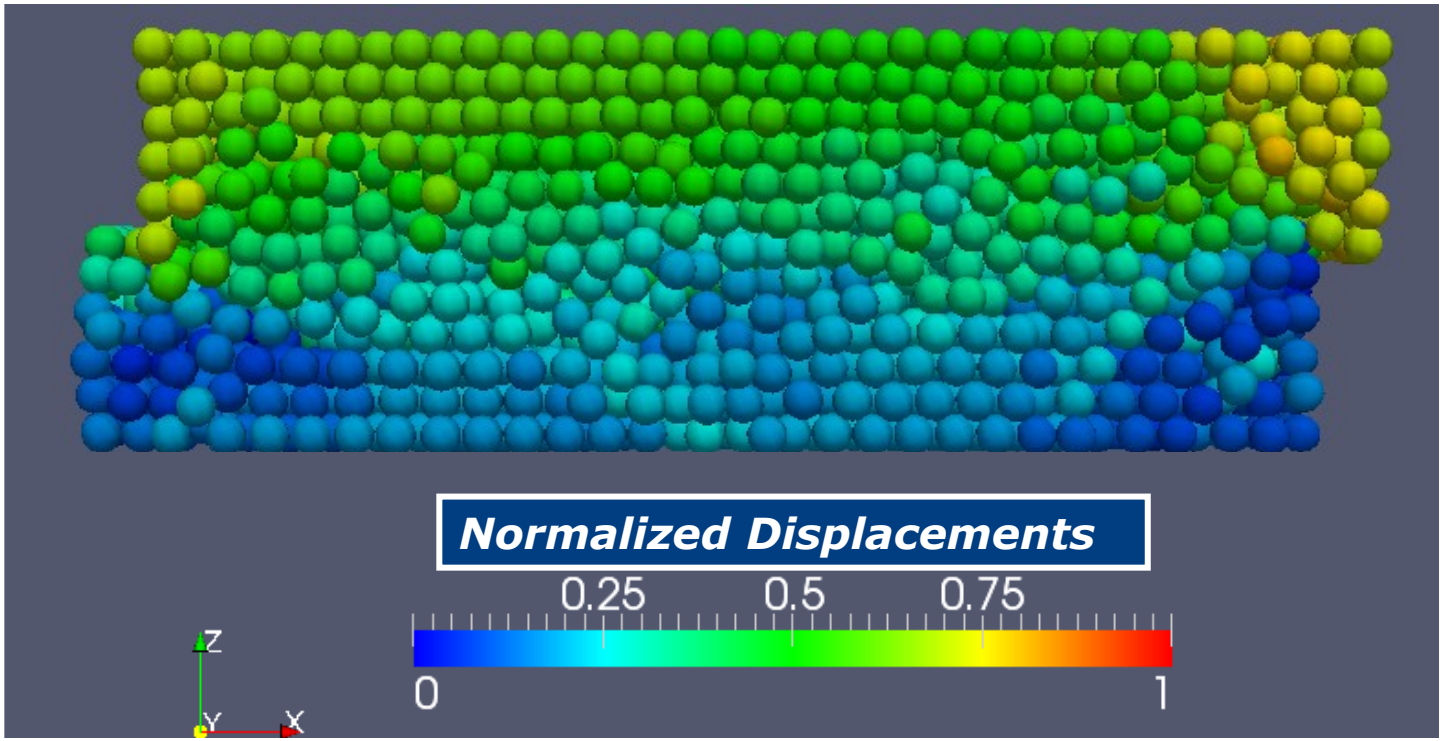
Normalized Displacements
0.25
0.5
0.75
0
1
Z
Y
X

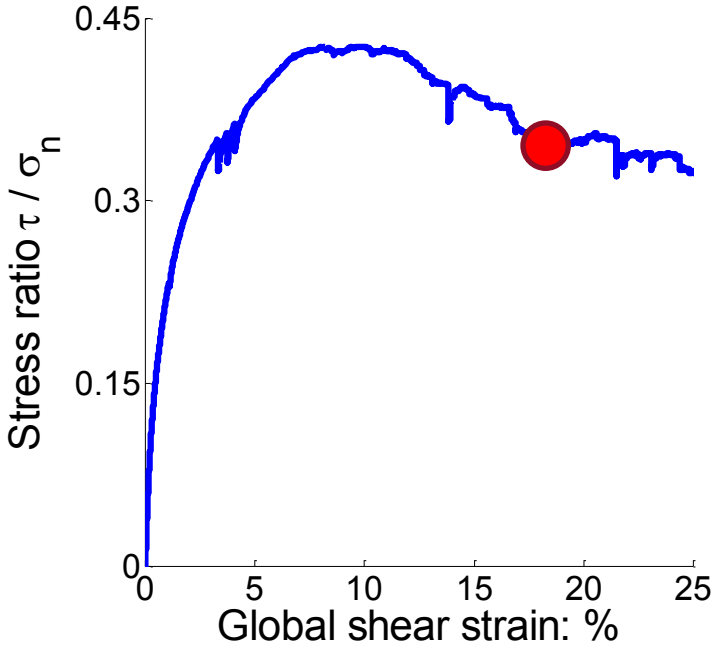
Stress ratio τ / σ_n
0.45
0.3
0.15
0
0
5
10
15
20
25
Global shear strain: %

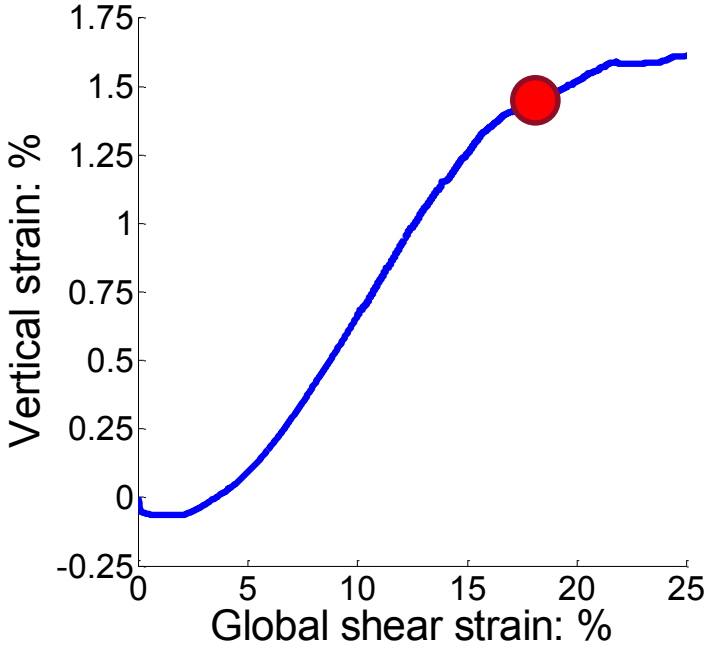
Vertical strain: %
1.75
1.5
1.25
1
0.75
0.5
0.25
0
-0.25
0
5
10
15
20
25
Global shear strain: %

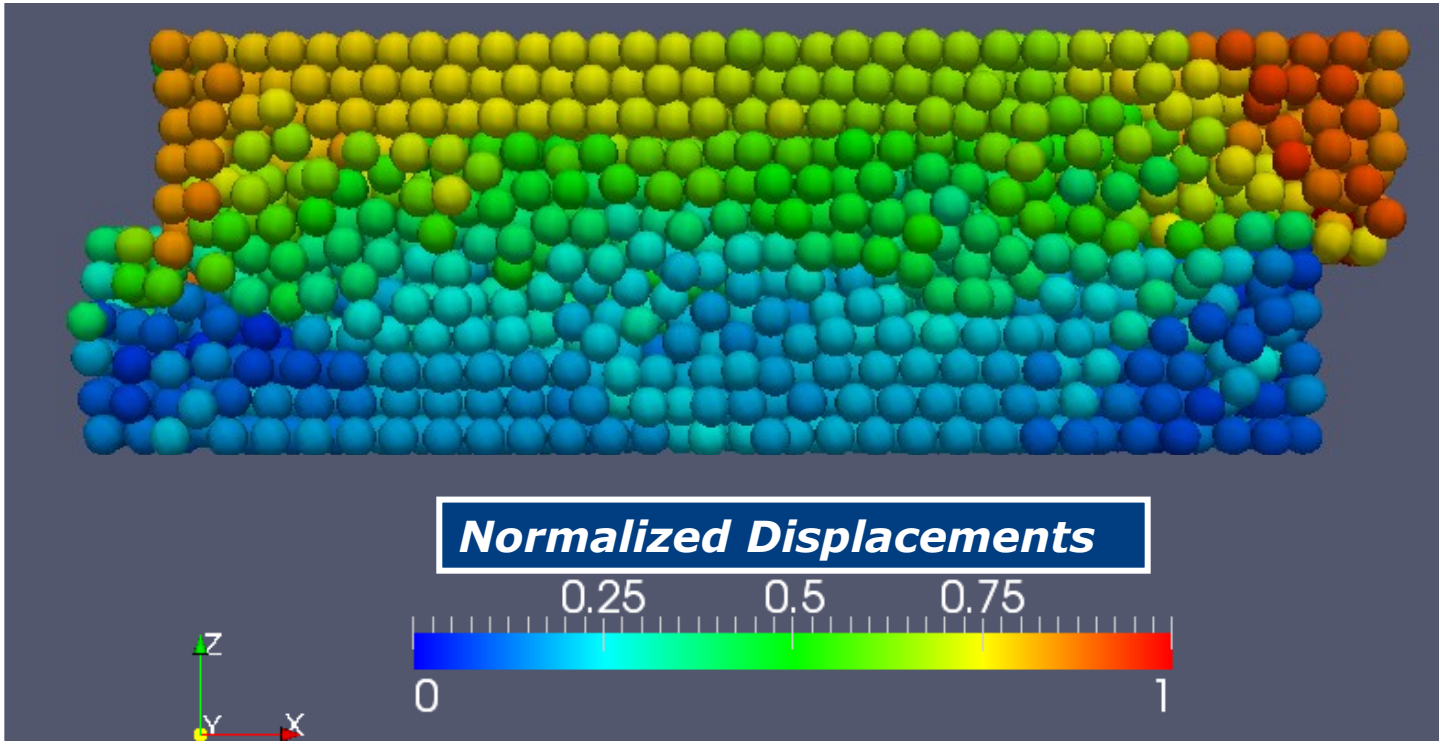
Normalized Displacements
0.25
0.5
0.75
0
1
Z
Y
X

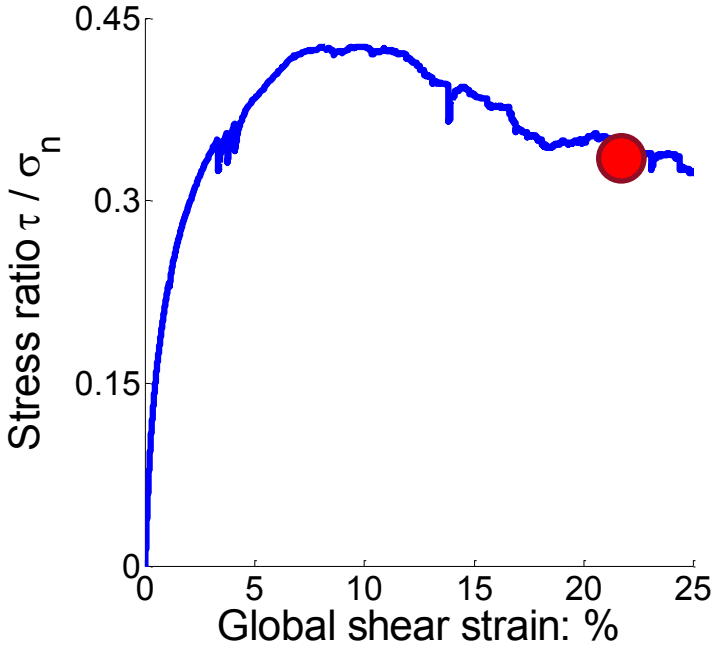
Stress ratio τ / σ_n
0.45
0.3
0.15
0
0
5
10
15
20
25
Global shear strain: %

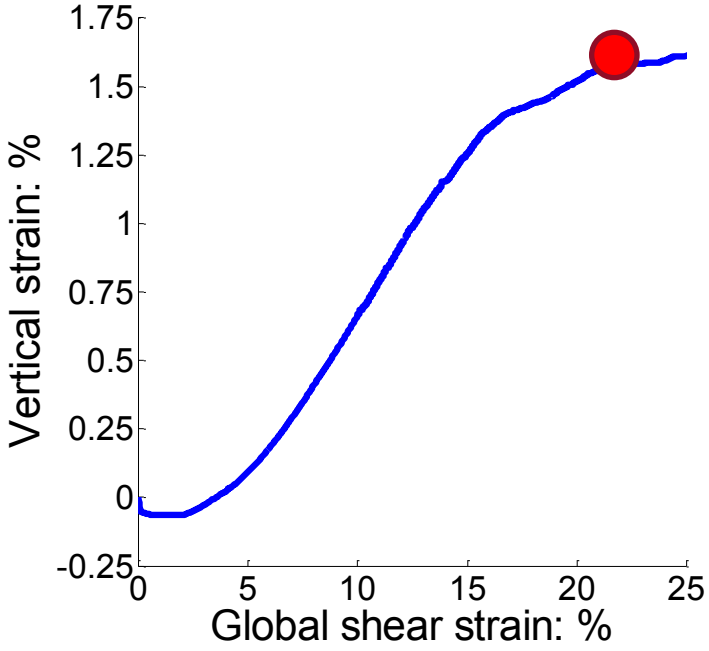
Vertical strain: %
1.75
1.5
1.25
1
0.75
0.5
0.25
0
-0.25
0
5
10
15
20
25
Global shear strain: %

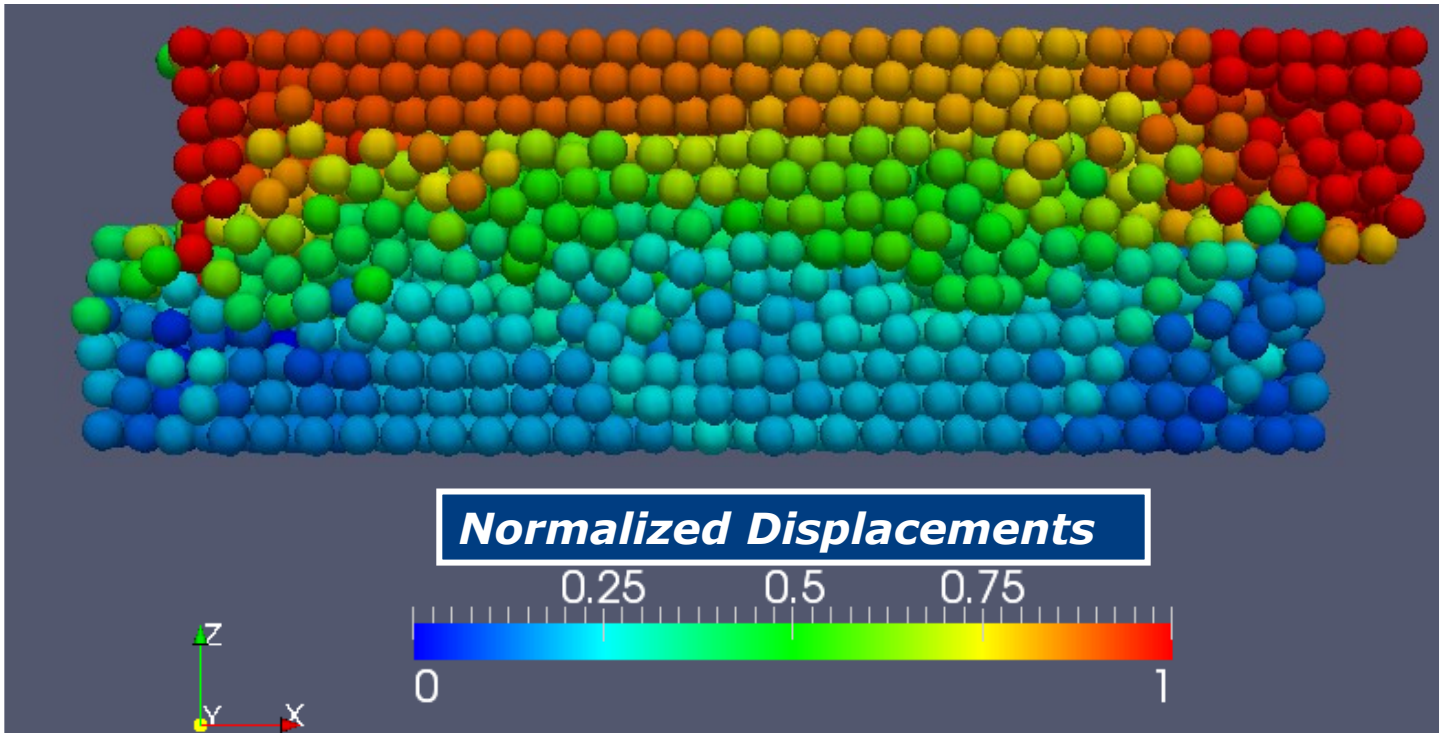
Normalized Displacements
0.25
0.5
0.75
0
1
Z
Y
X

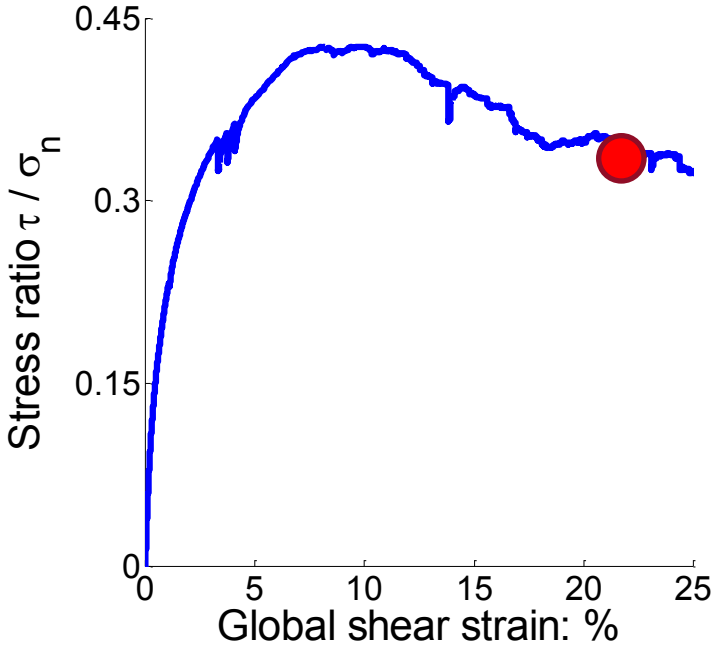
Stress ratio τ / σn
0.45
0.3
0.15
0
0
5
10
15
20
25
Global shear strain: %

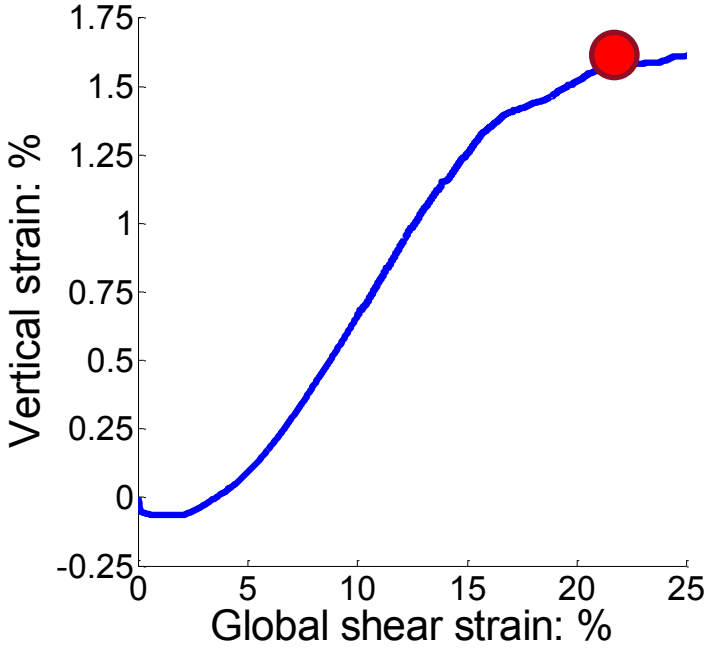
Vertical strain: %
1.75
1.5
1.25
1
0.75
0.5
0.25
0
-0.25
0
5
10
15
20
25
Global shear strain: %

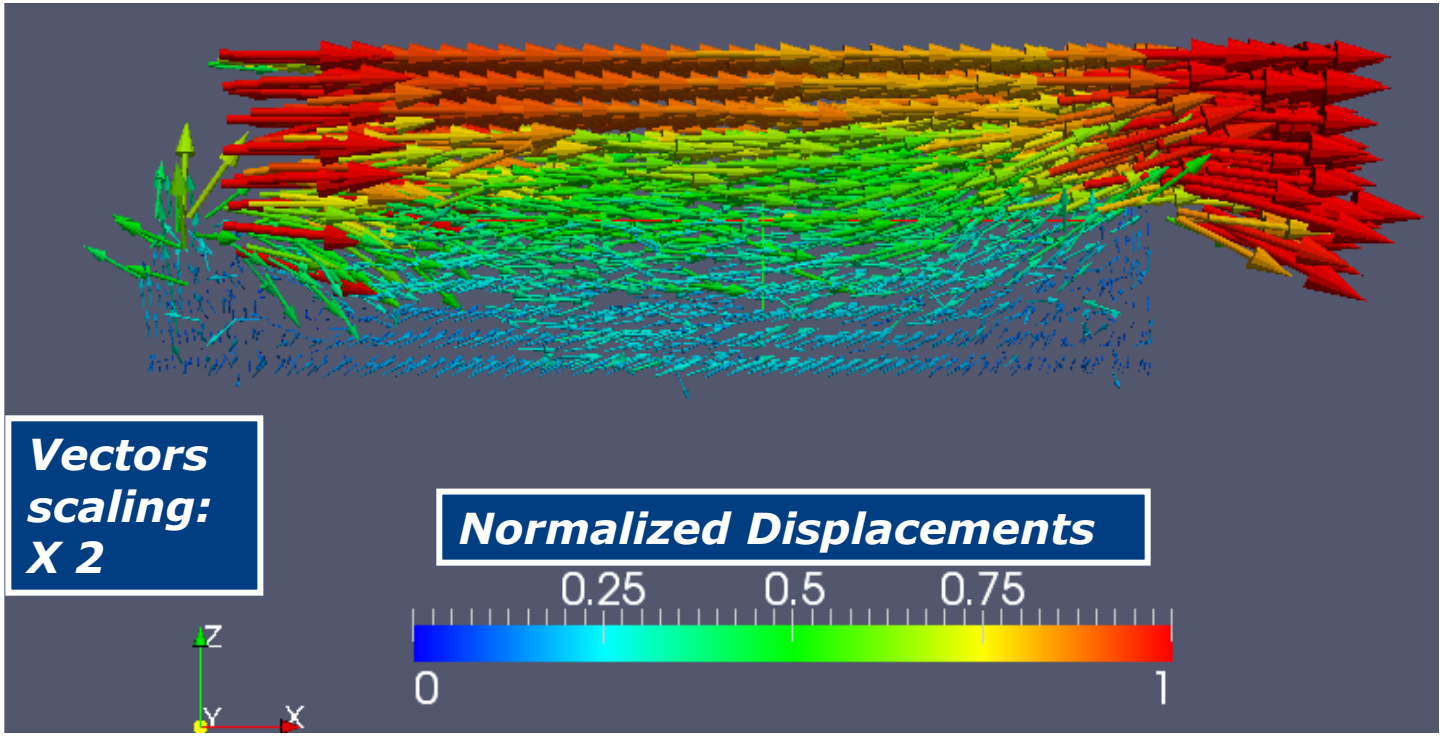
Vectors scaling: X 2
Normalized Displacements
0.25
0.5
0.75
0
1
Z
Y
X

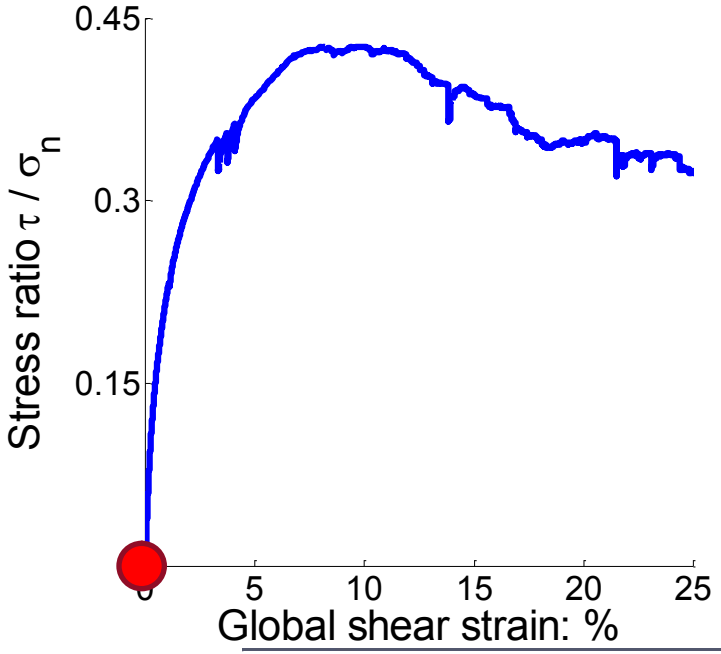
0.45
0.3
0.15
Stress ratio τ / σn
0
5
10
15
20
25
Global shear strain: %

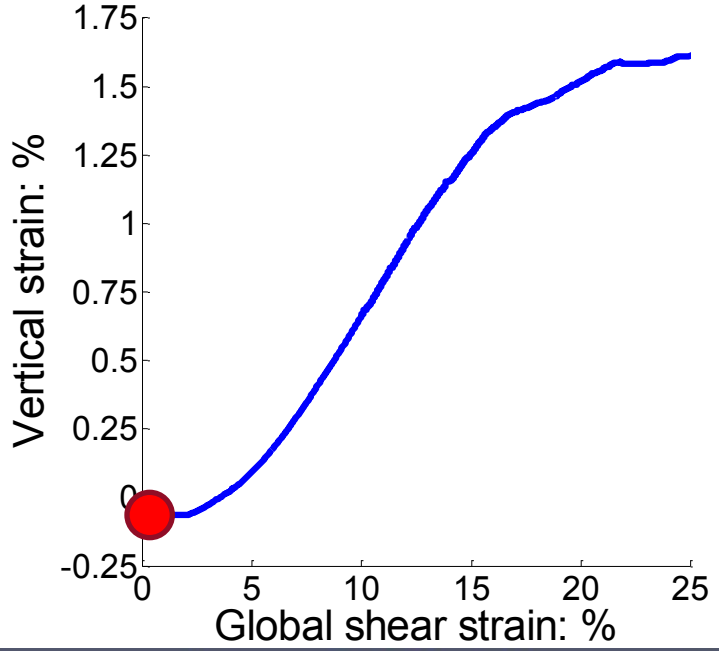
1.75
1.5
1.25
1
0.75
0.5
0.25
0
-0.25
Vertical strain: %
0
5
10
15
20
25
Global shear strain: %

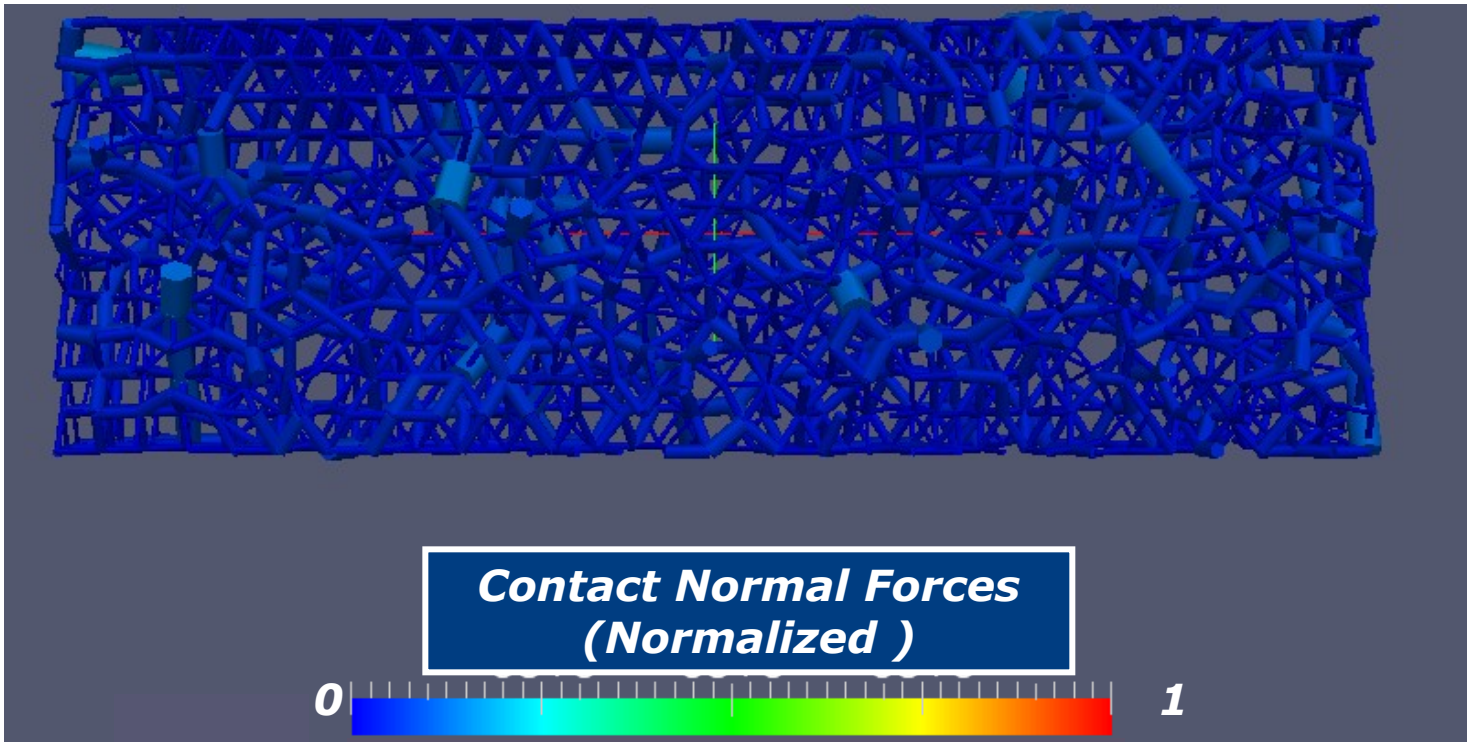
Contact Normal Forces
(Normalized)
0
1

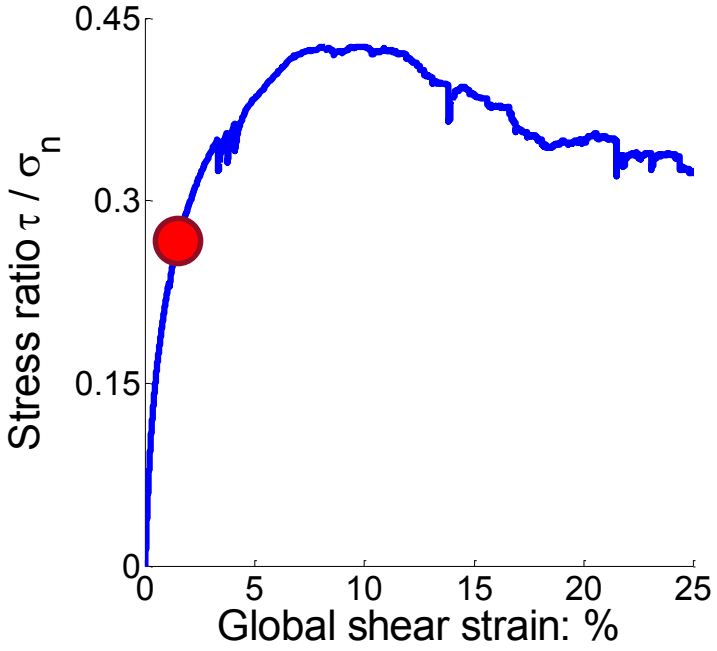
Stress ratio τ / σ_n
0.45
0.3
0.15
0
0
5
10
15
20
25
Global shear strain: %

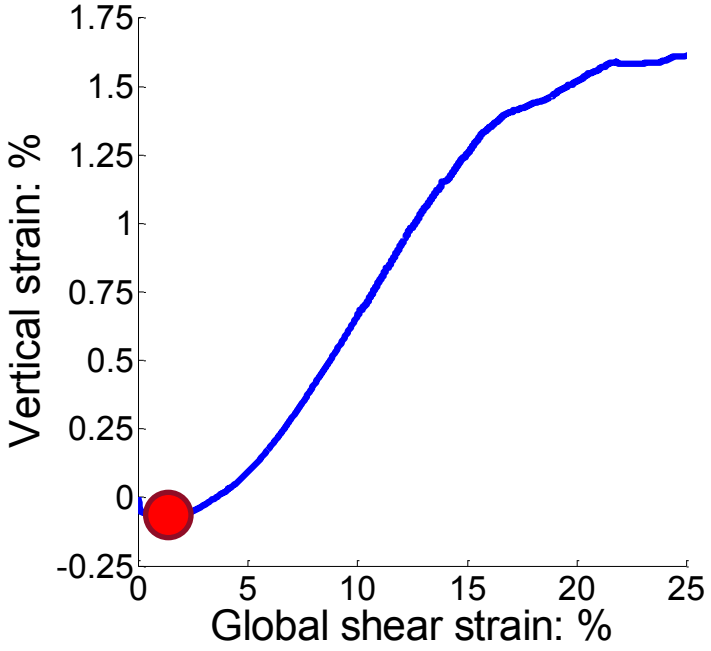
Vertical strain: %
1.75
1.5
1.25
1
0.75
0.5
0.25
0
-0.25
0
5
10
15
20
25
Global shear strain: %

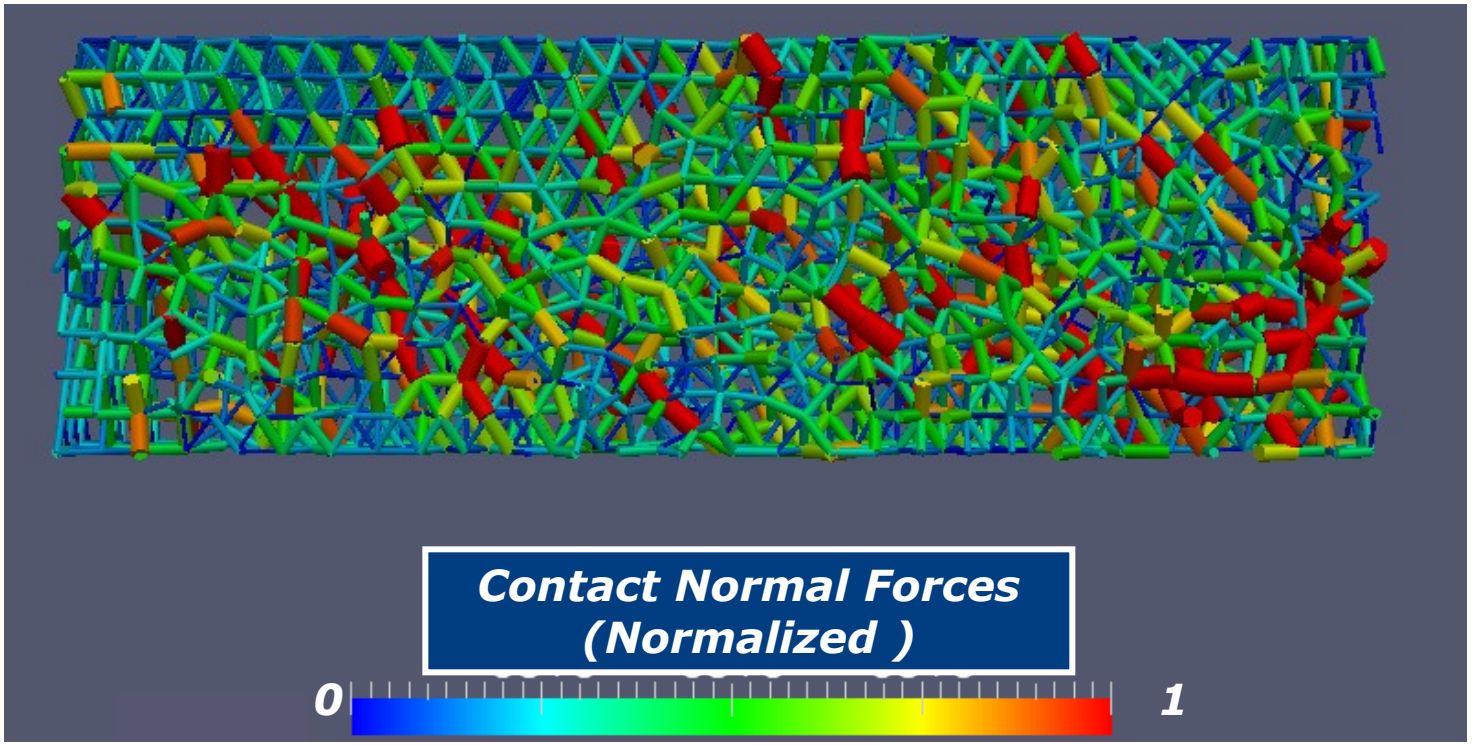
Contact Normal Forces
(Normalized)
0
1

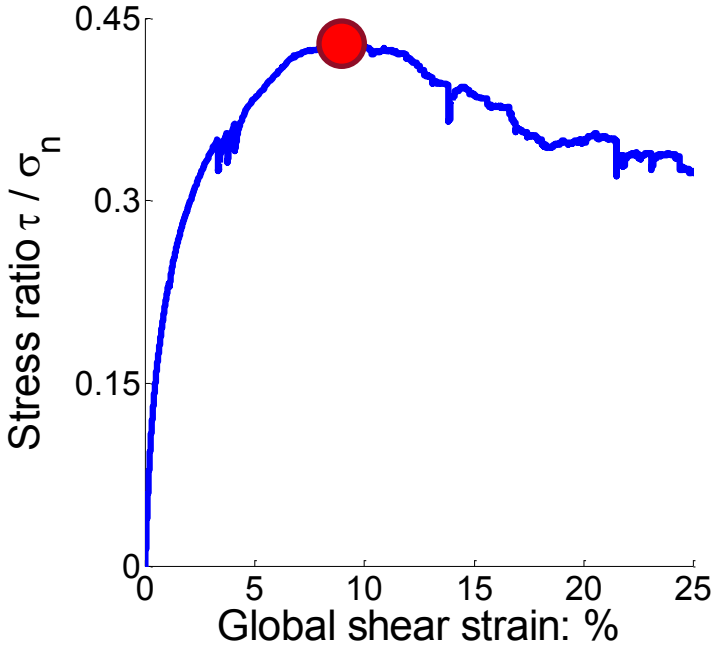
Stress ratio τ / σ_n
0.45
0.3
0.15
0
0
5
10
15
20
25
Global shear strain: %

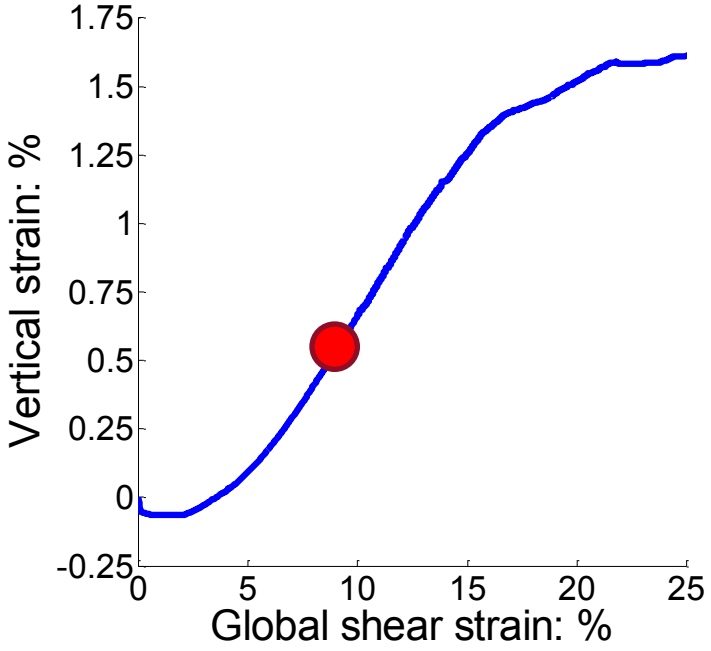
Vertical strain: %
1.75
1.5
1.25
1
0.75
0.5
0.25
0
-0.25
0
5
10
15
20
25
Global shear strain: %

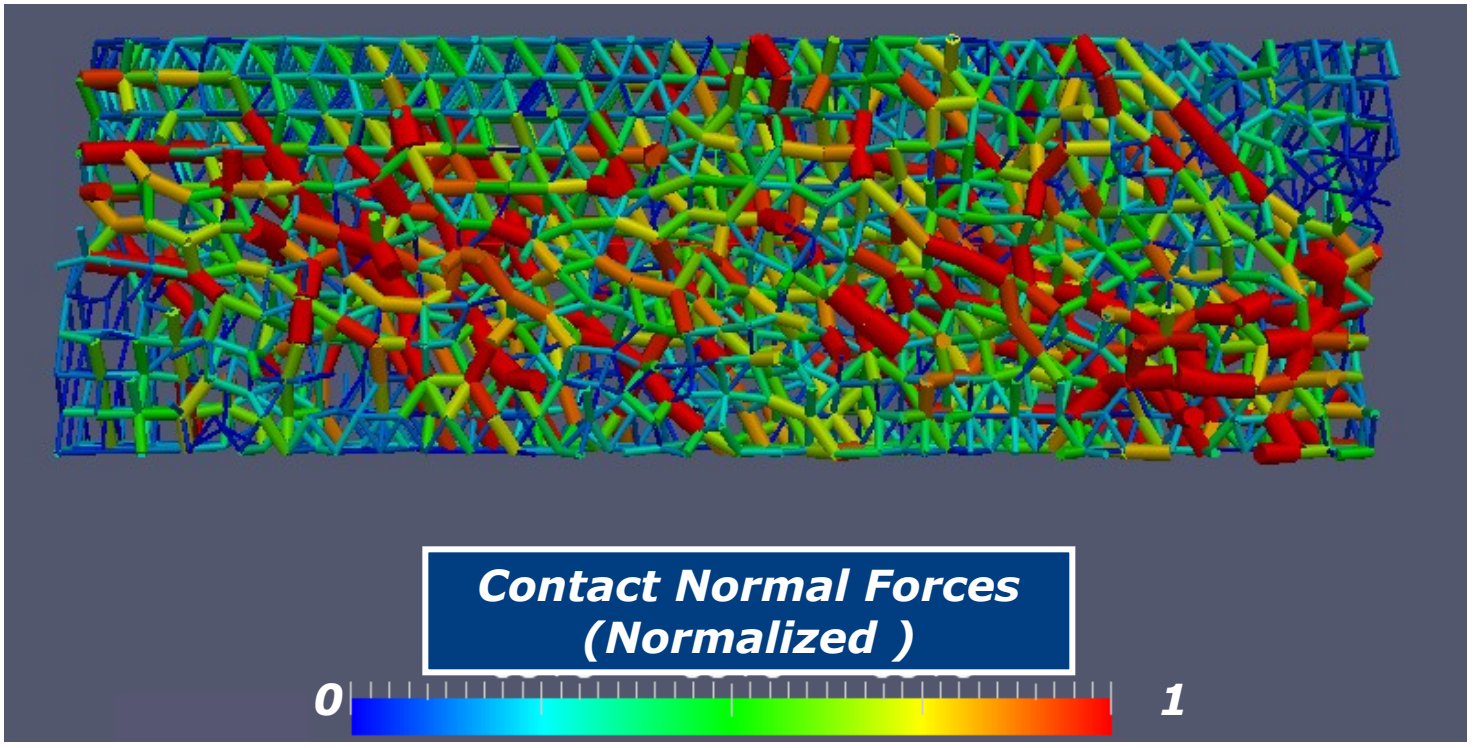
Contact Normal Forces
(Normalized)
0
1

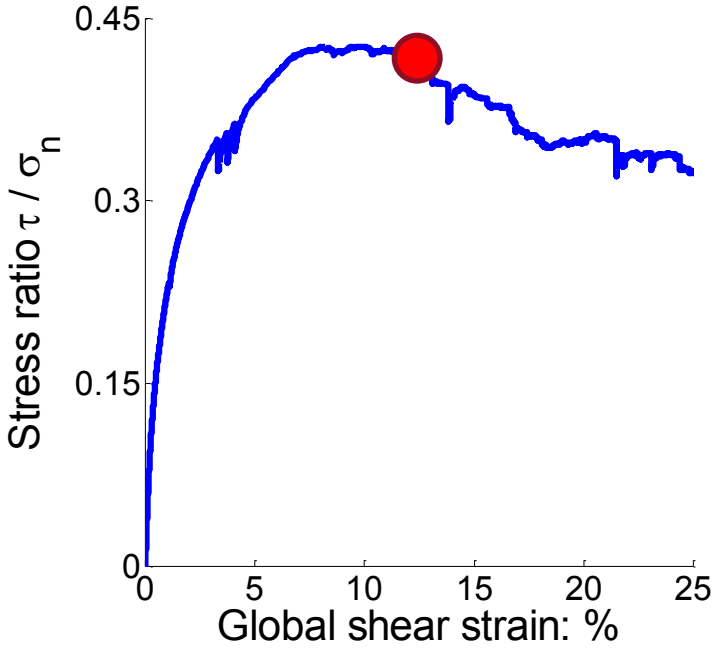
Stress ratio τ / σ_n
0.45
0.3
0.15
0
0
5
10
15
20
25
Global shear strain: %

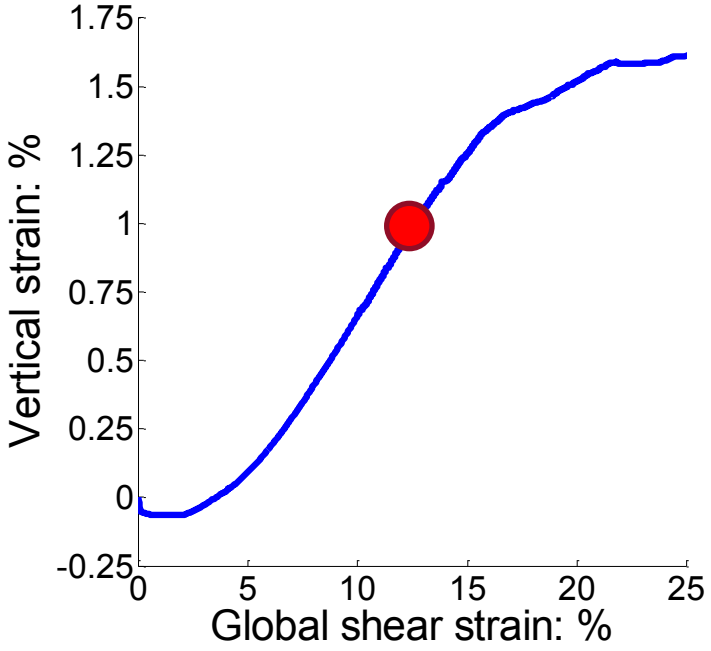
Vertical strain: %
1.75
1.5
1.25
1
0.75
0.5
0.25
0
-0.25
0
5
10
15
20
25
Global shear strain: %

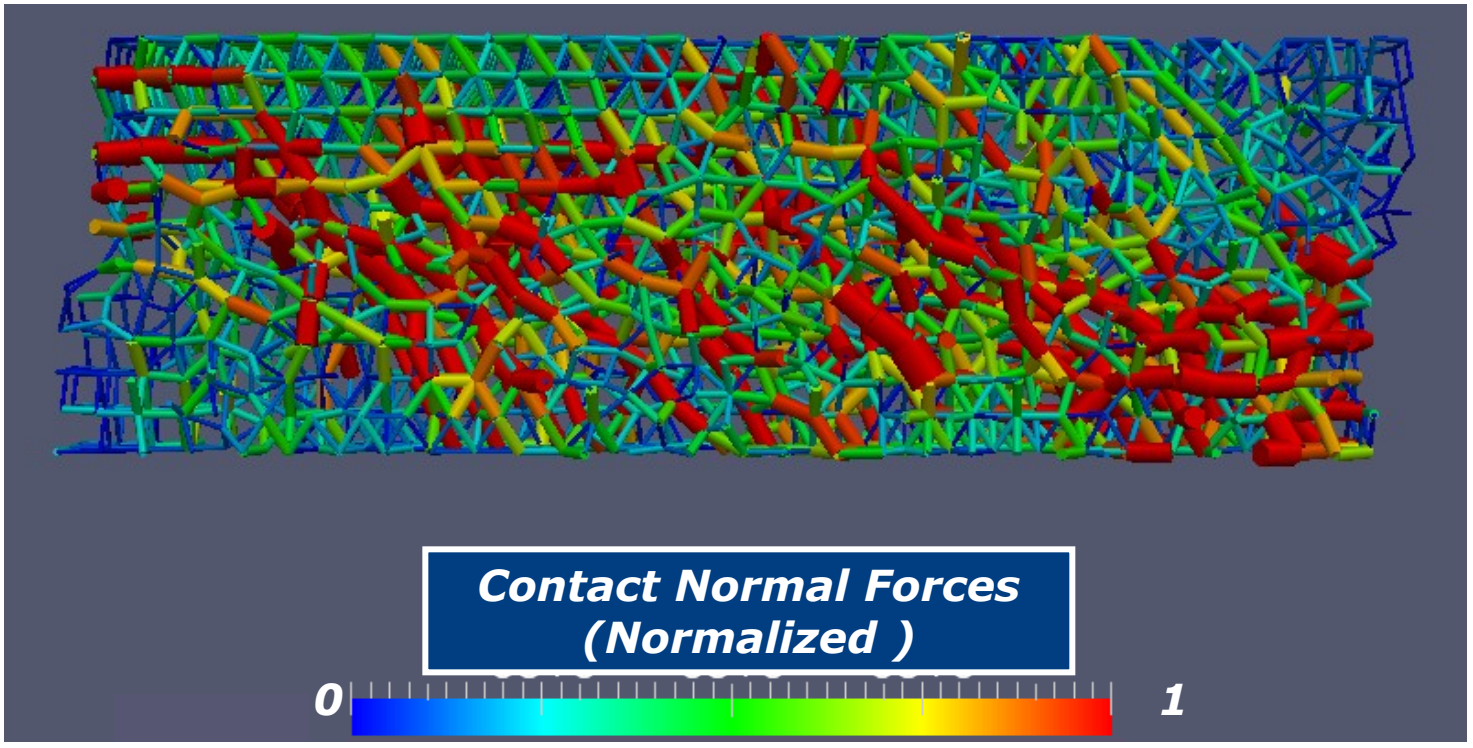
Contact Normal Forces
(Normalized)
0
1

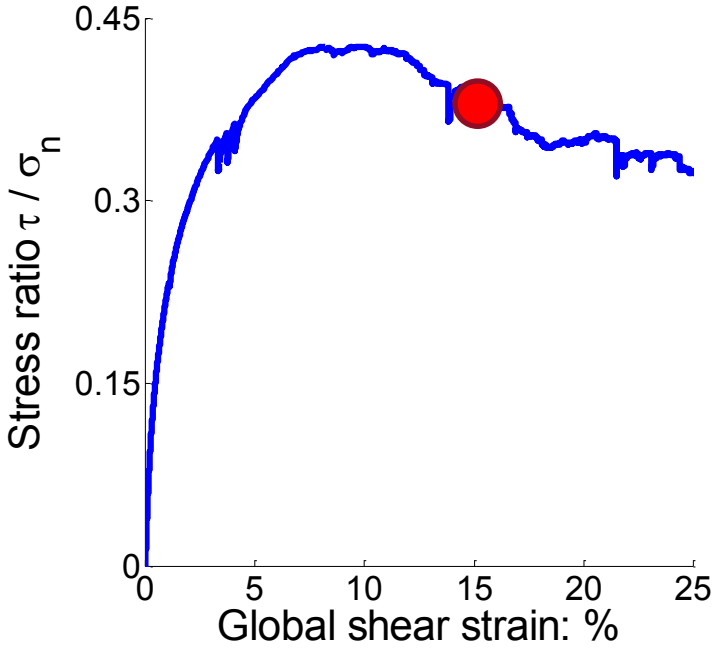
Stress ratio τ / σ_n
0.45
0.3
0.15
0
0
5
10
15
20
25
Global shear strain: %

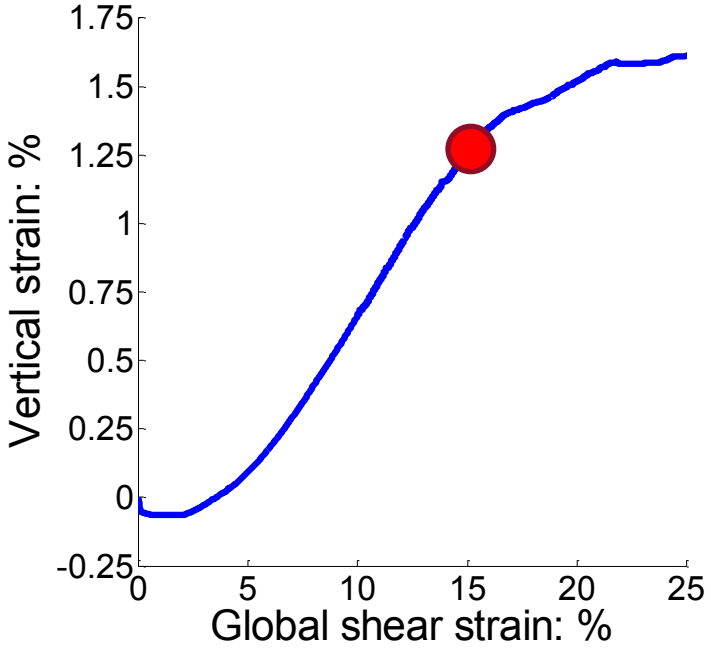
Vertical strain: %
1.75
1.5
1.25
1
0.75
0.5
0.25
0
-0.25
0
5
10
15
20
25
Global shear strain: %

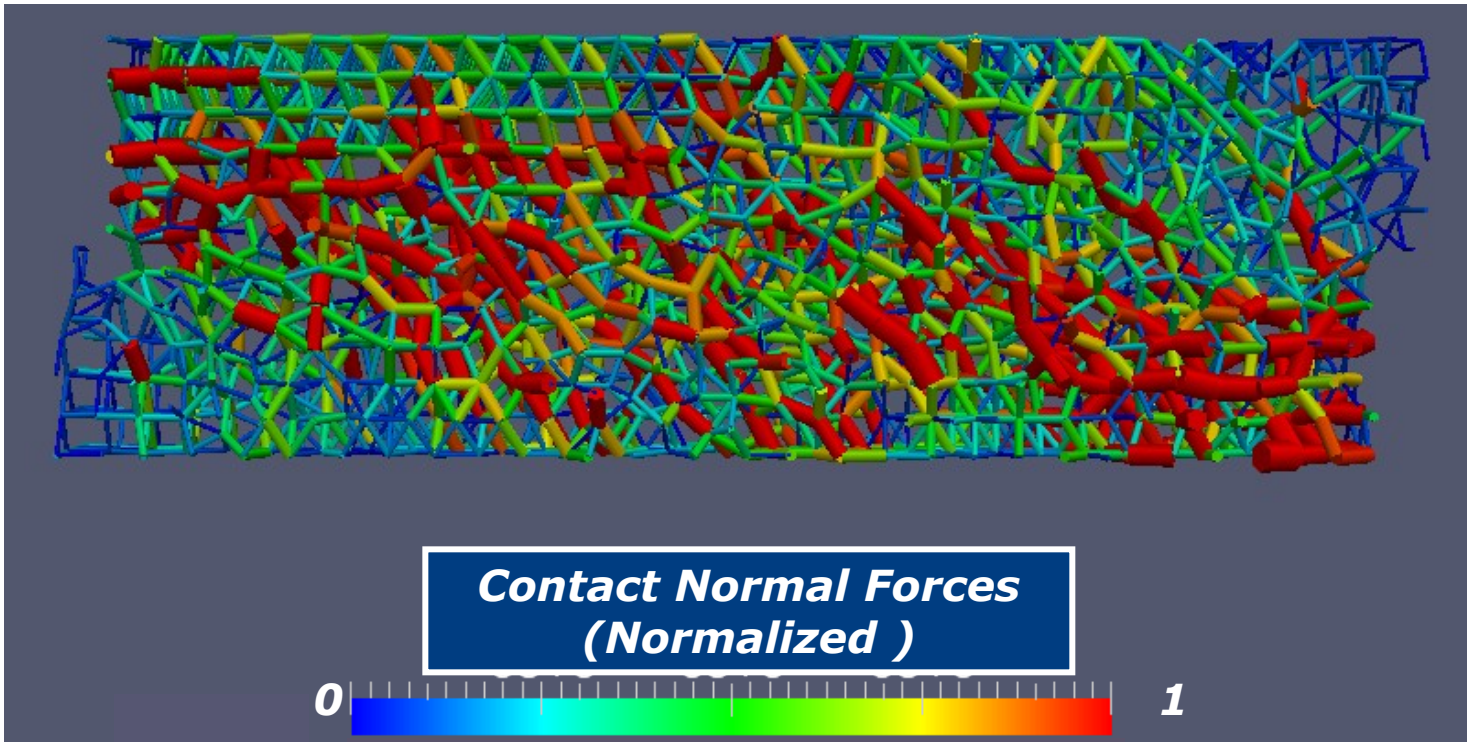
Contact Normal Forces
(Normalized)
0
1

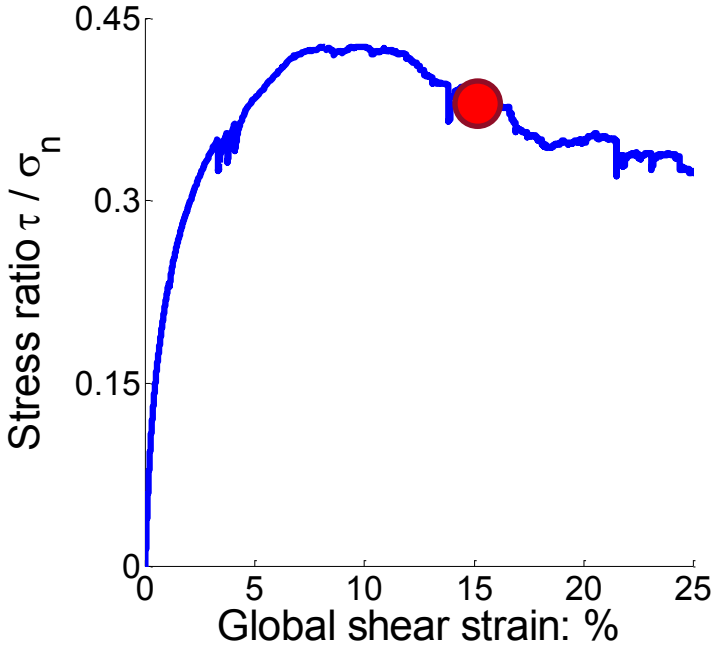
Stress ratio τ / σ_n
0.45
0.3
0.15
0
0
5
10
15
20
25
Global shear strain: %

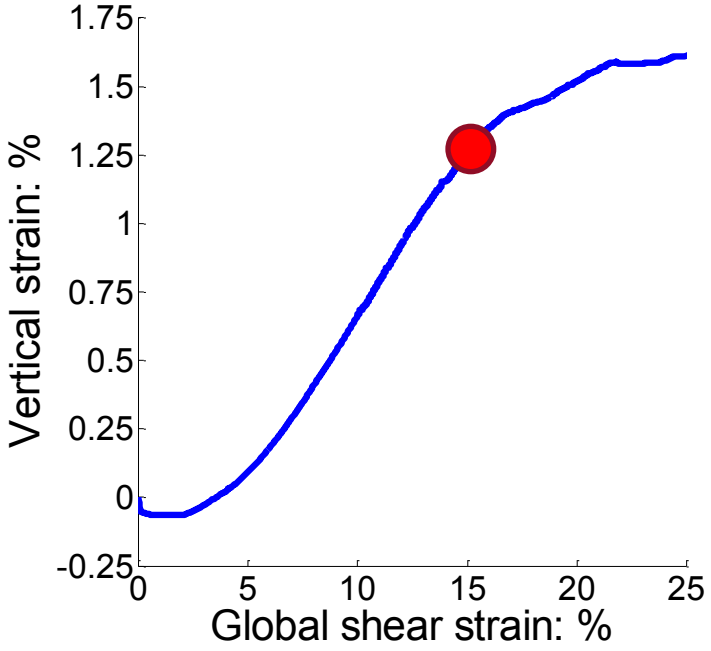
Vertical strain: %
1.75
1.5
1.25
1
0.75
0.5
0.25
0
-0.25
0
5
10
15
20
25
Global shear strain: %

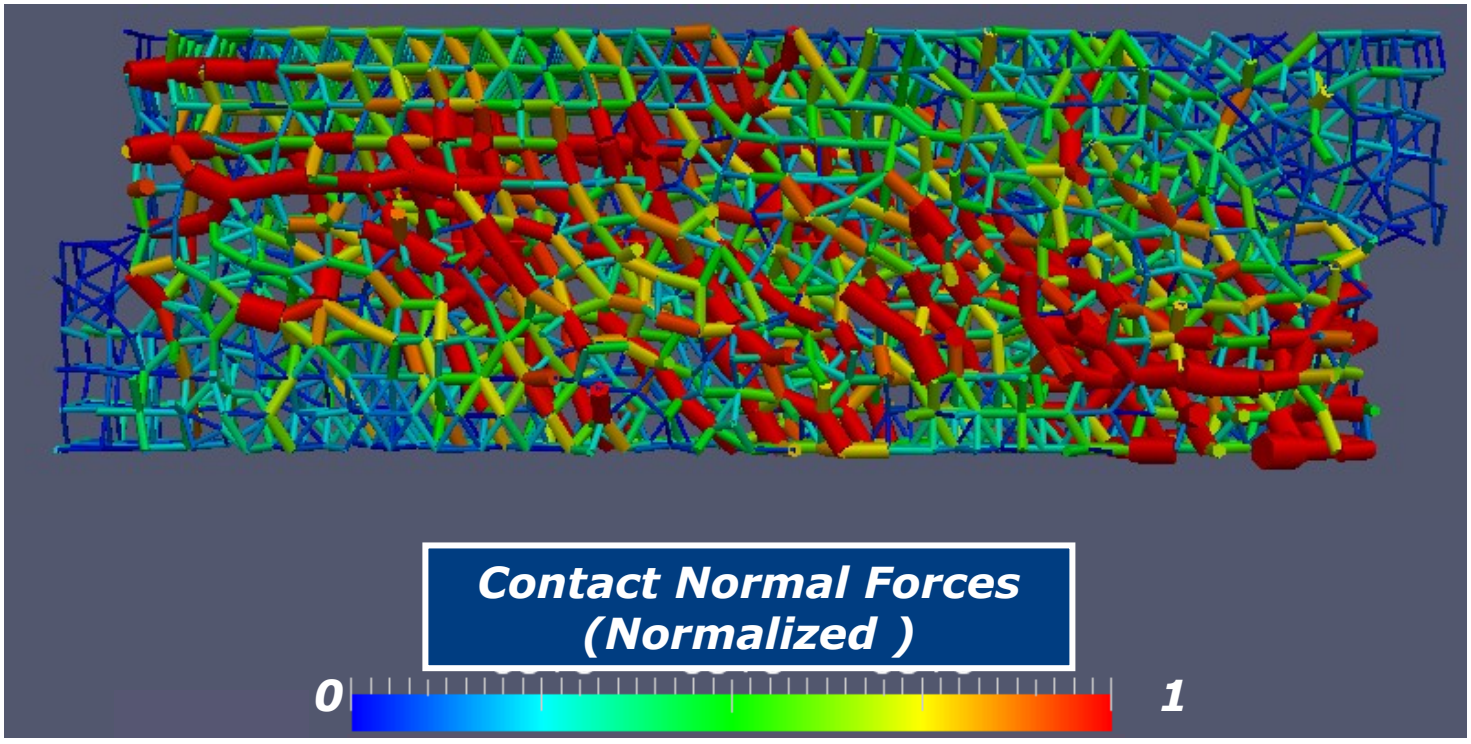
Contact Normal Forces
(Normalized)
0
1

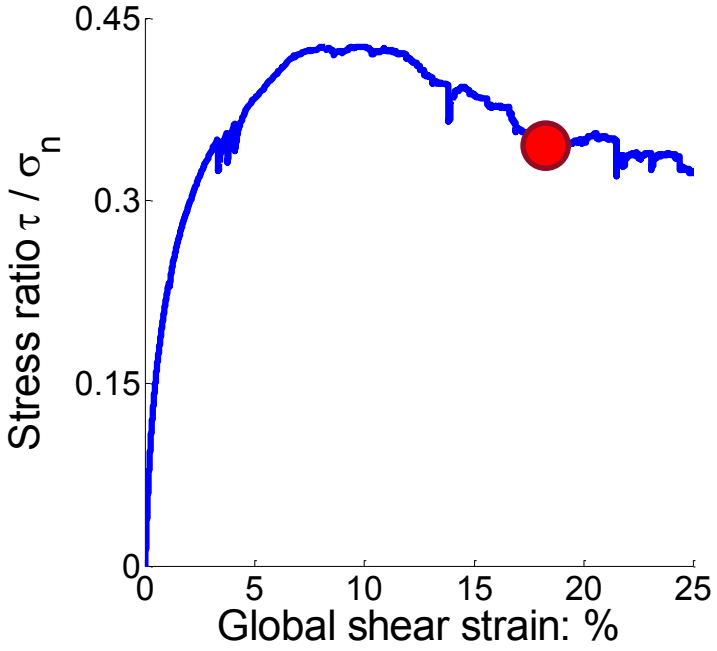
Stress ratio τ / σ_n
0.45
0.3
0.15
0
0
5
10
15
20
25
Global shear strain: %

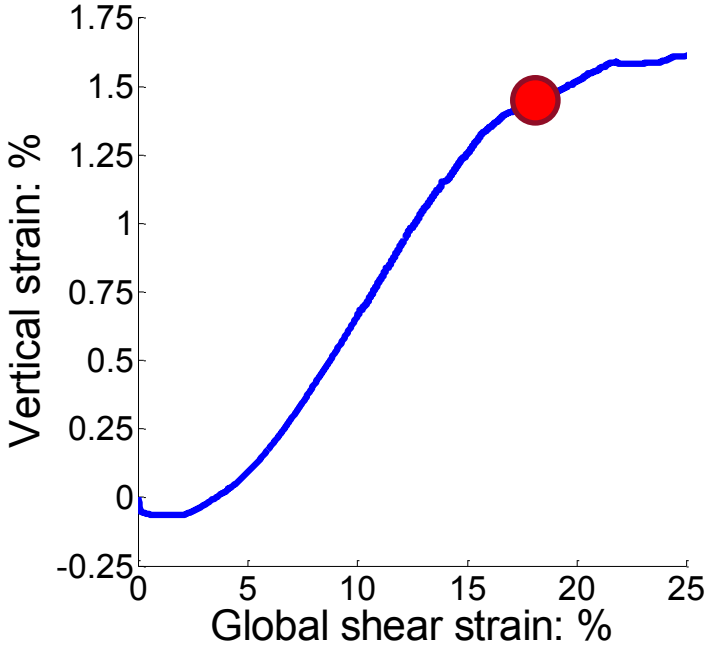
Vertical strain: %
1.75
1.5
1.25
1
0.75
0.5
0.25
0
-0.25
0
5
10
15
20
25
Global shear strain: %

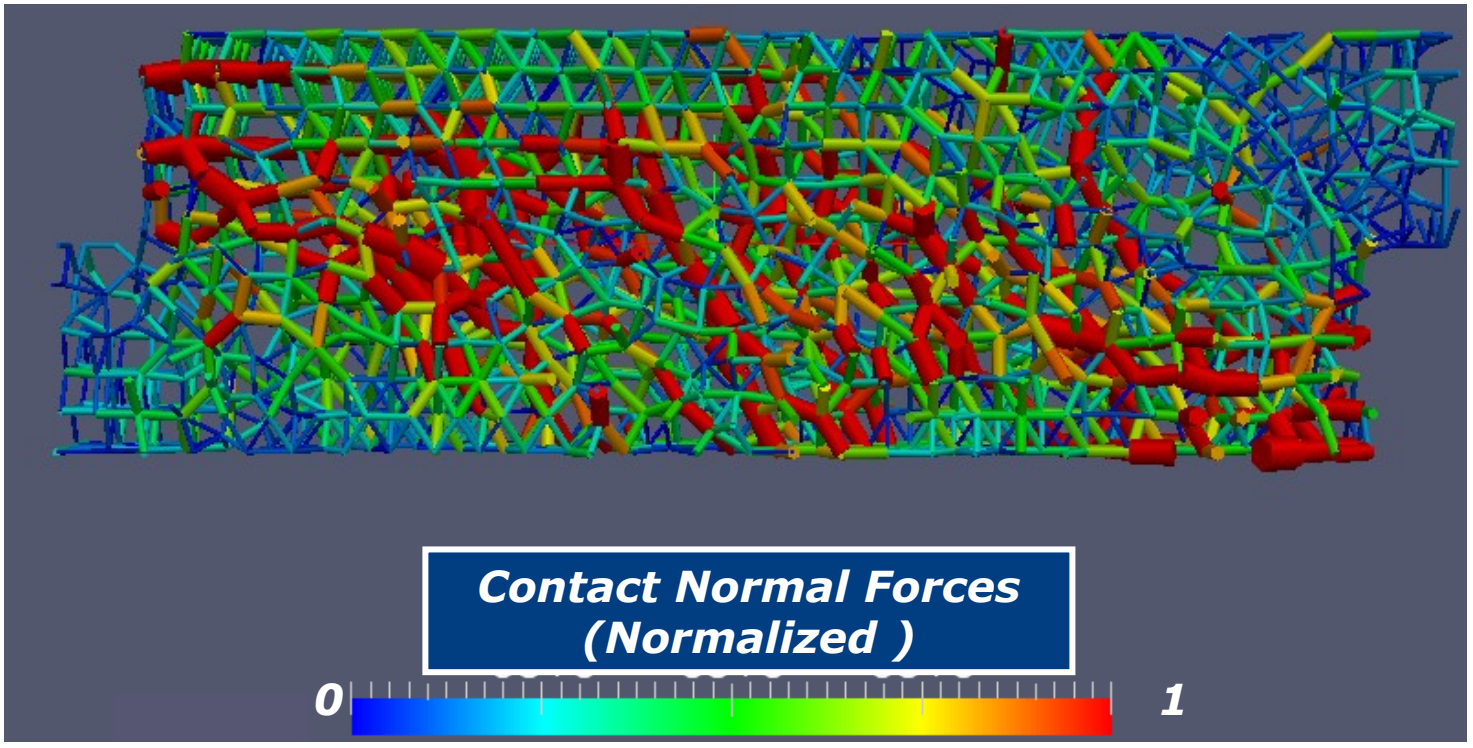
Contact Normal Forces
(Normalized)
0
1

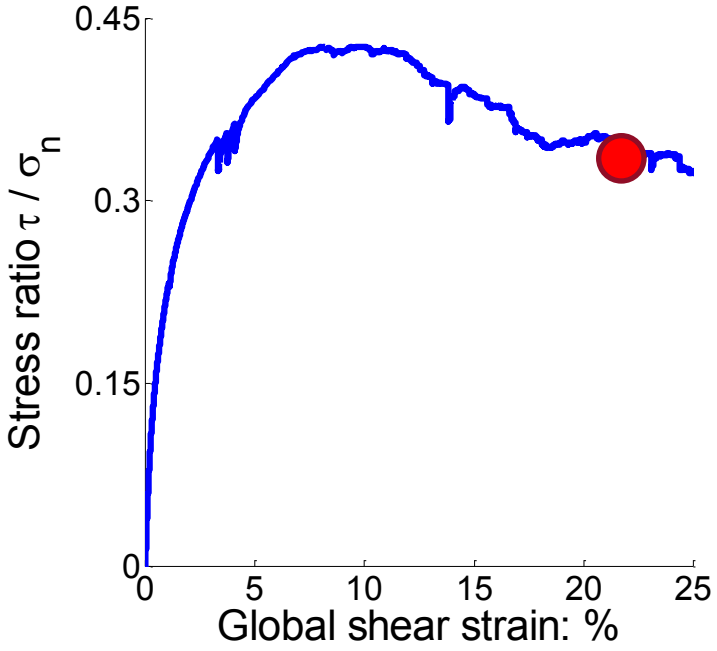
Stress ratio τ / σ_n
0.45
0.3
0.15
0
0
5
10
15
20
25
Global shear strain: %

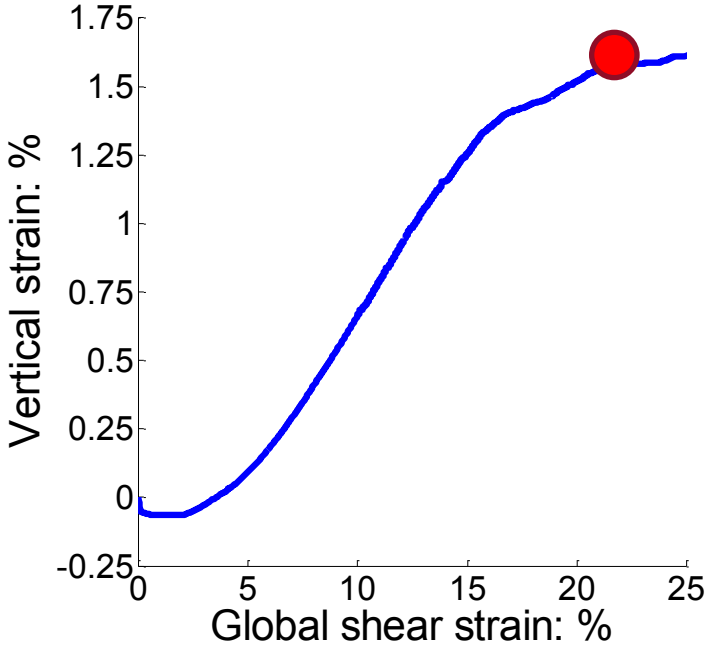
Vertical strain: %
1.75
1.5
1.25
1
0.75
0.5
0.25
0
-0.25
0
5
10
15
20
25
Global shear strain: %

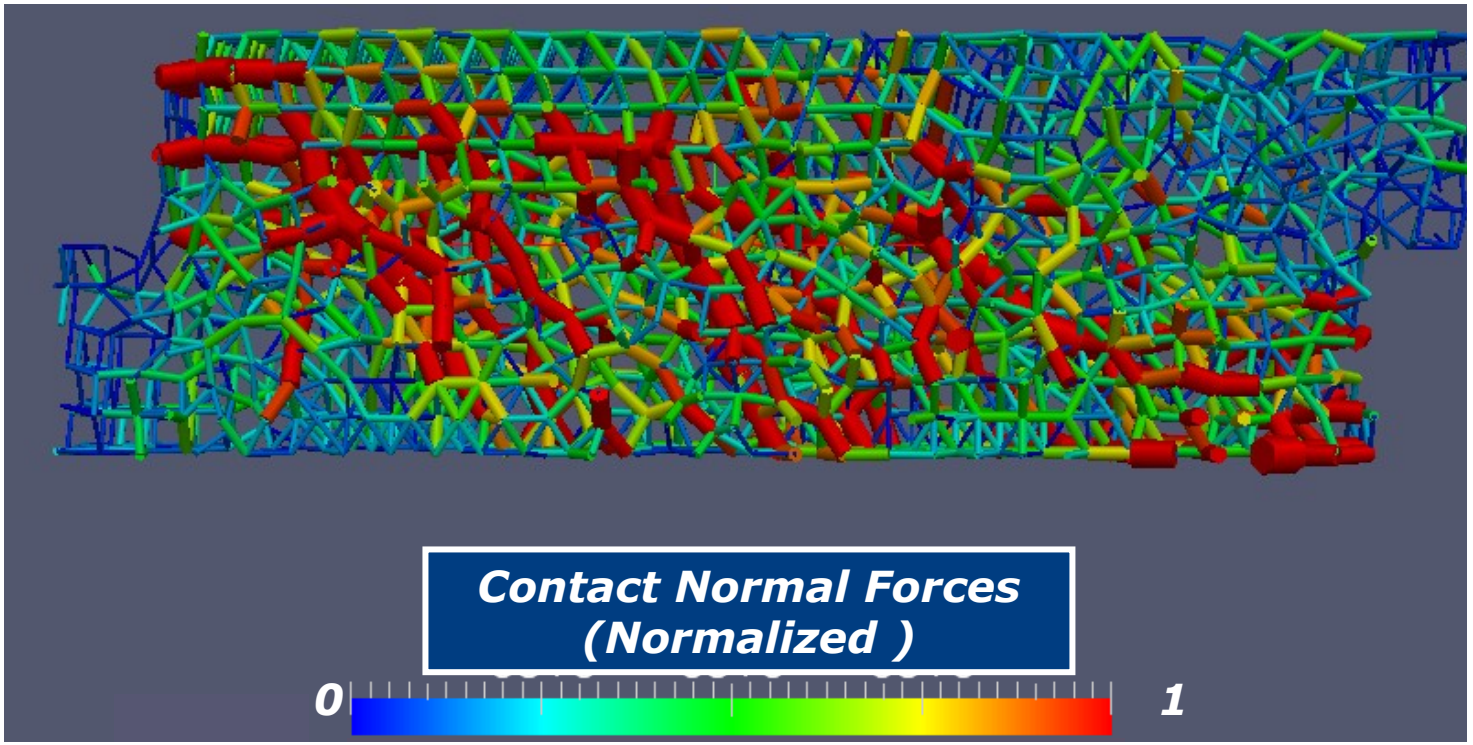
Contact Normal Forces
(Normalized)
0
1

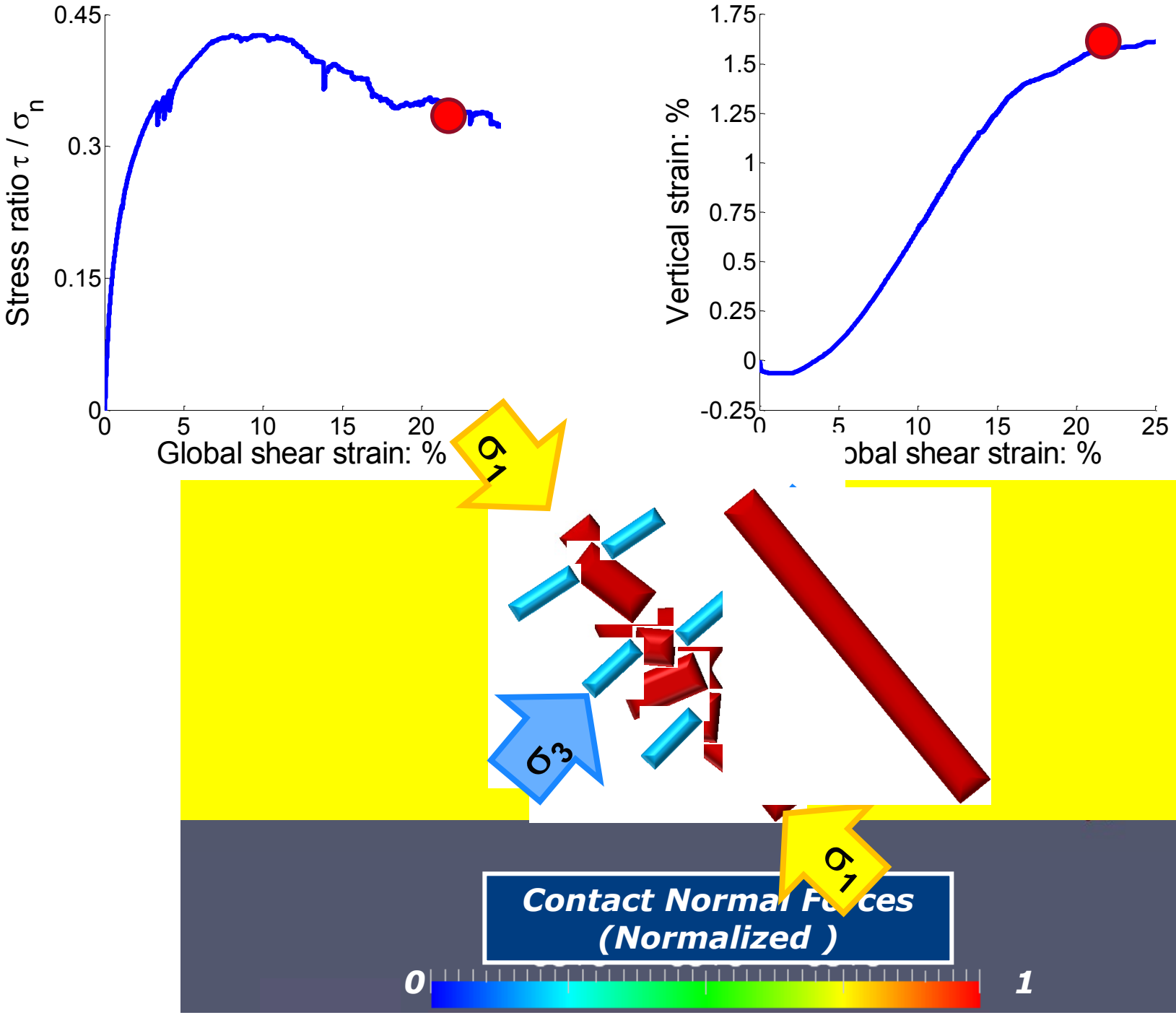
Stress ratio τ / σn
0.45
0.3
0.15
0
0
5
10
15
20
Global shear strain: %
Vertical strain: %
1.75
1.5
1.25
1
0.75
0.5
0.25
0
-0.25
0
5
10
15
20
25
σ1
σ3
σ1
Contact Normal Forces
(Normalized)
0
1

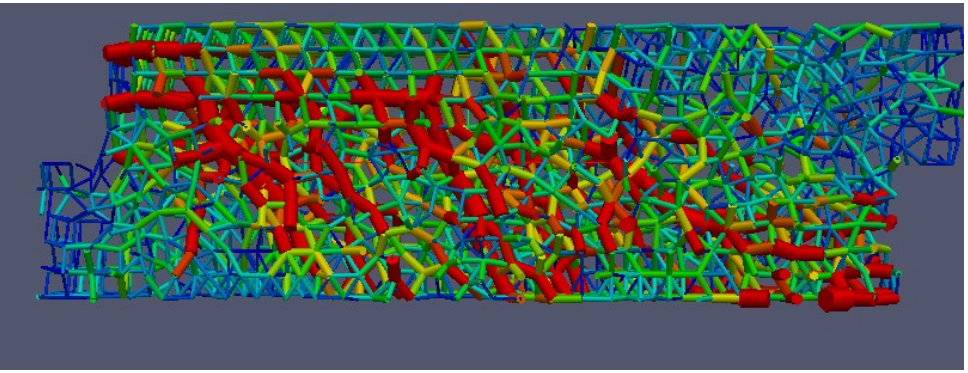

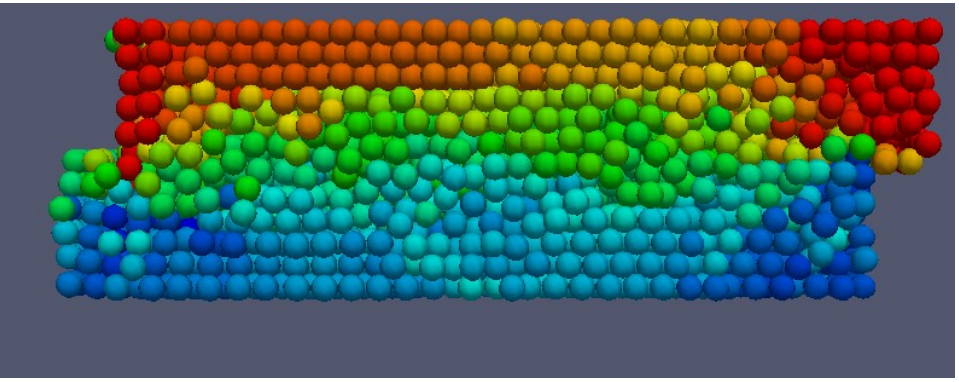

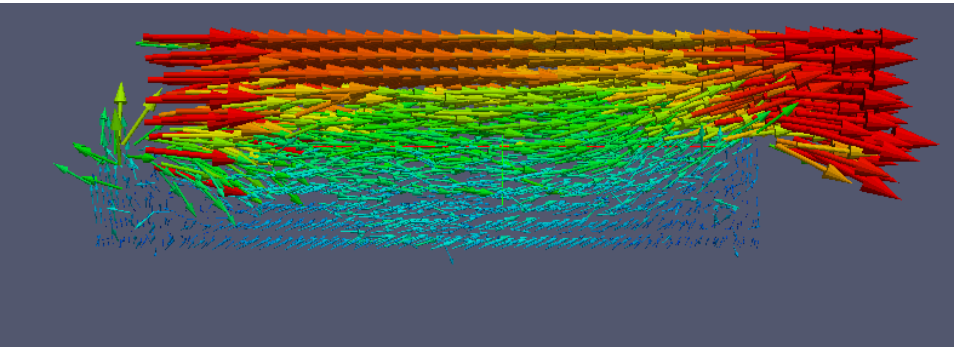

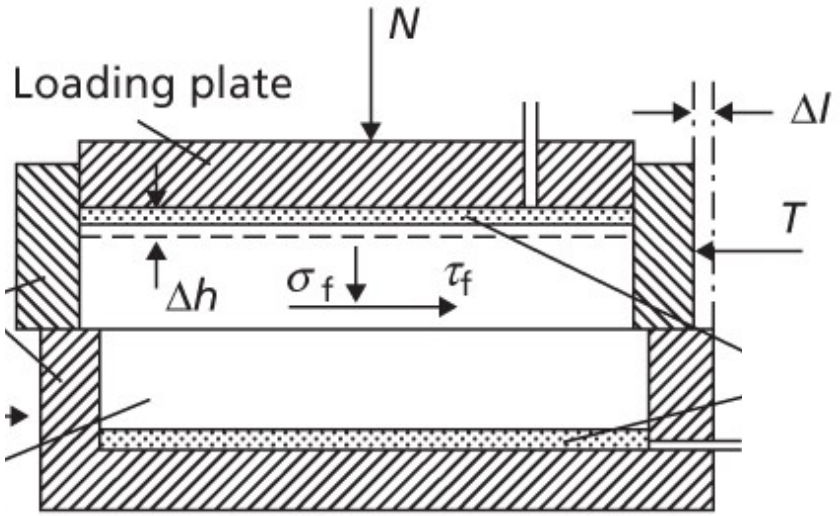

Diagram from
Craig's Soil Mechanics
Knappett and Craig(2012)

Direct Shear Test

- Reasonable correlation with physical test
- DEM gives insight into kinematics and failure mechanisms
- Limited number of particles (11,700)

No. of Particles in Geomechanics DEM Simulations

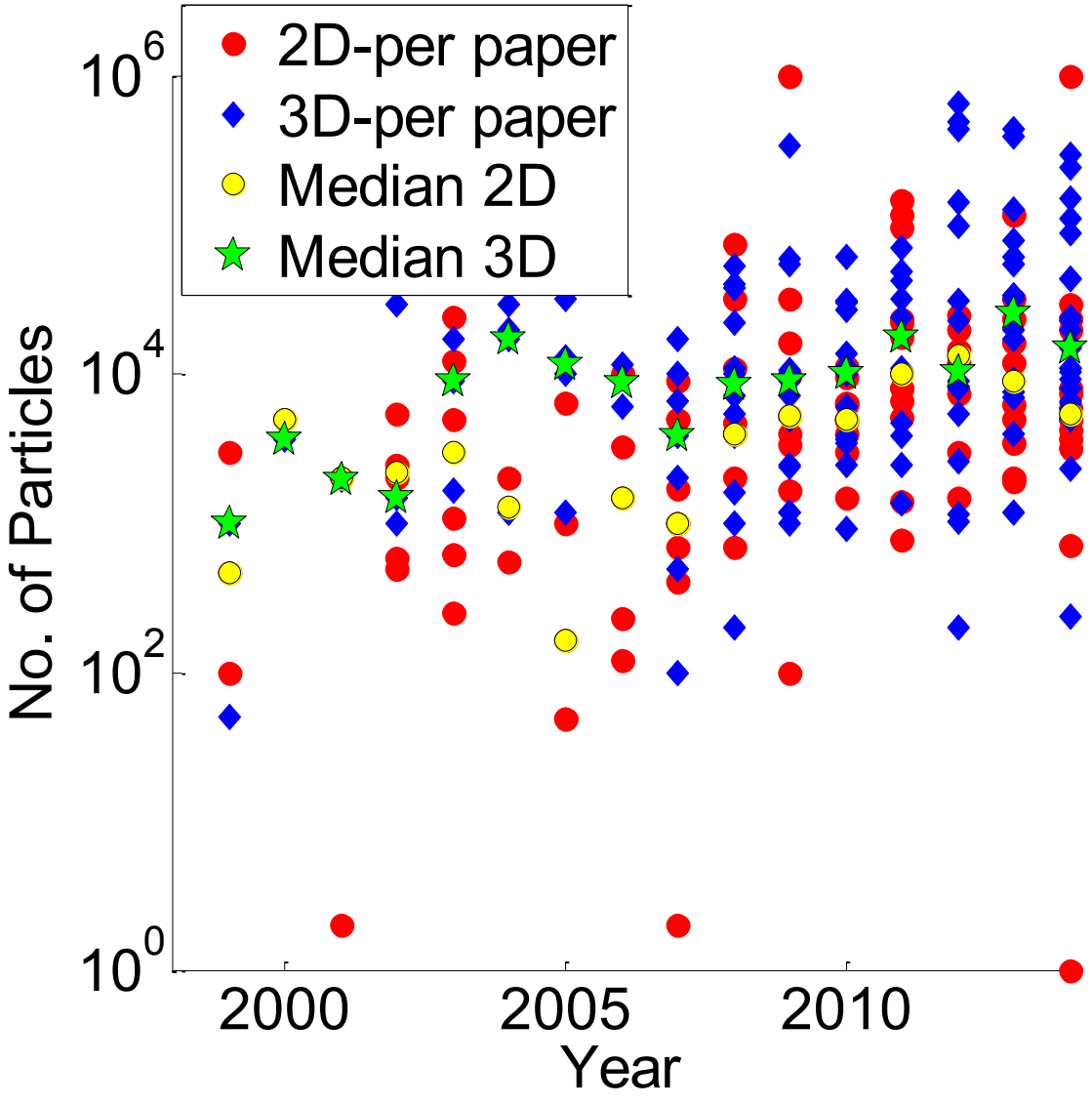

D_{50}=200 micron
>150,000 particles

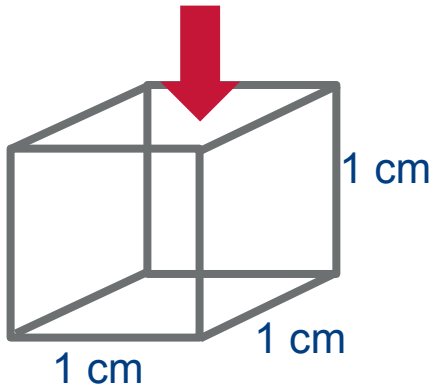

Use of High Performance Computing to Increase Sample Size

- LAMMPS (http://lammps.sandia.gov/)
- Classical molecular dynamics code that can be used for DEM
- Uses spatial decomposition and MPI (message passage interface)
- Can run large high performance computers (hpc) with distributed memory
- Researchers at IC (Marketos, Hanley, Shire, Huang, Otsubo) have been working to modify the granular LAMMPS package

Validation of Granular LAMMPS

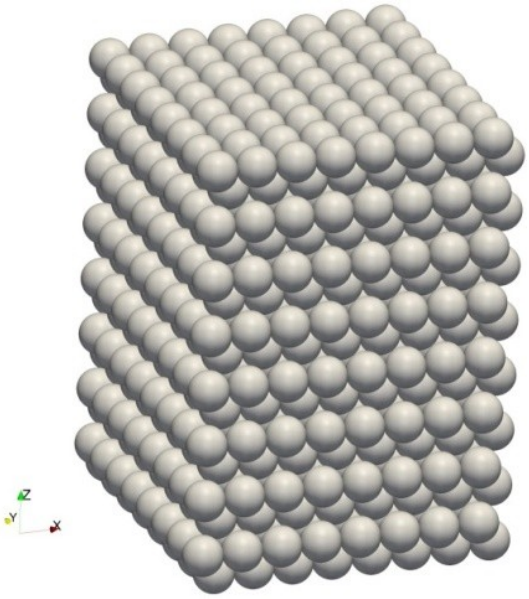

Compression of face-centred-cubic array of spheres.

Analytical solution documented in *Thornton (1979) Géotechnique*

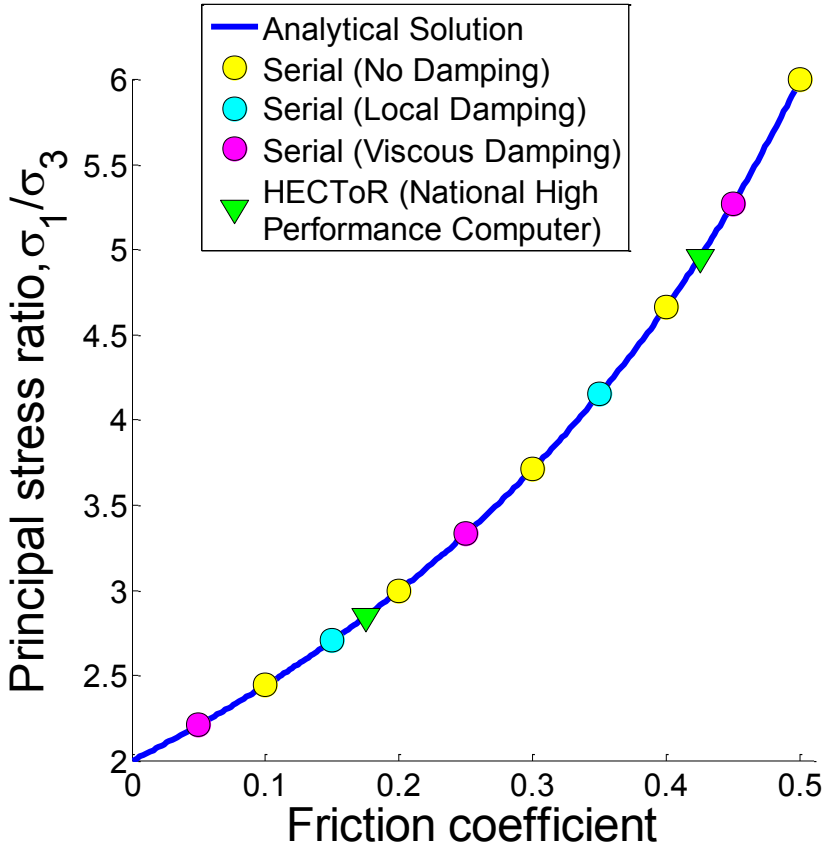

Validations by
K. Hanley and X. Huang

A State Parameter for Sands: ψ

Critical state is a state where the soil deforms at constant stress and constant void ratio

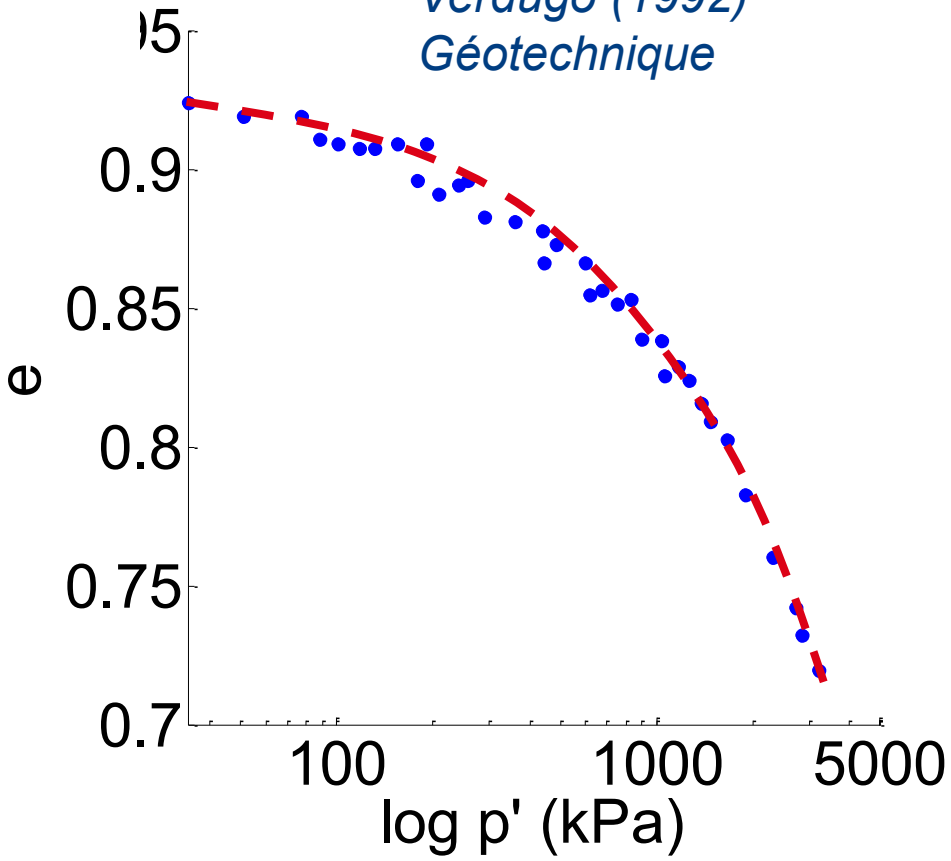

Been and Jefferies (1985)
Géotechnique

A State Parameter for Sands: ψ

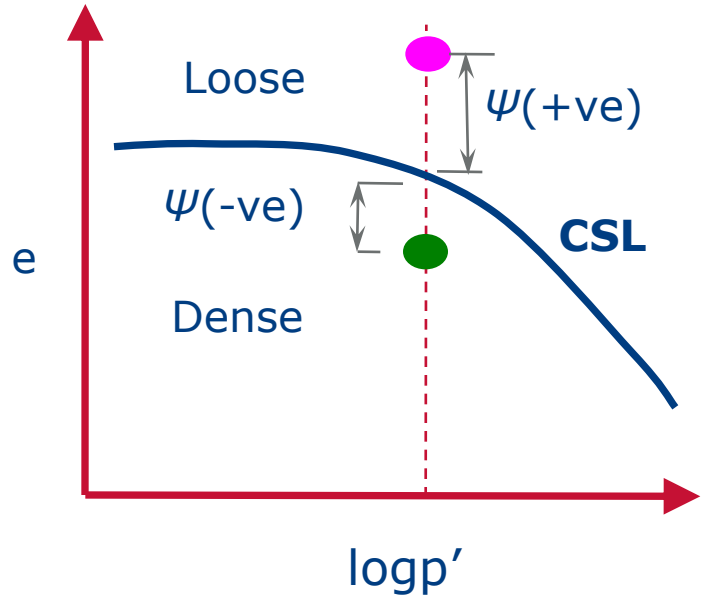

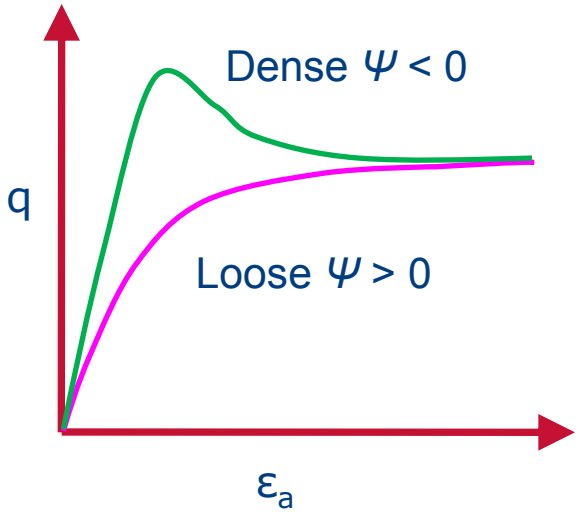

e void ratio
q deviatoric stress
p' mean effective stress

$q = \sigma'_1 - \sigma'_3$

$p' = {}^1/_3(\sigma'_1 + 2\sigma'_3)$

(triaxial case)

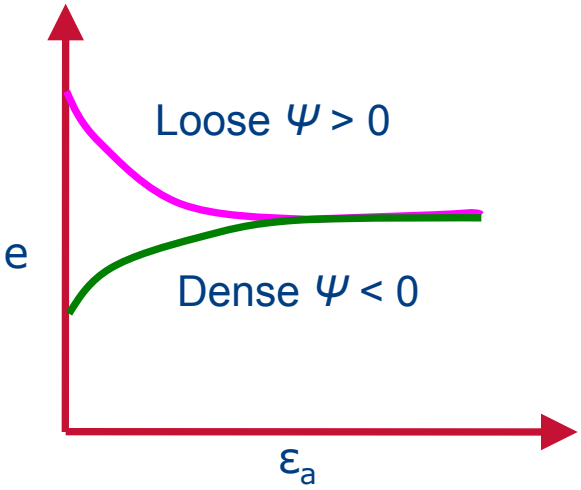

Been and Jefferies (1985)
Géotechnique

Variation in Φ'_p with ψ_0

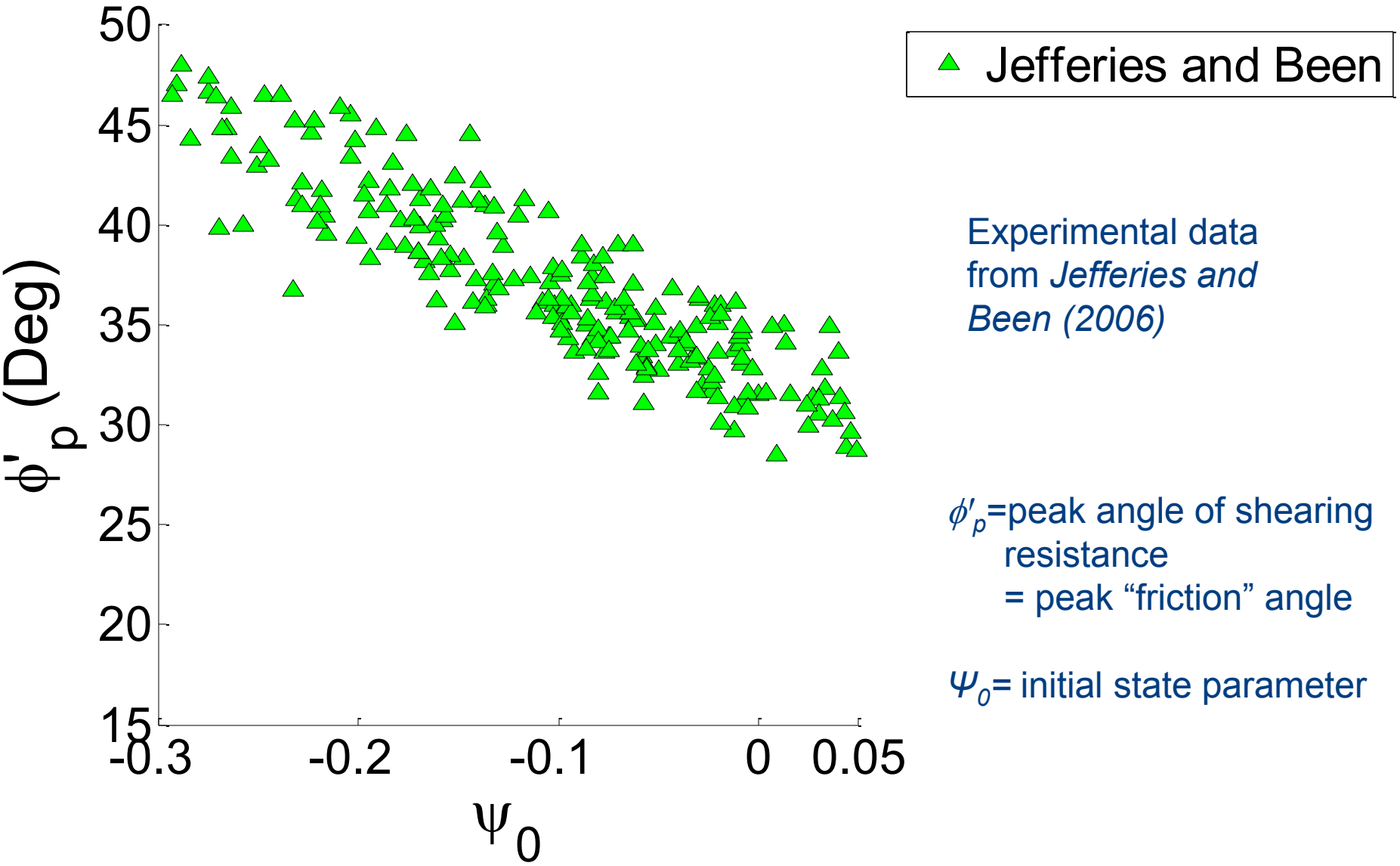

Experimental data from *Jefferies and Been (2006)*

ϕ'_p=peak angle of shearing resistance
= peak "friction" angle

Ψ_0= initial state parameter

Variation in Φ'_p with ψ_0

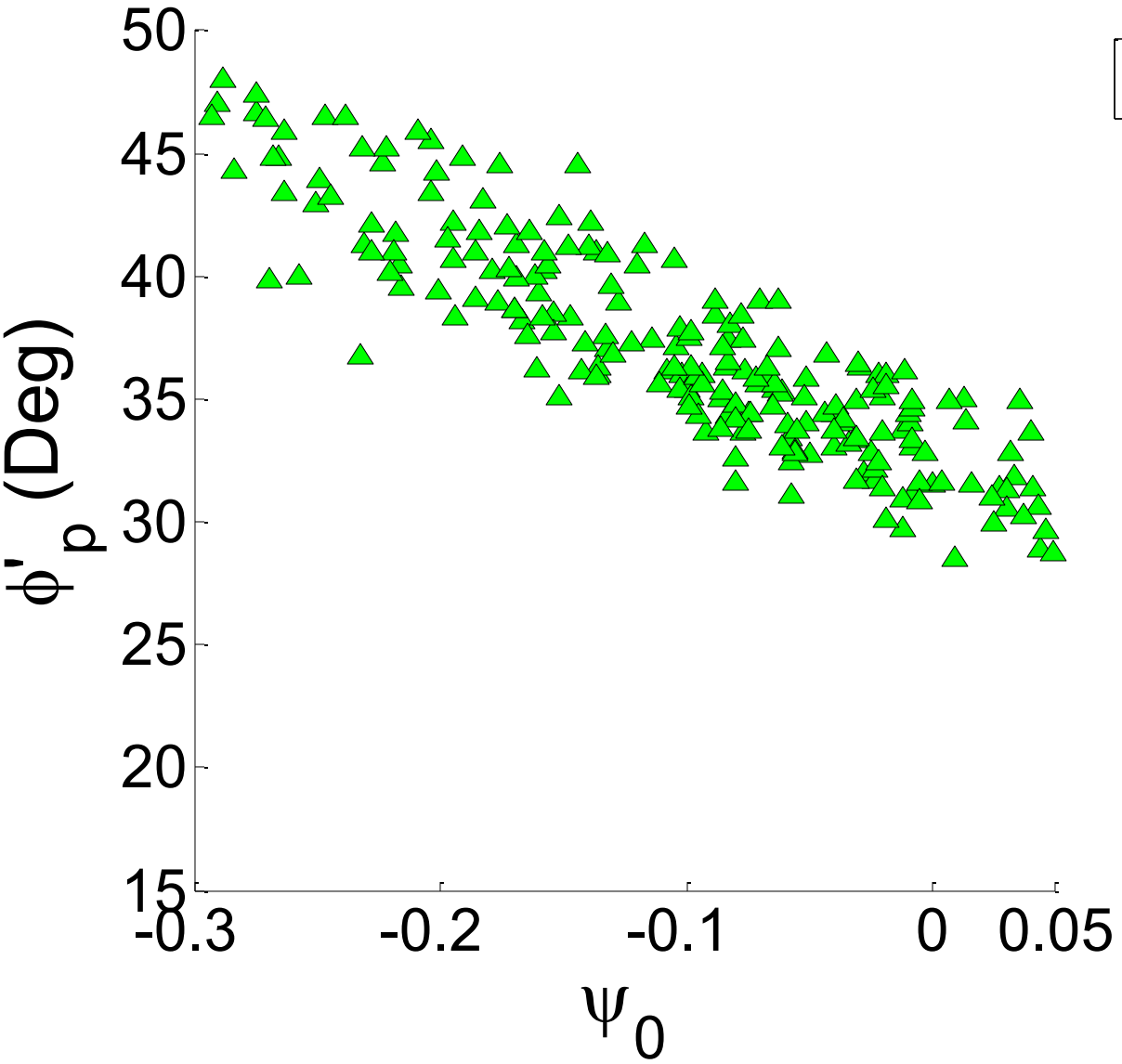

Triaxial cell at IC

In Situ Stresses

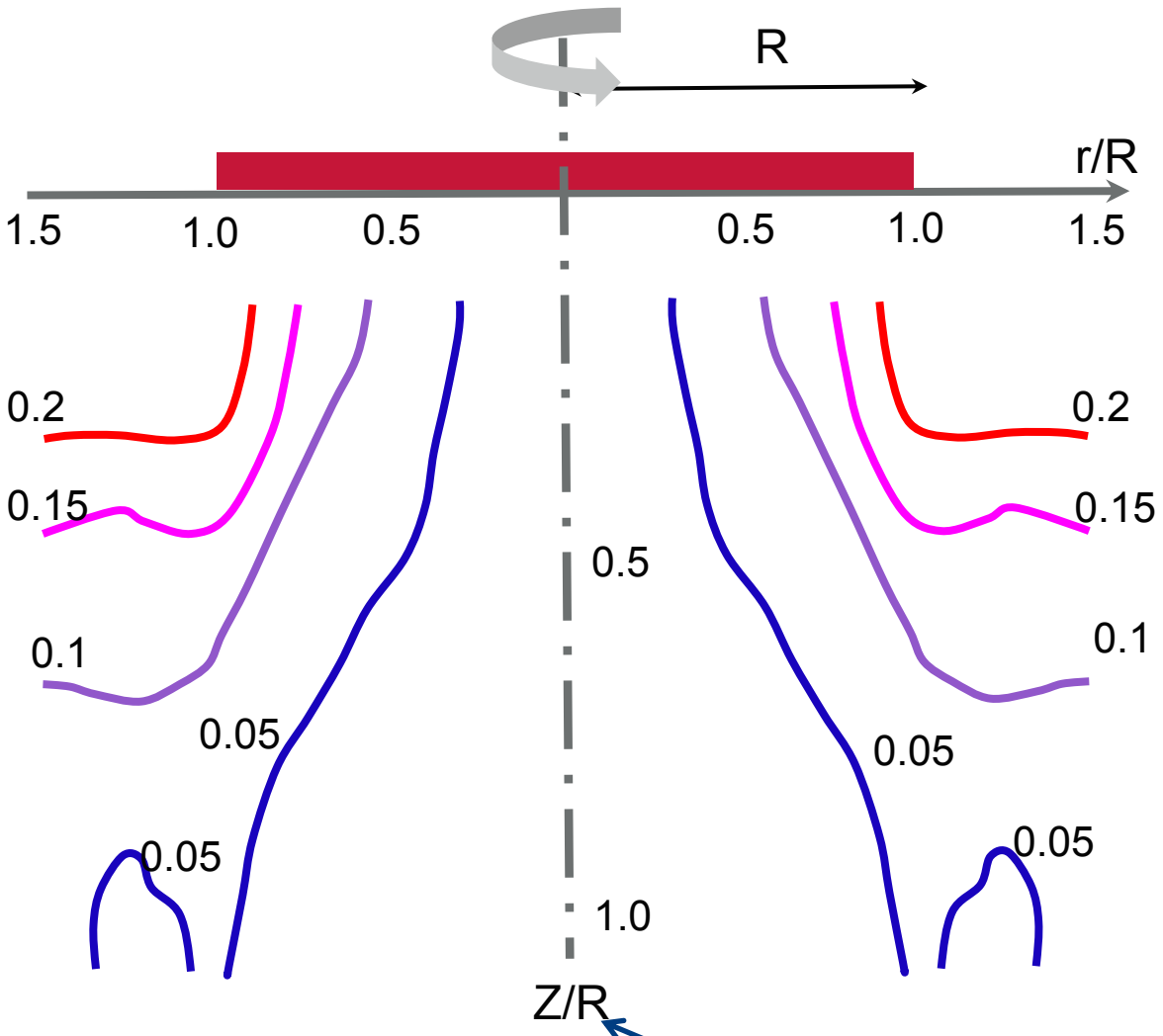

Hight (1983)

Stress increments beneath a circular footing on isotropic, linear elastic foundation

Contours of

$$\frac{\Delta\sigma'_2 - \Delta\sigma'_3}{\Delta\sigma'_1 - \Delta\sigma'_3}$$

σ'_1=major principal stress
σ'_2=intermediate principal stress
σ'_3=minor principal stress

$\sigma'_1 > \sigma'_2 > \sigma'_3$

Along CL:

- $\Delta\sigma'_2 = \Delta\sigma'_3$
- Triaxial conditions

Variation in Soil Strength with Principal Stress Ratio

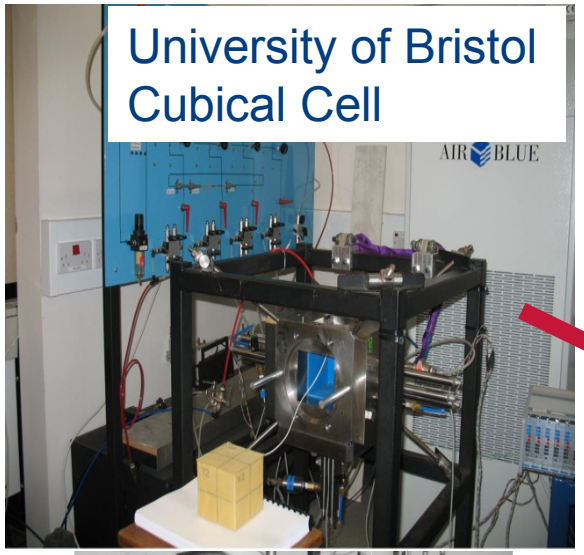

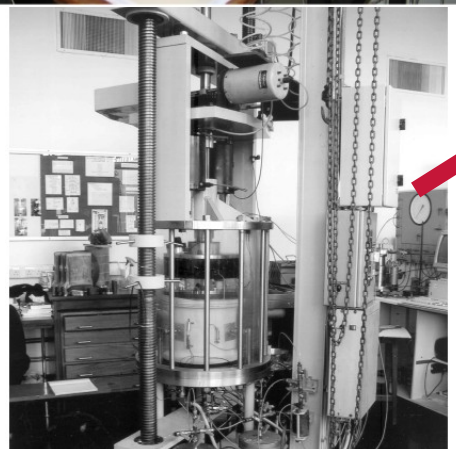

Large Hollow Cylinder Apparatus at IC

Can control *b*

b= intermediate stress ratio

$$b = \frac{\sigma'_2 - \sigma'_3}{\sigma'_1 - \sigma'_3}$$

- *b*=0:Triaxial compression
- *b*=1:Triaxial extension
- *b*≈0.5: Plane strain

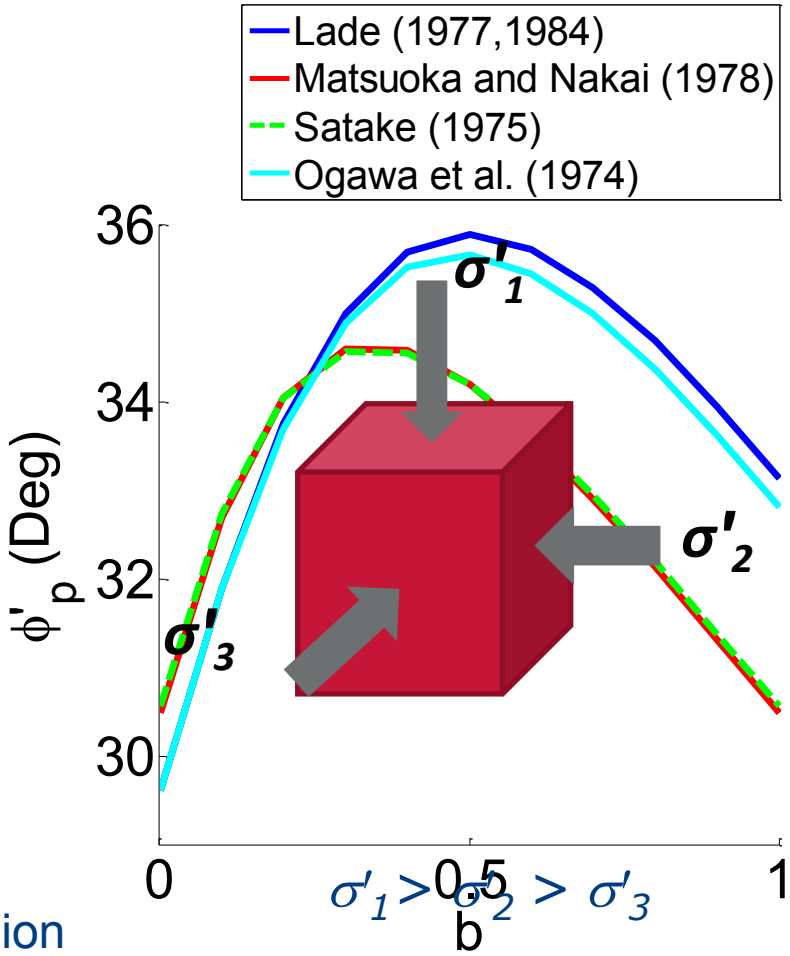

ϕ'_p= peak angle of shearing resistance
= peak "friction" angle

O'Sullivan et al. (2015) Géotechnique

DEM Analysis of ψ for a 3D Stress State

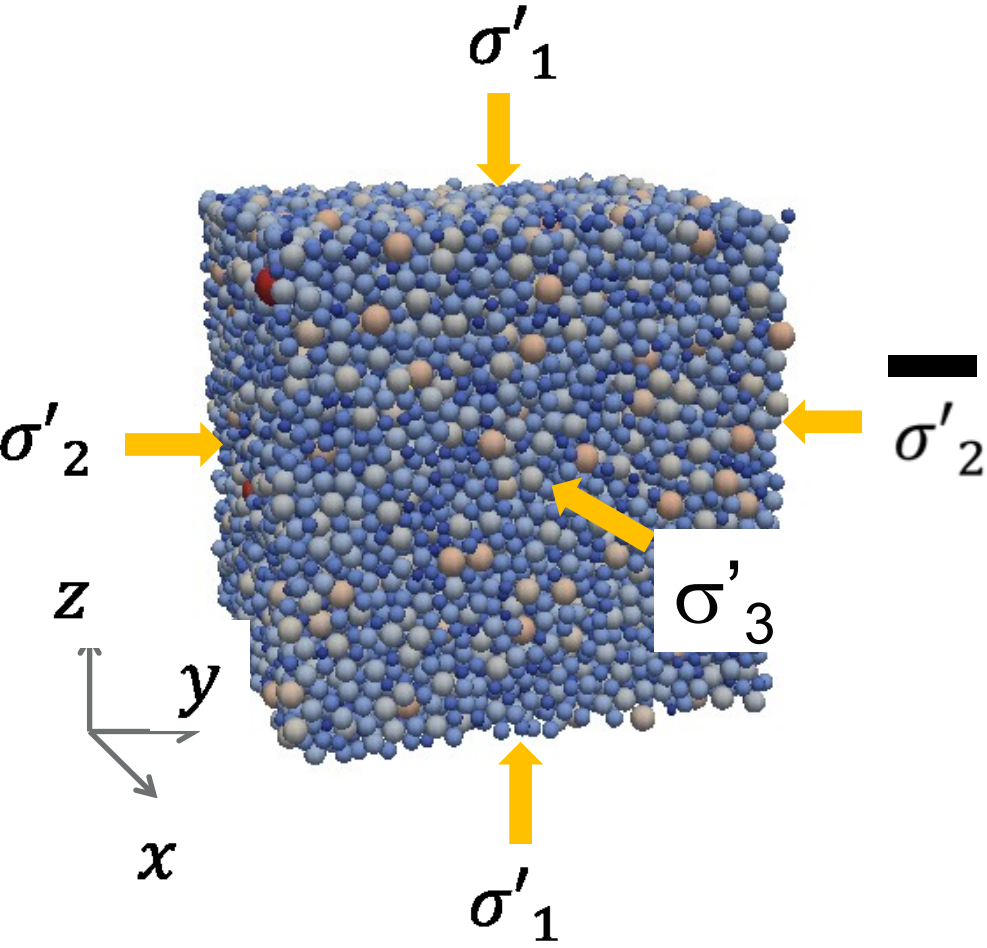

- 20,164 spherical particles
- Periodic boundaries
- Grading similar to Toyoura sand
- Friction coefficient μ=0.25
- Controlled *b*
- Deformed to large strain
- Varied initial state parameter (ψ_0)
- Most of simulations used LAMMPS

Huang et al. (2014)
Géotechnique

Variation in Peak and Critical State Friction Angles with *b*

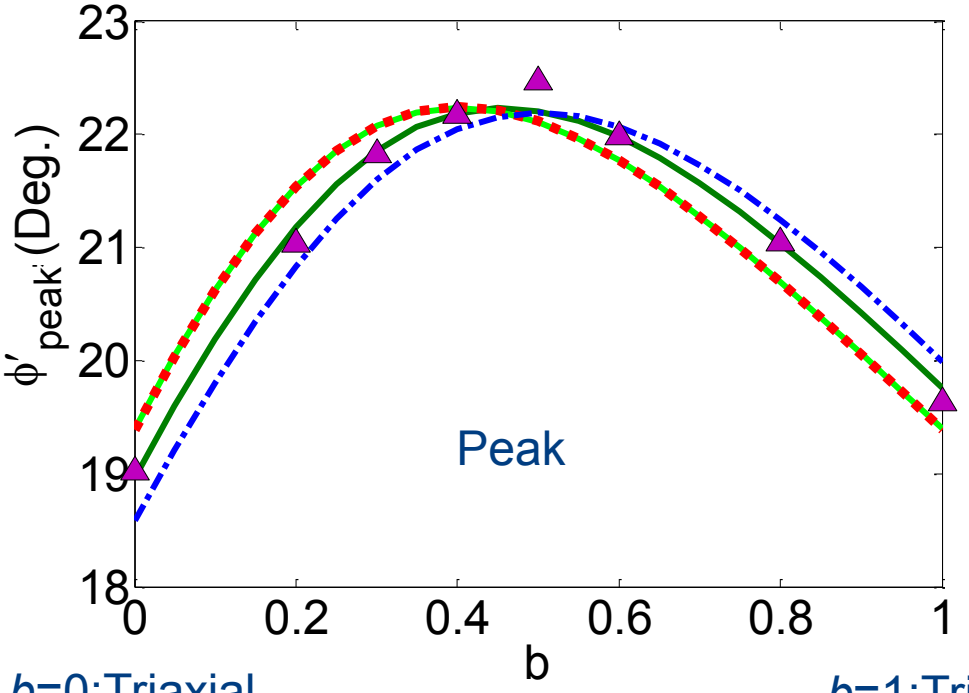

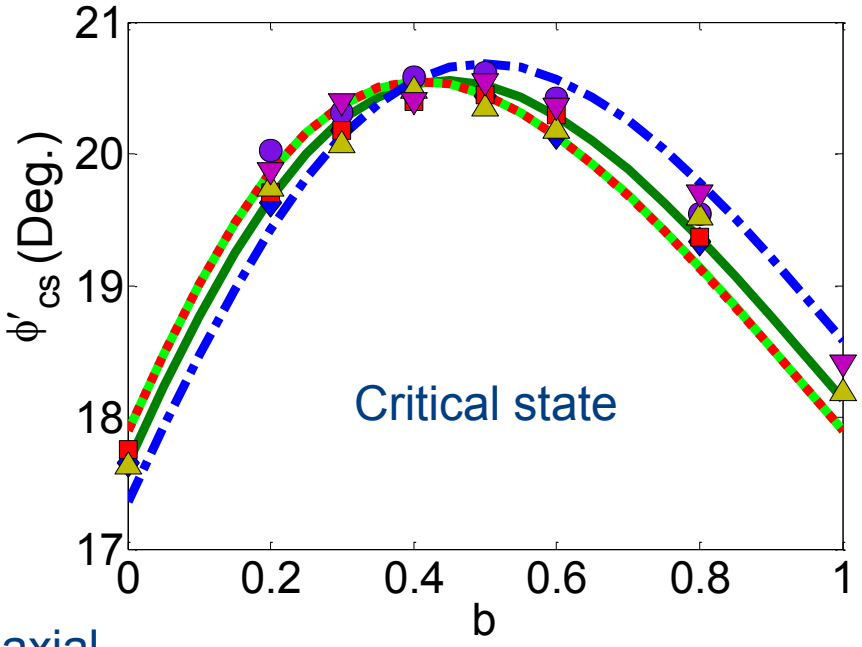

b=0:Triaxial Compression

b=1:Triaxial Extension

Ogawa
Satake
Matsuoka-Nakai
Lade
e_0=0.646, σ'_3=500 kPa

$$b = \frac{\sigma'_2 - \sigma'_3}{\sigma'_1 - \sigma'_3}$$

Huang et al. (2014) Granular Matter

e_o=0.533, σ'_3=100 kPa
e_0=0.612, σ'_3=5000 kPa
e_0=0.625, σ'_3=2000 kPa
e_0=0.625, σ'_3=1000 kPa
e_0=0.646, σ'_3=500 kPa

DEM Analysis of ψ for a 3D Stress State

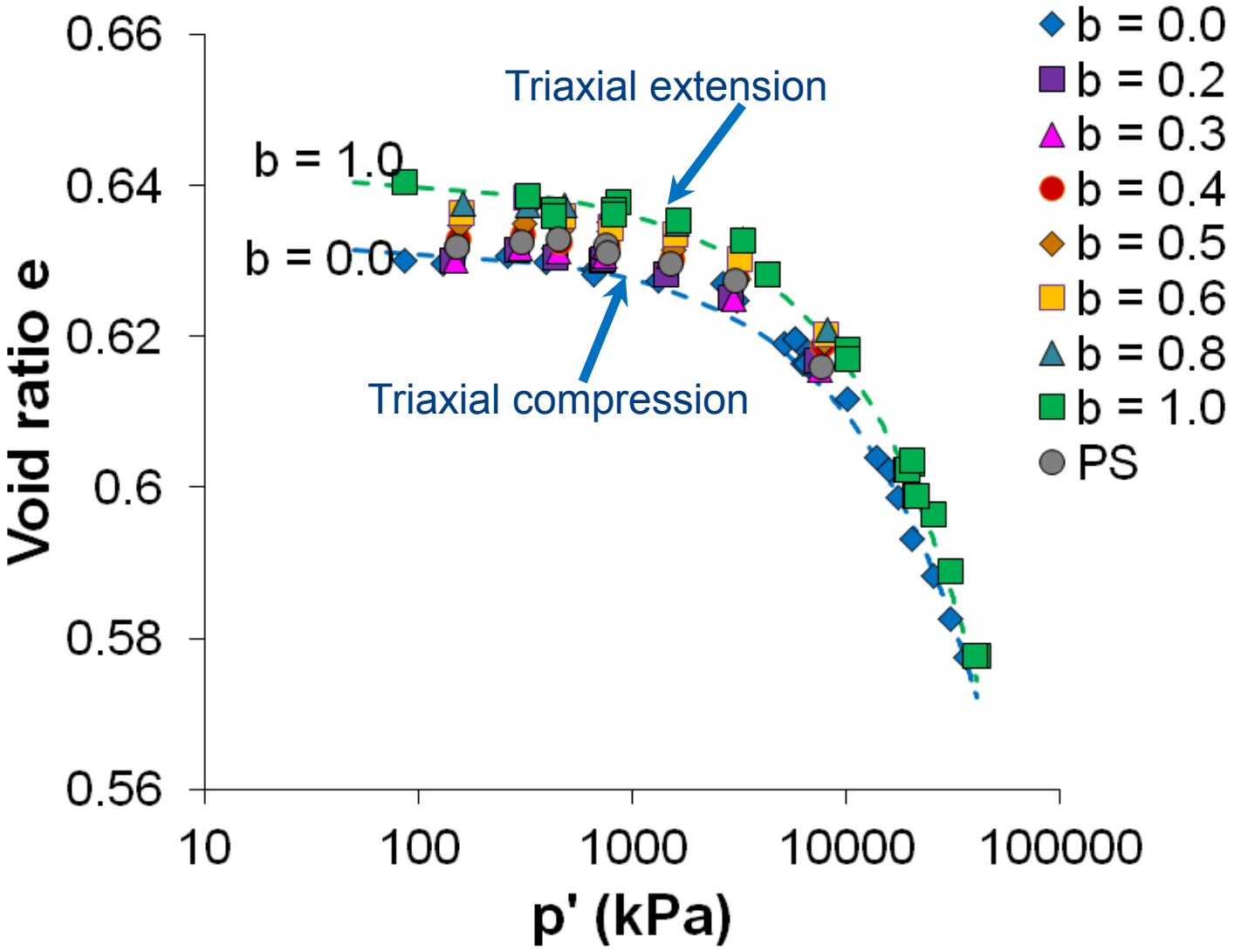

State Dependent Response

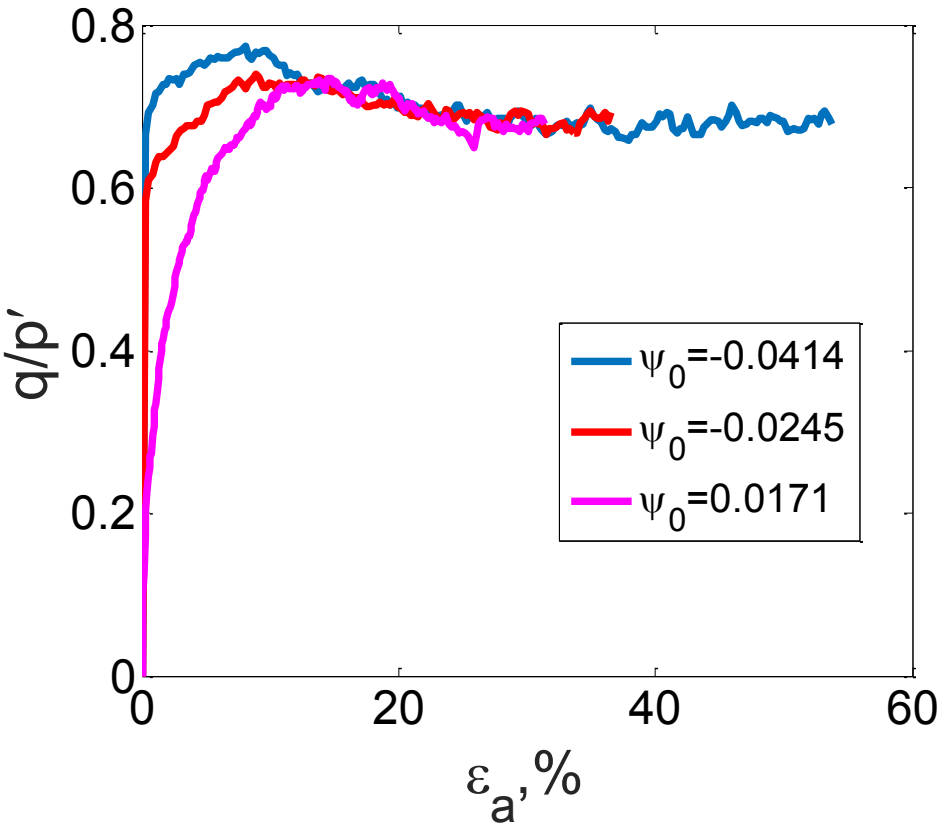

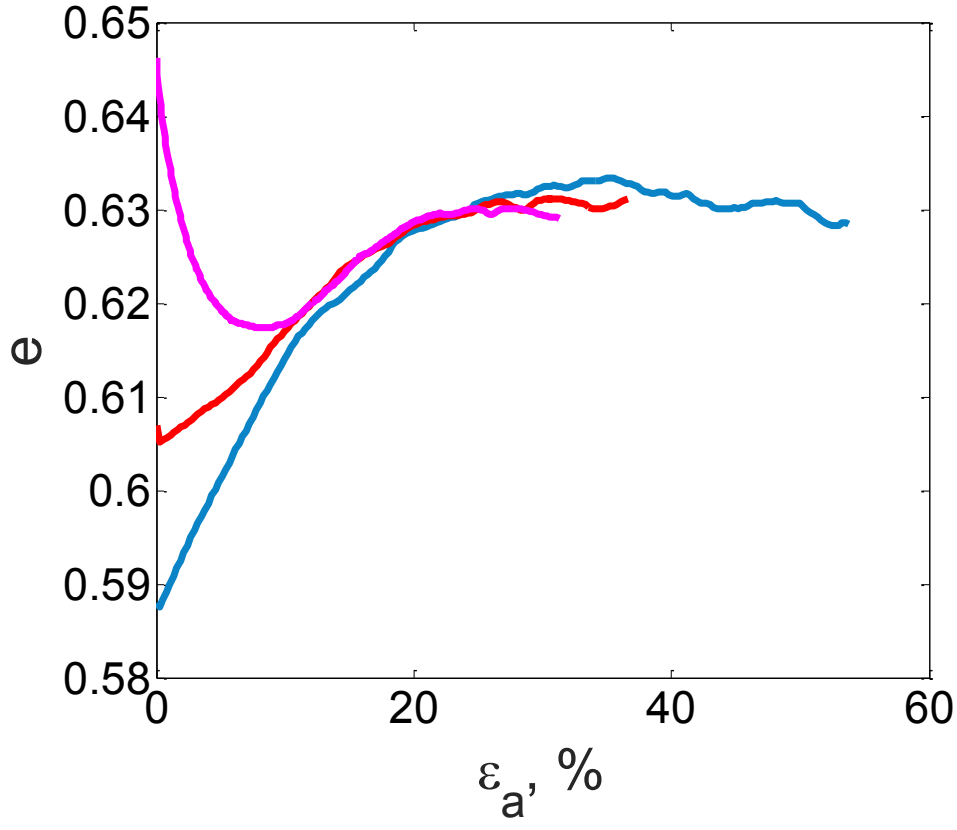

$\Psi > 0$ loose

$\Psi < 0$ dense

$q=\sigma'_1-\sigma'_3$

$p'=1/3(\sigma'_1+2\sigma'_3)$

(triaxial)

σ'_3=500kPa

Huang et al. (2014) Géotechnique

Variation in Φ'_p with ψ_0

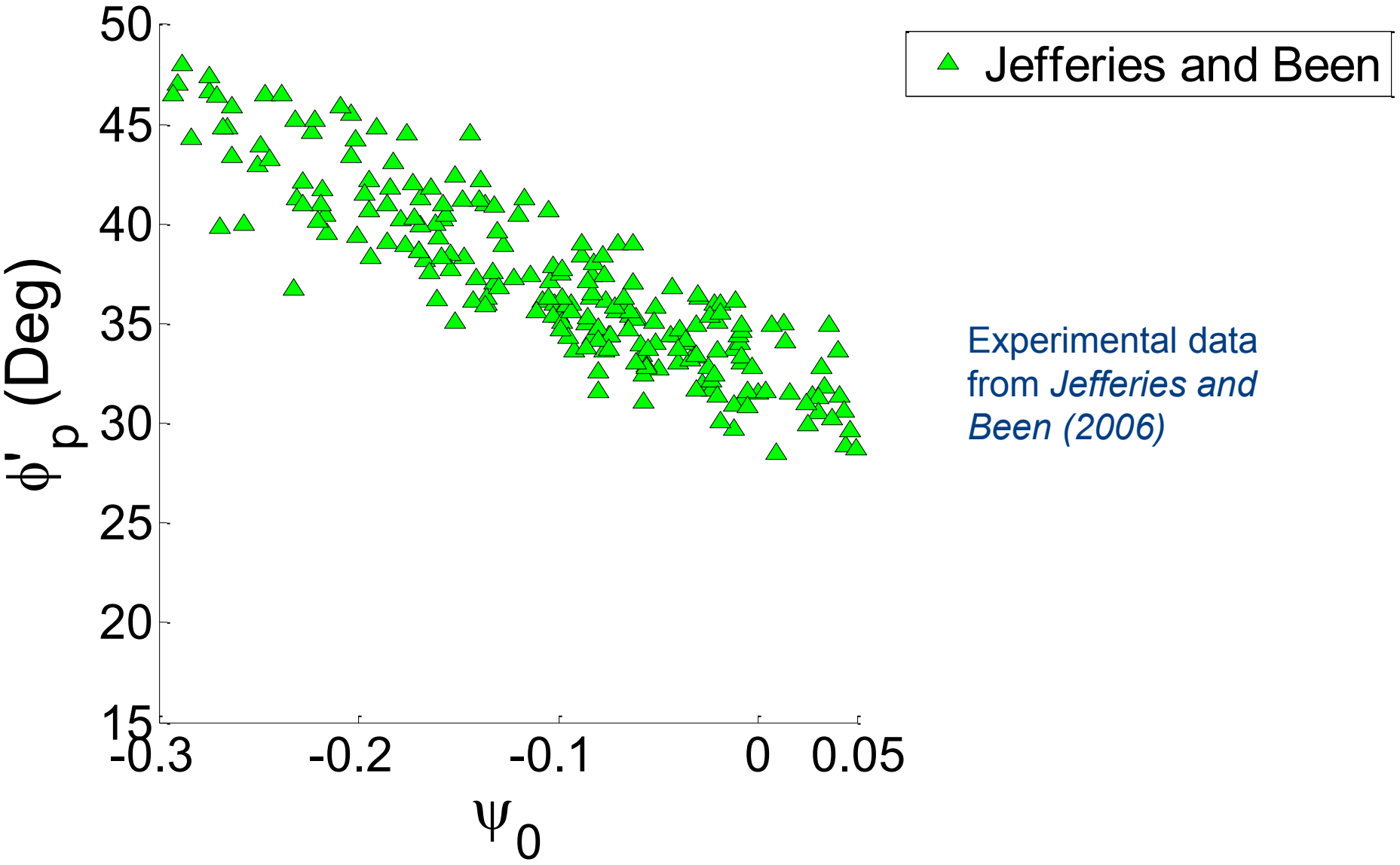

Experimental data from *Jefferies and Been (2006)*

Variation in Φ'_p with ψ_0

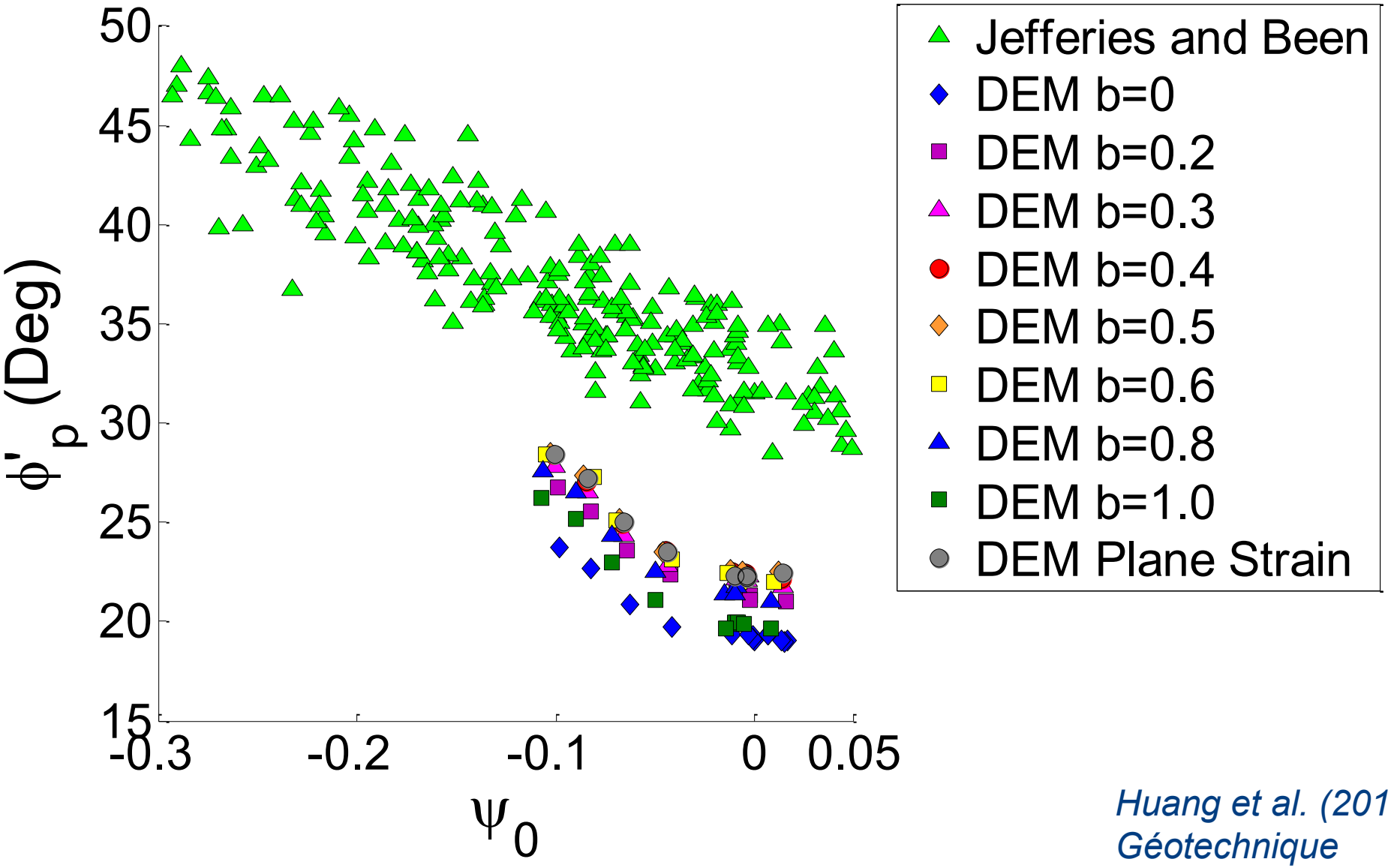

Huang et al. (2014)
Géotechnique

Variation in $\Phi'_p - \Phi'_{cs}$ with ψ_0

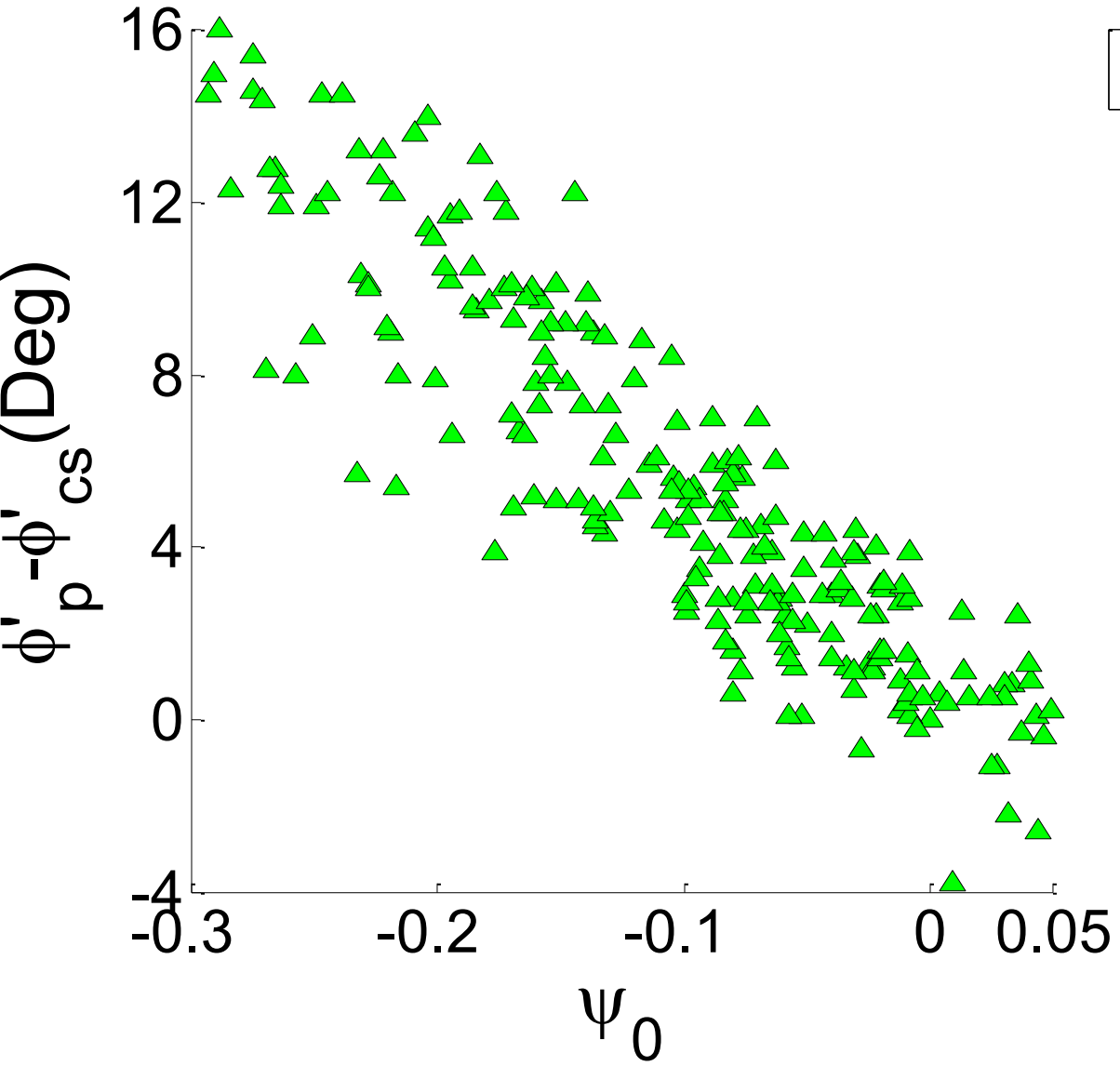

Experimental data from *Jefferies and Been (2006)*

Variation in $\Phi'_p - \Phi'_{cs}$ with ψ_0

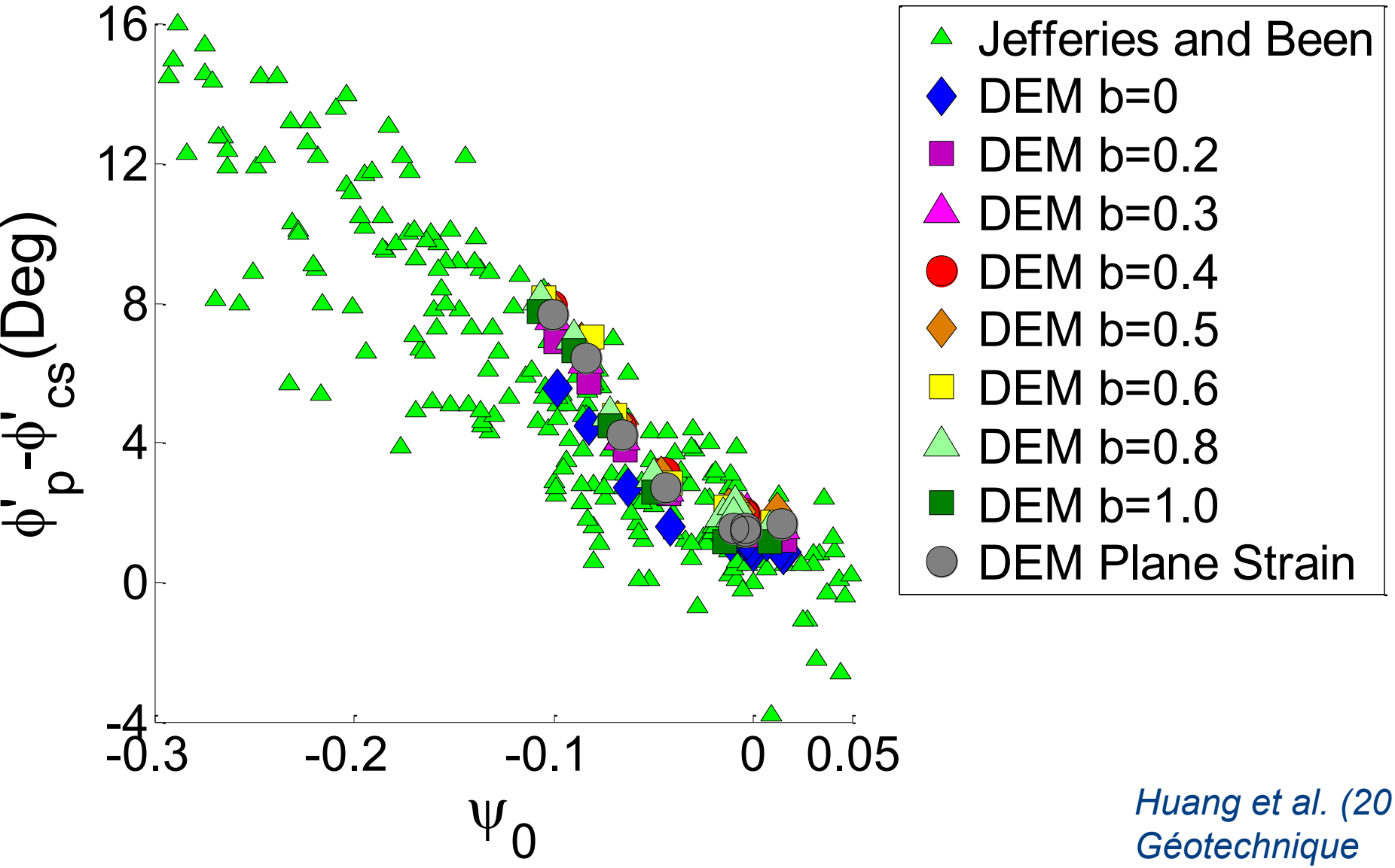

Huang et al. (2014) Géotechnique

Variation in D_p with ψ_0

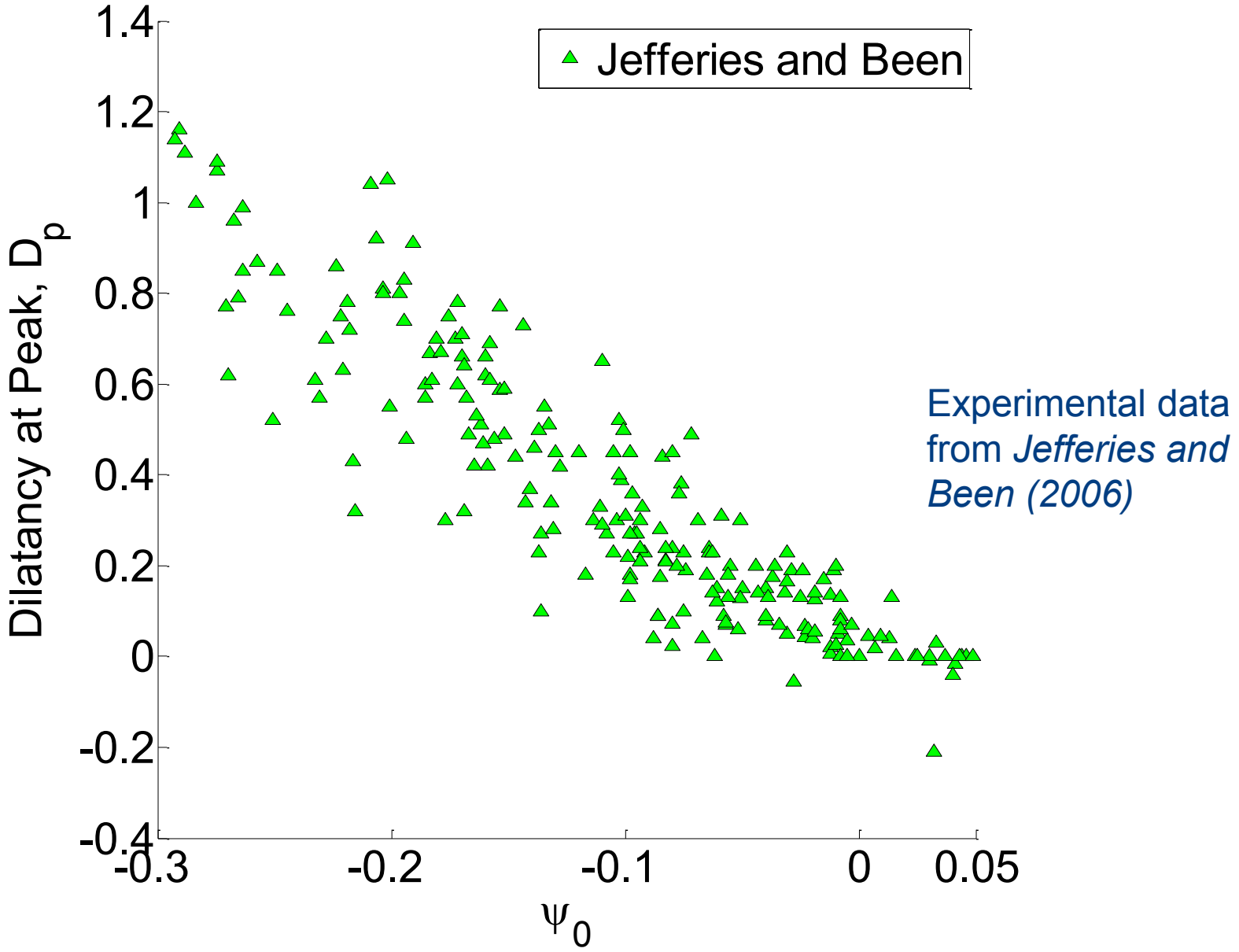

Experimental data from *Jefferies and Been (2006)*

Variation in D_p with ψ_0

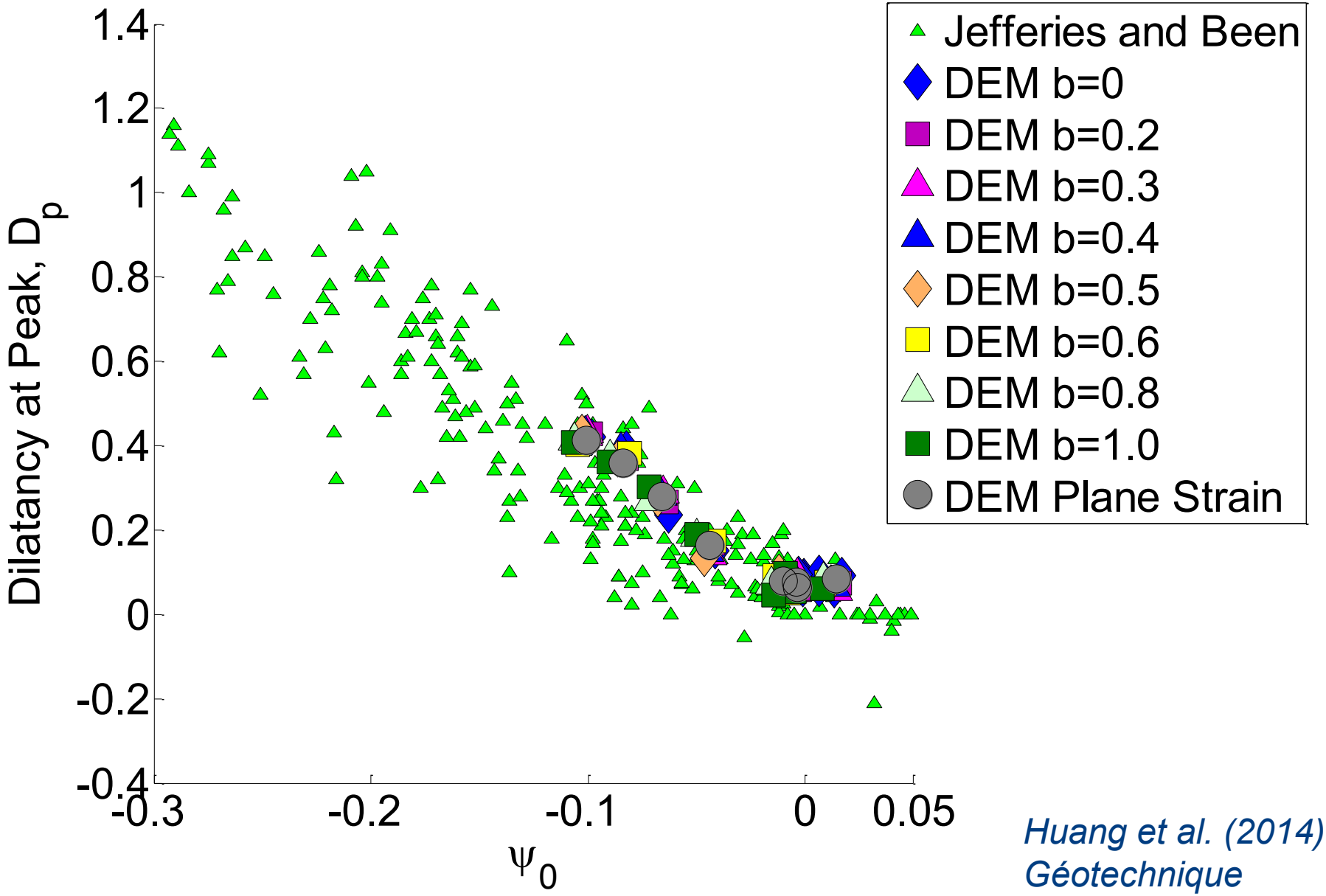

Huang et al. (2014) Géotechnique

Huang et al. (2014)
Géotechnique

Performance of Norsand Model

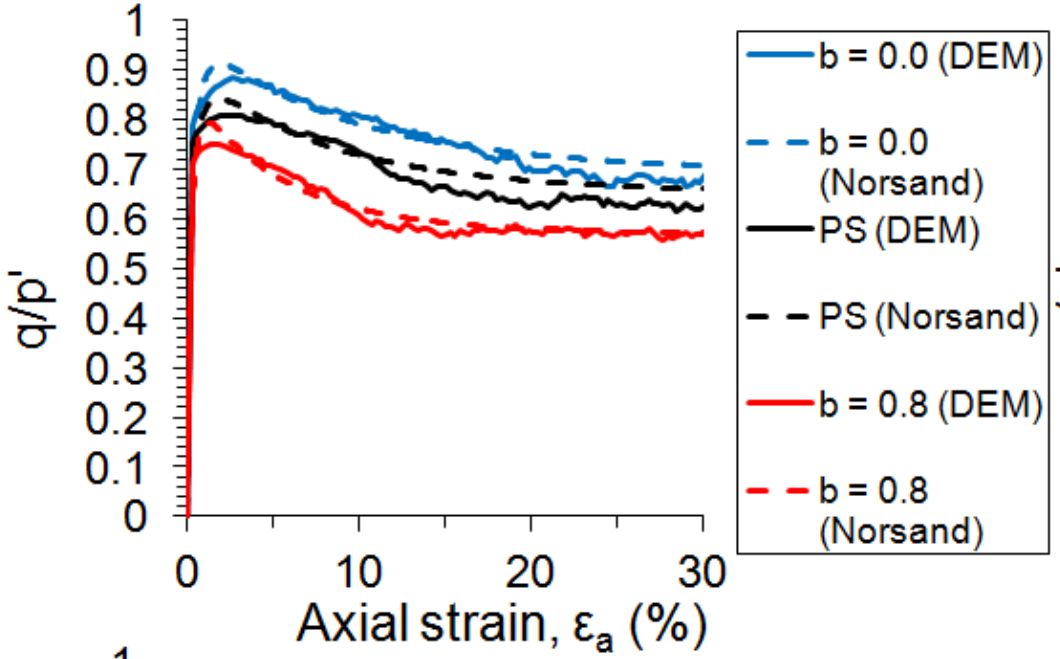

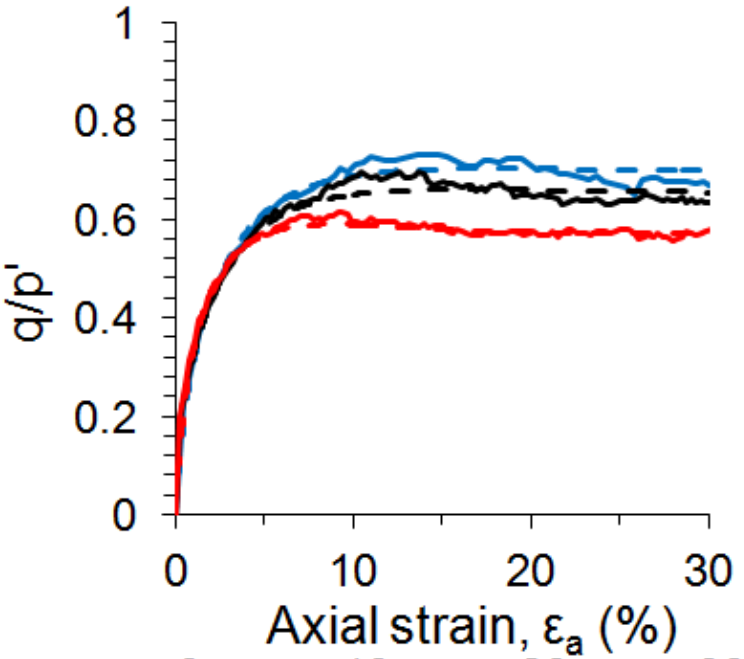

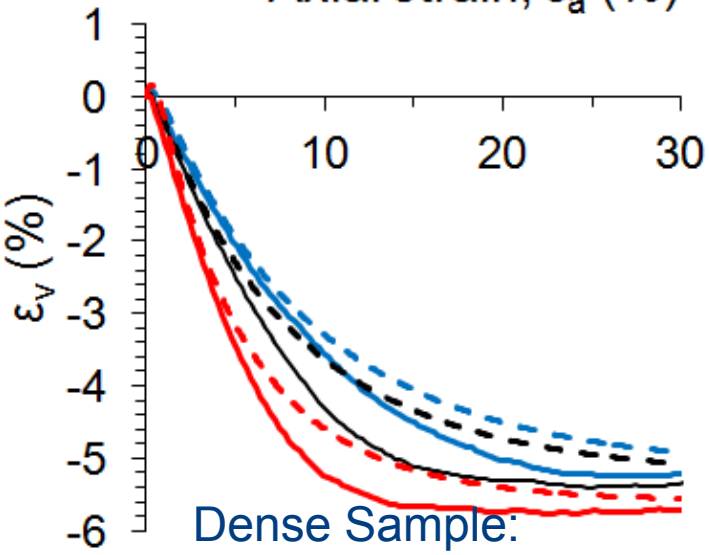

Dense Sample:
σ'_3=300 kPa, ψ_0 =-0.0823

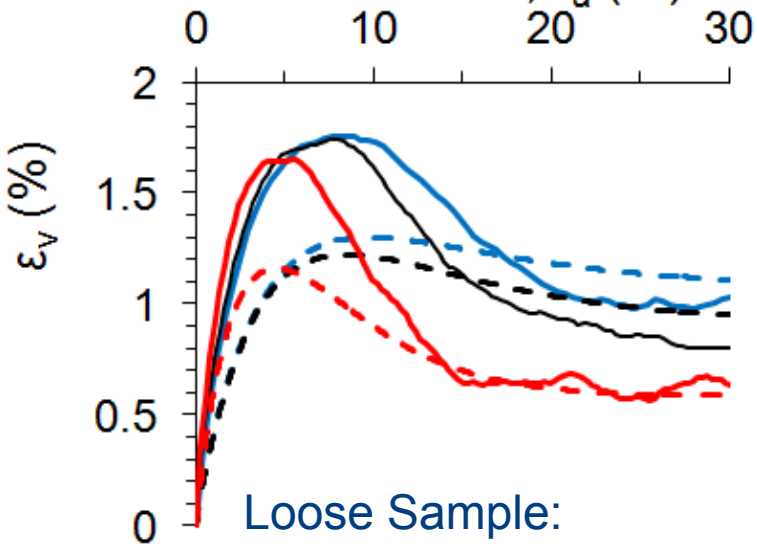

Loose Sample:
σ'_3=500 kPa, ψ_0 =0.0171

Reminder that Robust Constitutive Models are Needed

The remains of the village of Bento Rodrigues in Brazil following tailings dam collapse, Nov. 2015

http://www.theguardian.com

DEM Analysis of ψ for a 3D Stress State

- DEM simulations can capture influence of *b* on strength and the state-dependency of soil strength and dilation
- DEM data indicate that the correlations between ϕ'_p-ϕ'_{cs} and ψ_0 and D_p and ψ_0 are independent of particle morphology and *b*
- DEM simulations can be used to supplement experimental investigations when developing constitutive models for soil behaviour in a general stress space

DEM Limitations

- Spherical particles under-estimate soil strength (ϕ'_{cs} , ϕ'_{p})

Toyoura sand:

- $\phi'_{cs}=31^{o}$
- Subangular grains

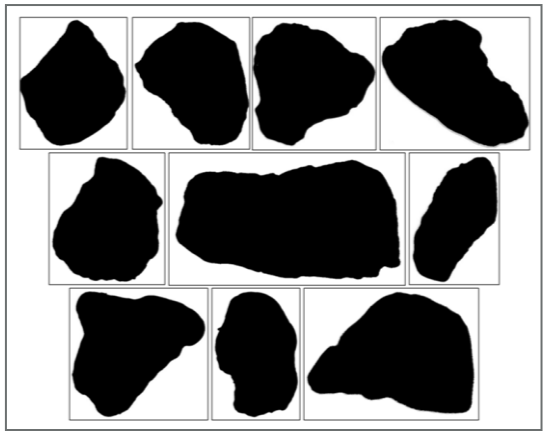

DEM model:

- $\phi'_{cs}=18.2^{o}$
- Spherical particles

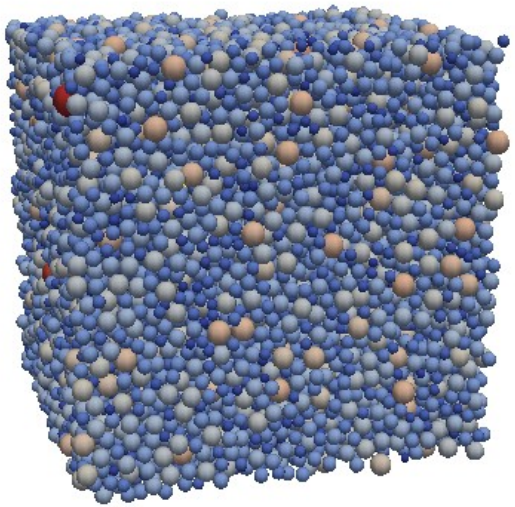

Influence of Morphology on ϕ'_p and ϕ'_{cs}

- Rotation of non-spherical particles will be frustrated by finite contact area

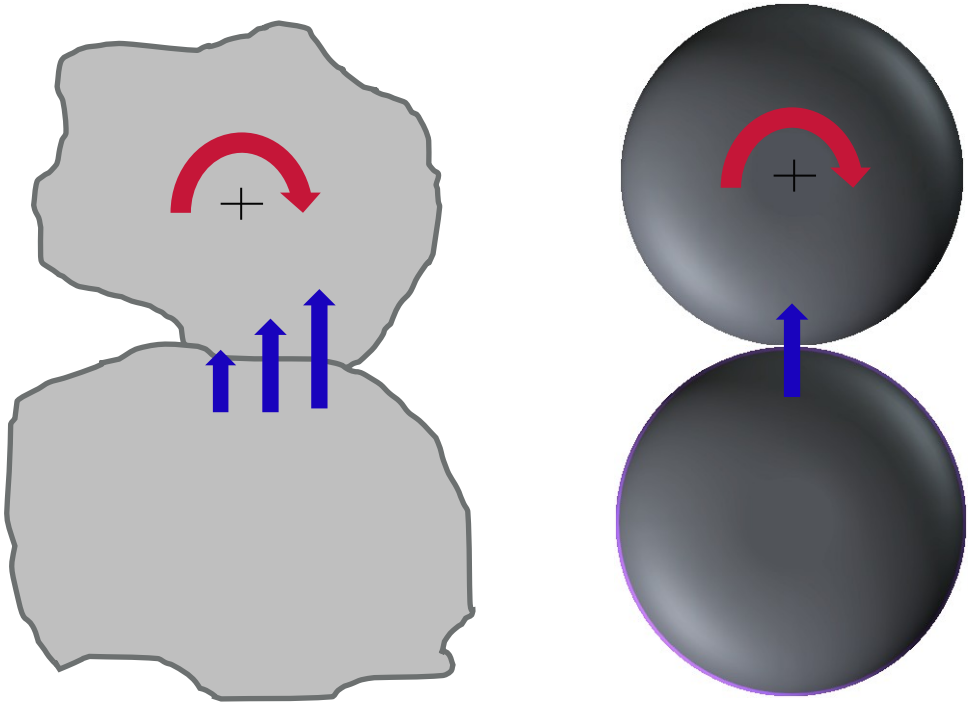

Influence of Morphology on ϕ'_p and ϕ'_{cs}

- Force chains between non-spherical particles are more stable

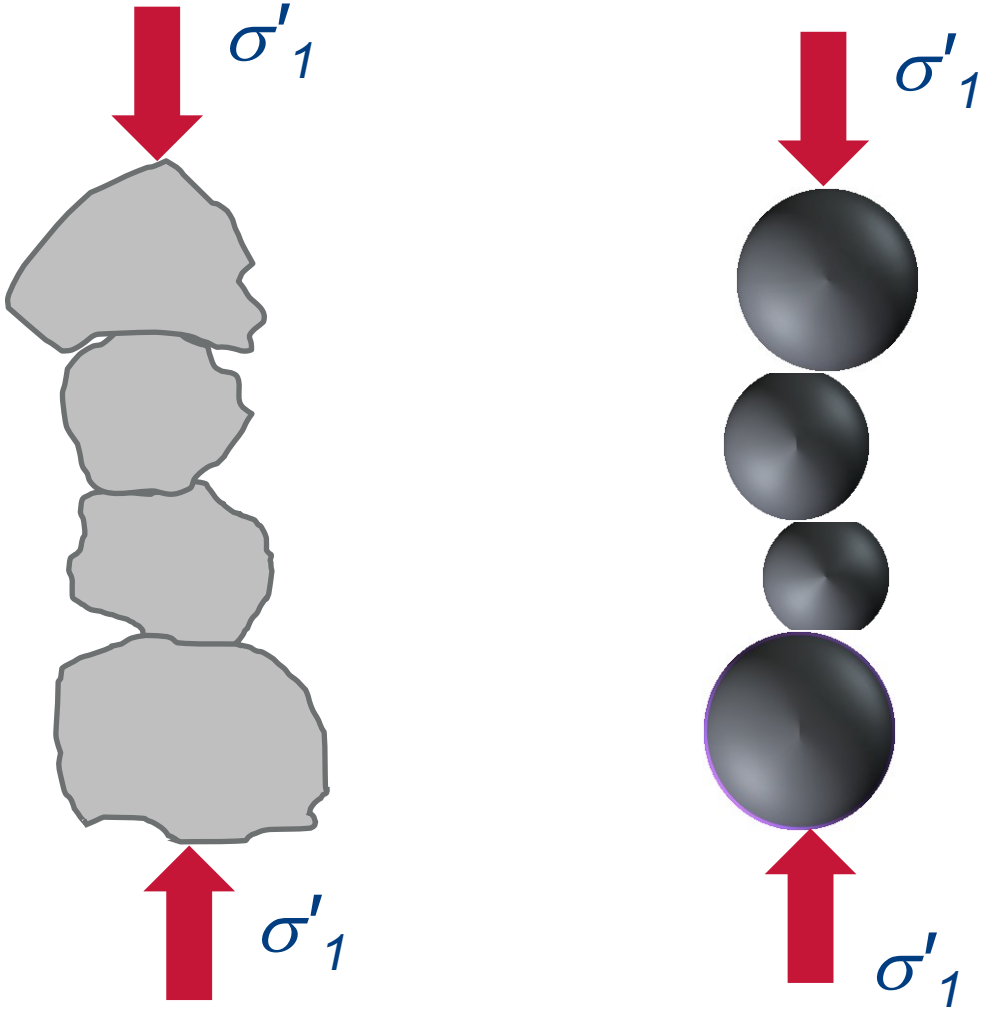

DEM and Particle Geometry

- Options for non-spherical particles include sphere clumps - computational cost increase

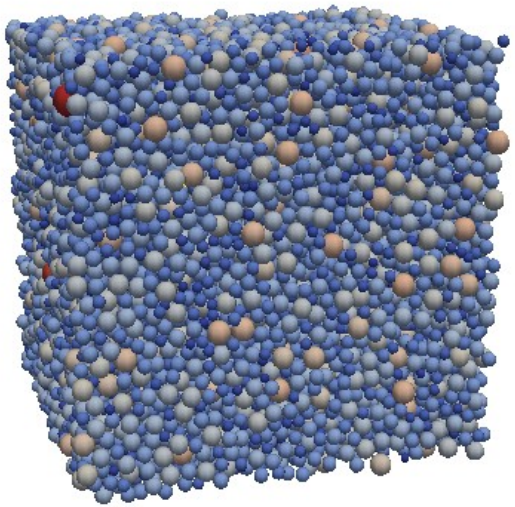

389 Agglomerates

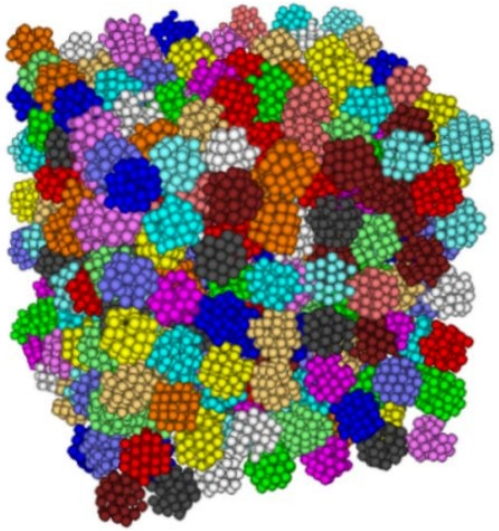

Cheng et al (2003) Géotechnique

Micro Computed Tomography (microCT)

- High resolution, three-dimensional images created using X-rays
- Non-destructive
- Computed tomography developed by Cormack and Hounsfield – Awarded Nobel Prize in Physiology or Medicine in 1979
- First paper in *Géotechnique* – *Oda et al. (2004)*

Micro Computed Tomography (microCT)

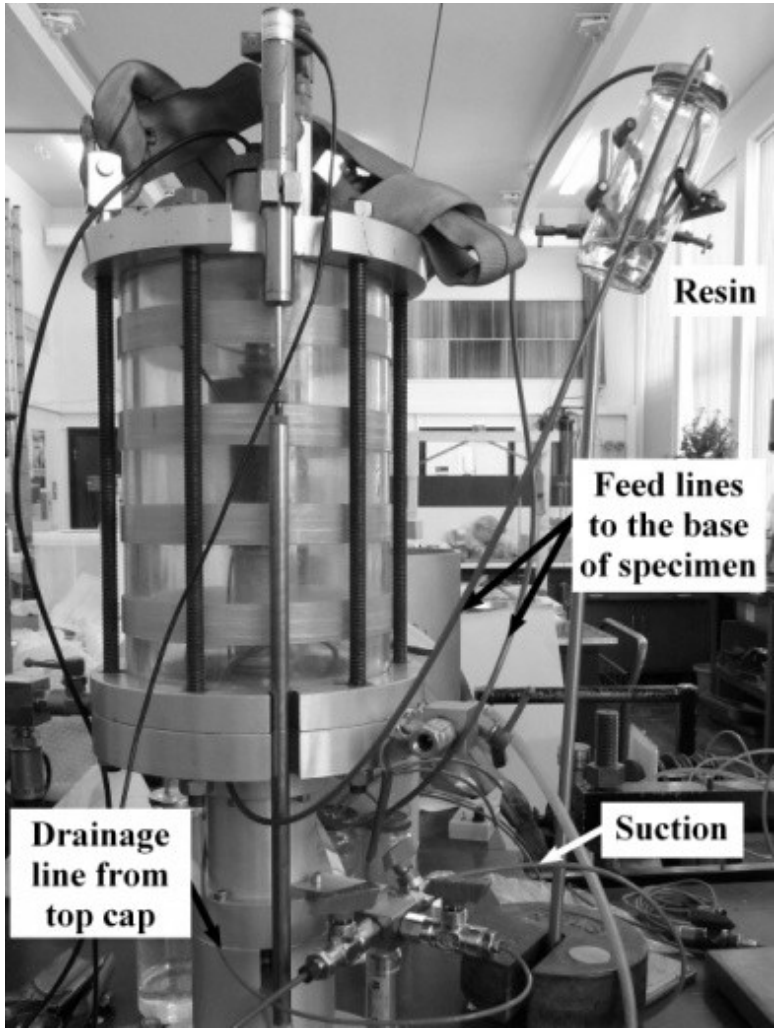

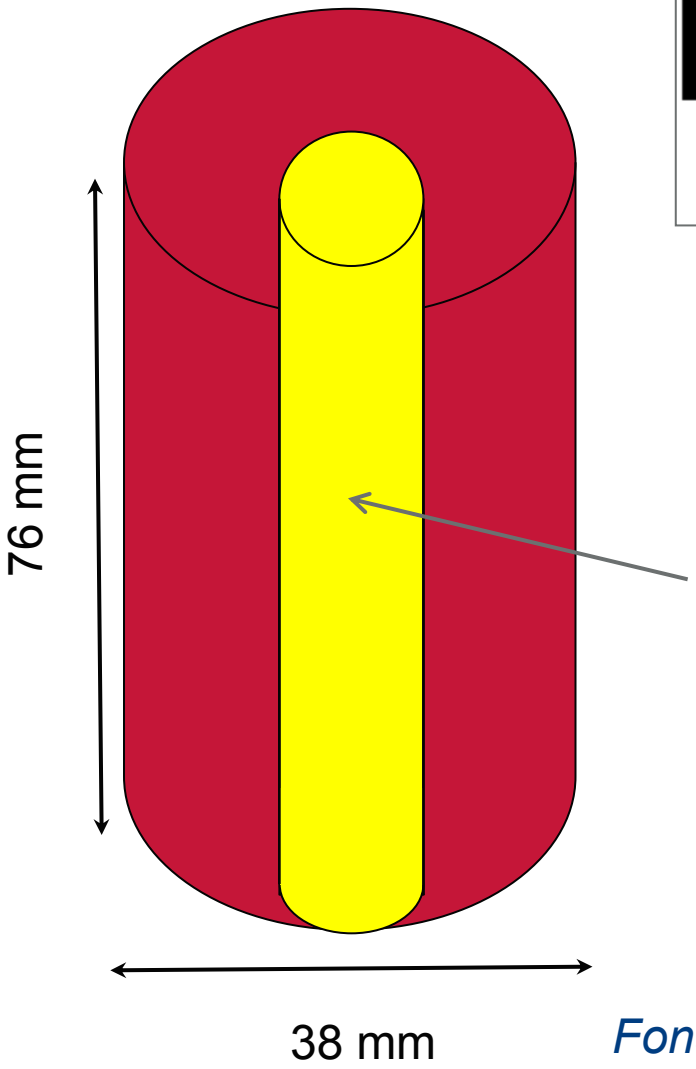

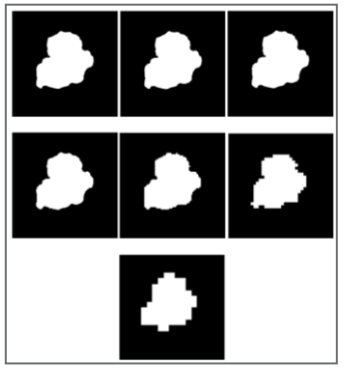

Central core extracted for scanning

3-10 mm in diameter

Fonseca et al. (2014) Géotechnique

MicroCT scanning

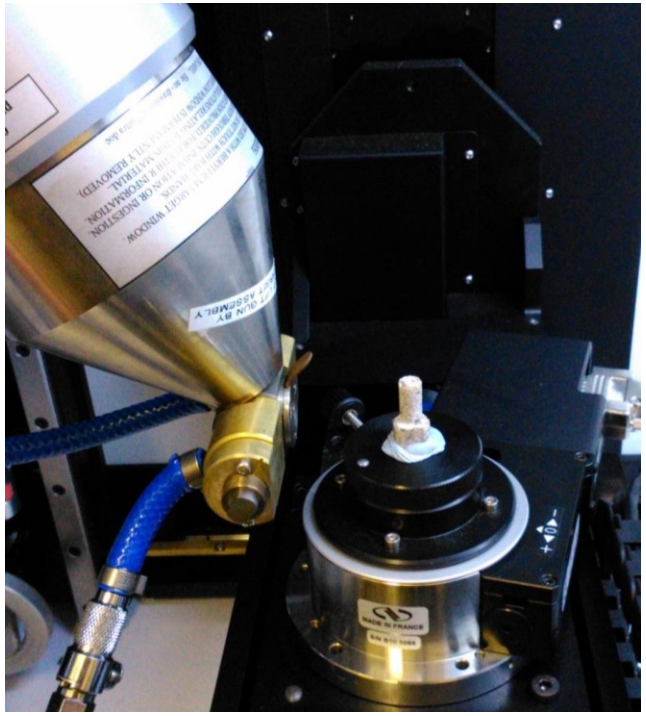

X-Ray source + typical sample for scanning

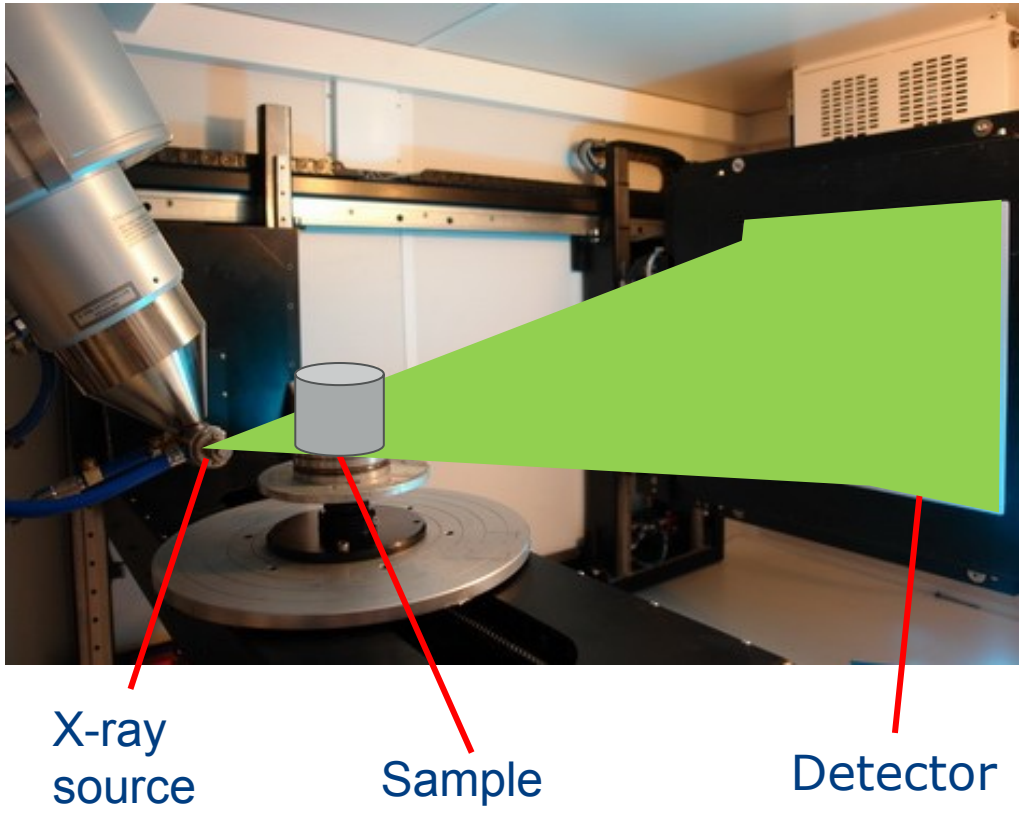

(H. Taylor, current PhD student)

Image source: http://www.nikonmetrology.com

MicroCT Data Analysis

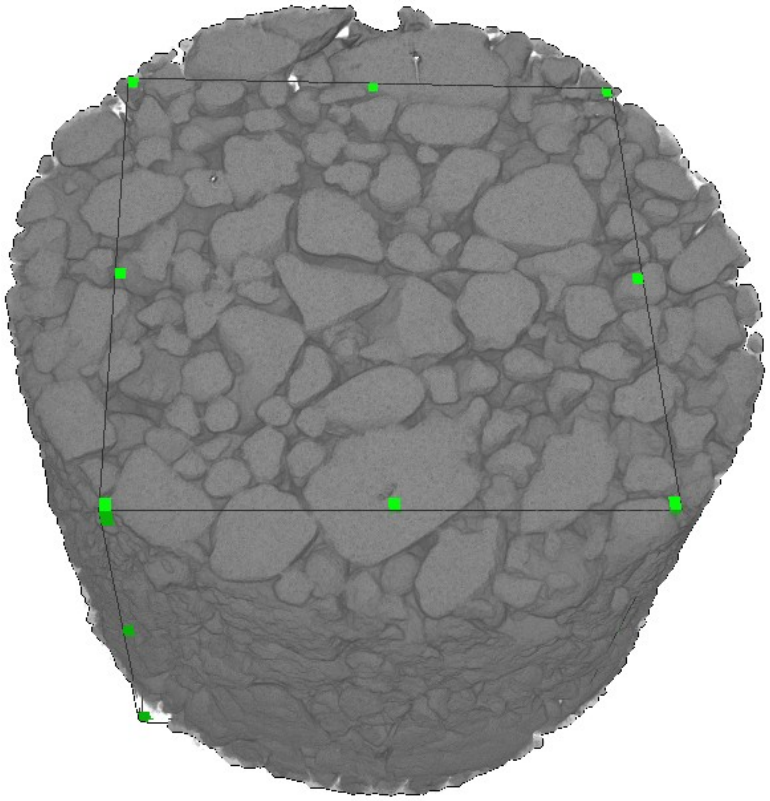

Raw output – 3D attenuation map

(H. Taylor)

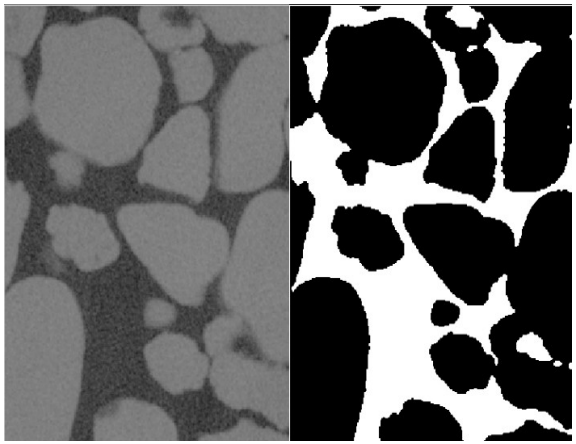

2D Slice from μCT image

Binary image

Taylor et al. (2015)
Computers and Geotechnics

MicroCT Data Analysis

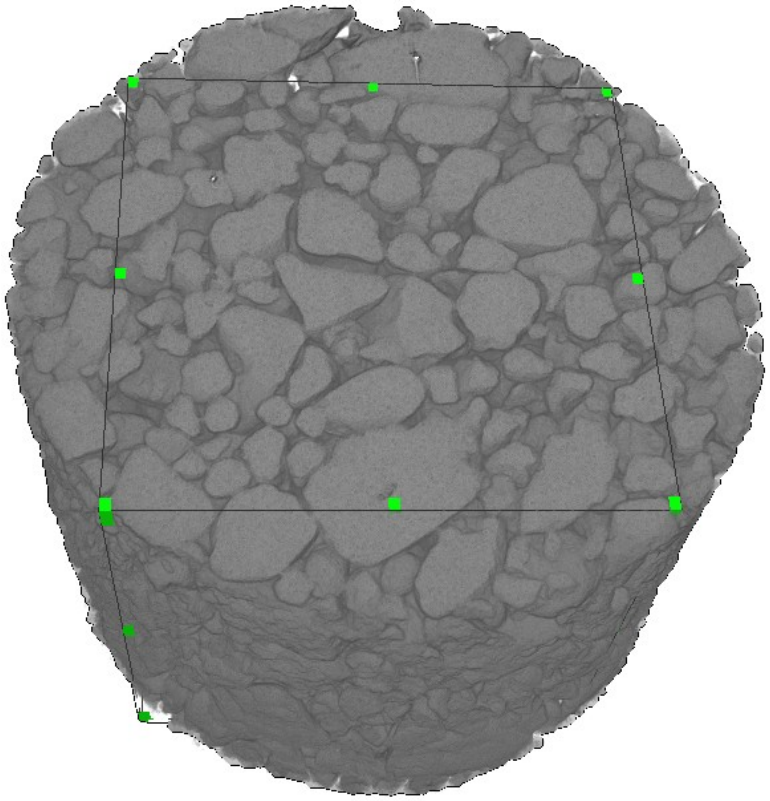

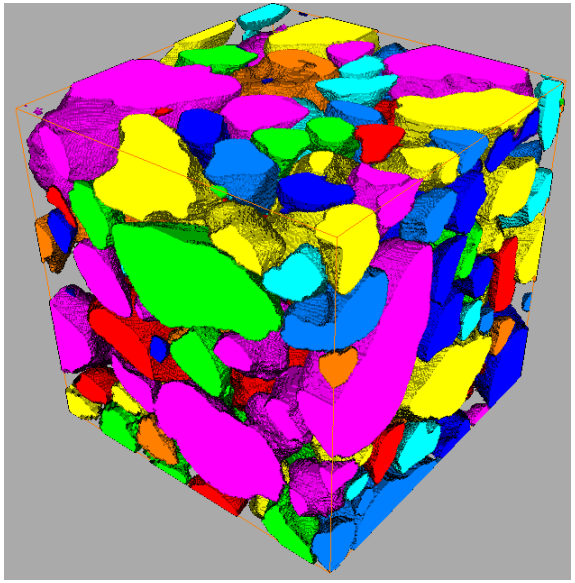

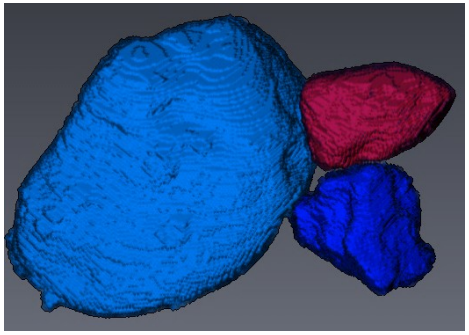

Individual particles and contacts from watershed segmentation

(H. Taylor)

Reigate Sand: A "Locked Sand"

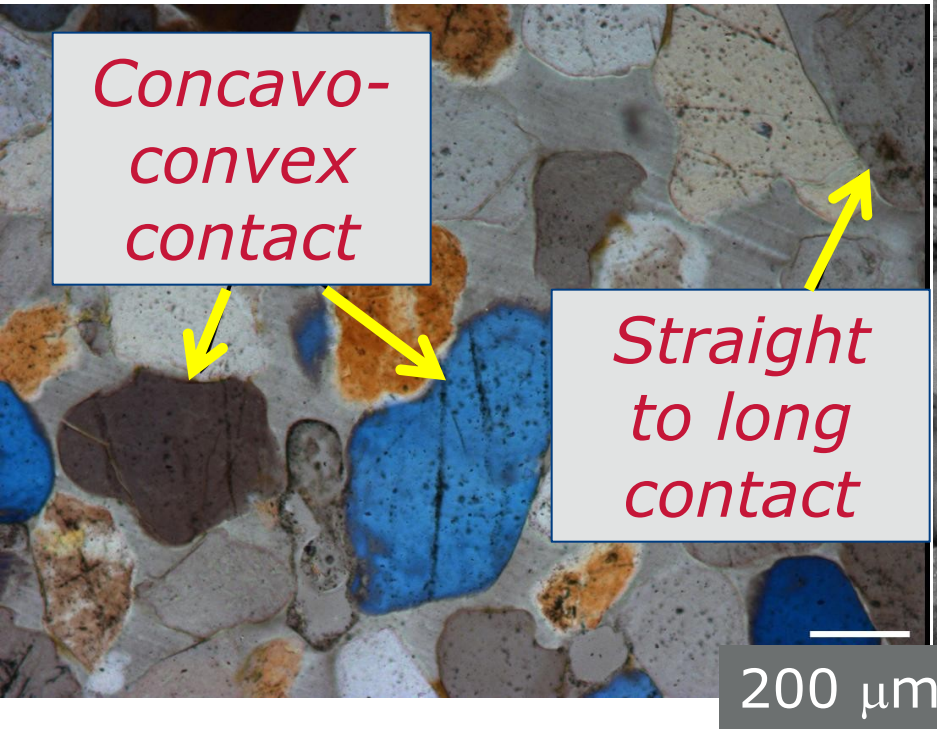

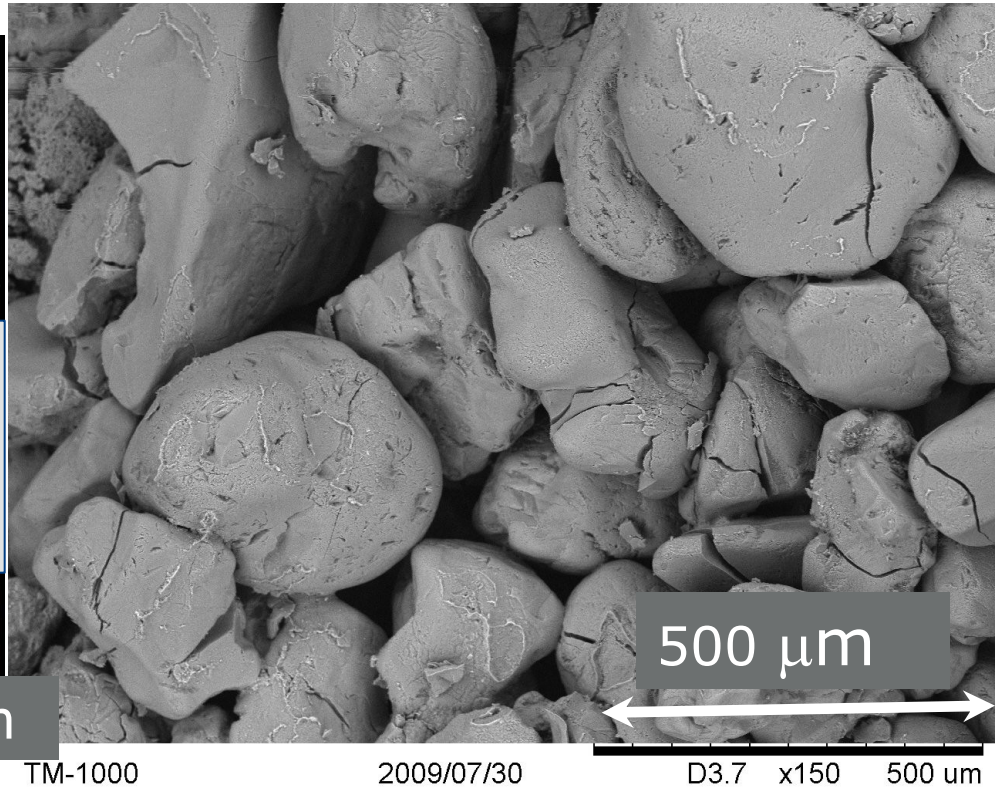

Transmitted light microscope image of thin section (cross-polarized light) (contact configurations proposed by *Dusseault and Morgensten (1979)*)

Scanning electron microscope (SEM) image

Doctoral Research of Dr. J. Fonseca

Reigate Sand Load:Deformation response

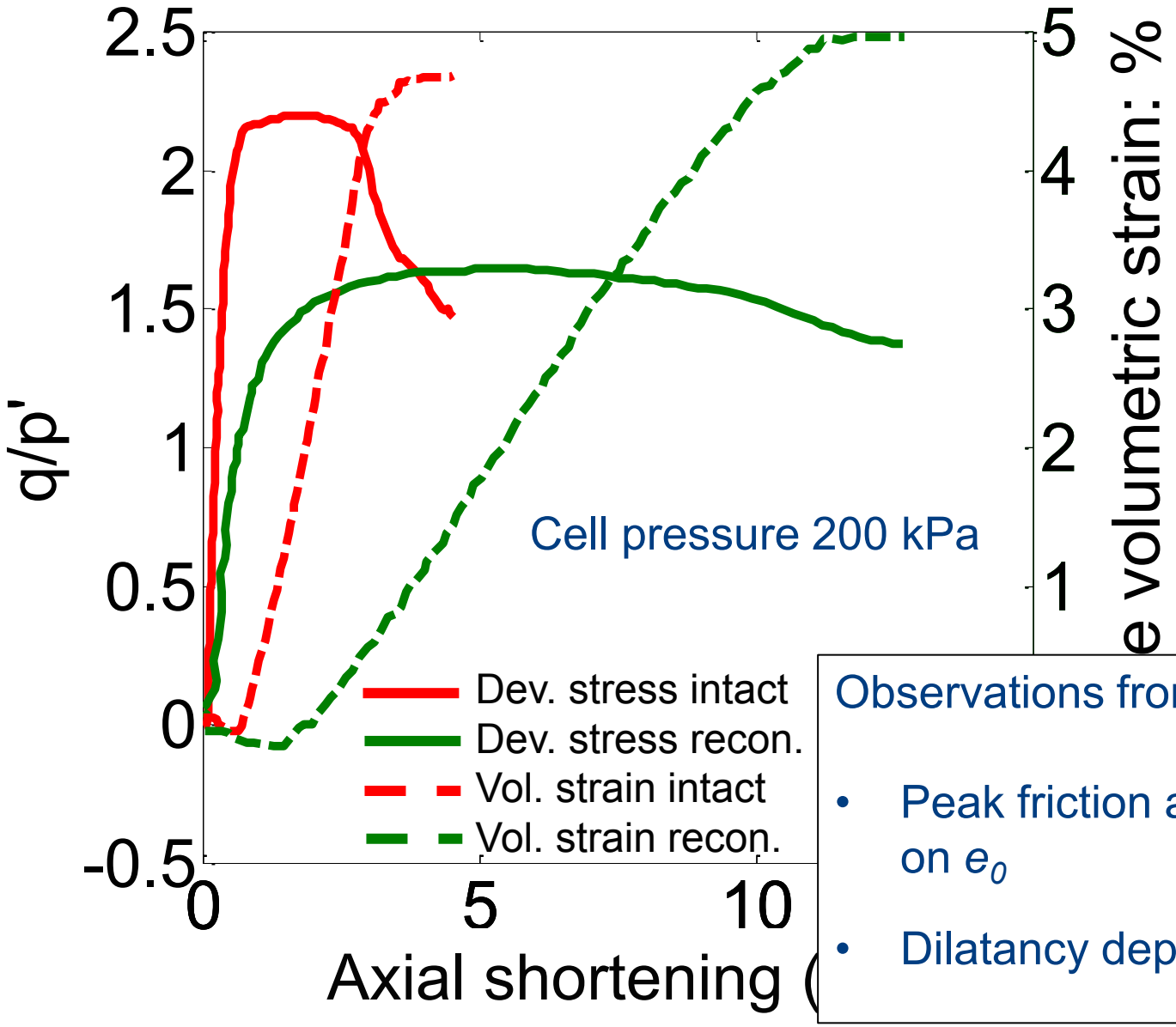

Cresswell and Powrie Géotechnique (2004)

Reconstituted sample "pluviated to highest possible density"

Observations from direct shear tests:

- Peak friction angle (ϕ'_p) depends on e_0
- Dilatancy depends on stress level

Reigate Sand – Site Location

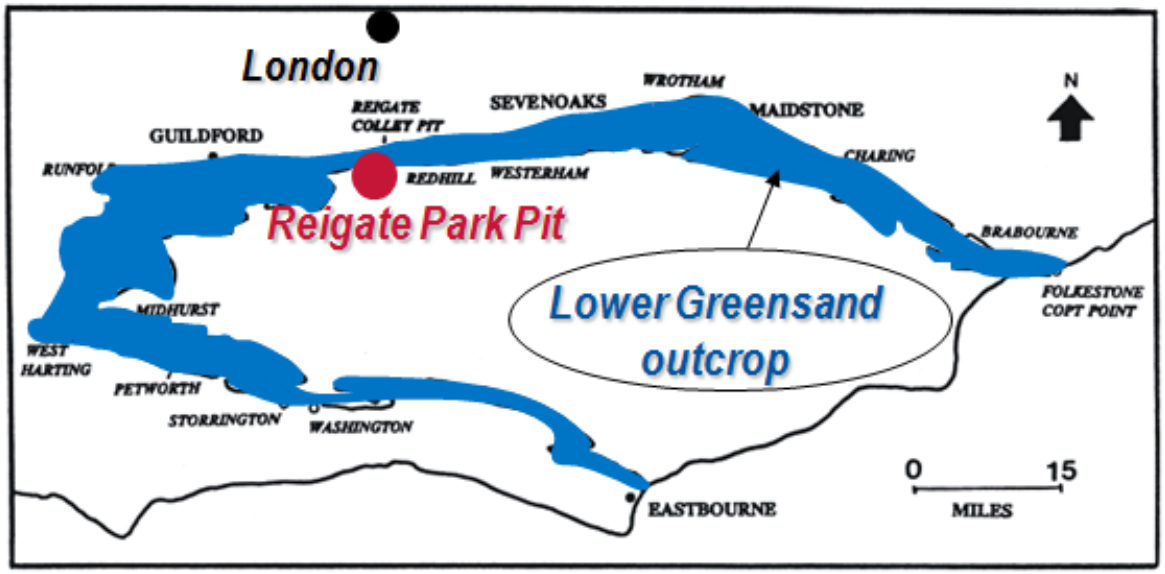

From Richards & Barton (1999)

Block Sampling

Triaxial Tests – Sample Preparation

Intact Sample

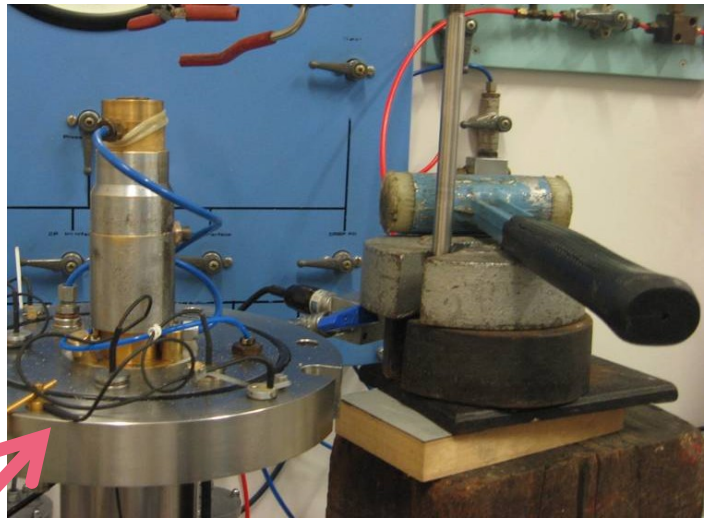

Reconstituted Sample (Prepared by pouring / tamping/ tapping)

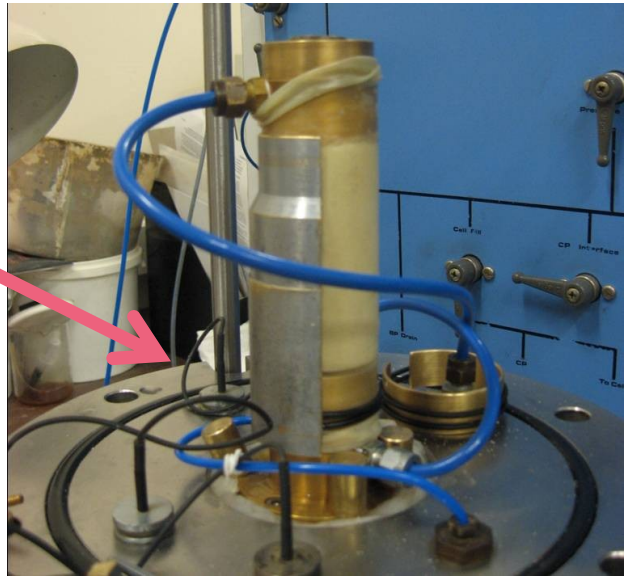

Doctoral Research of Dr. J. Fonseca

Triaxial Test Data

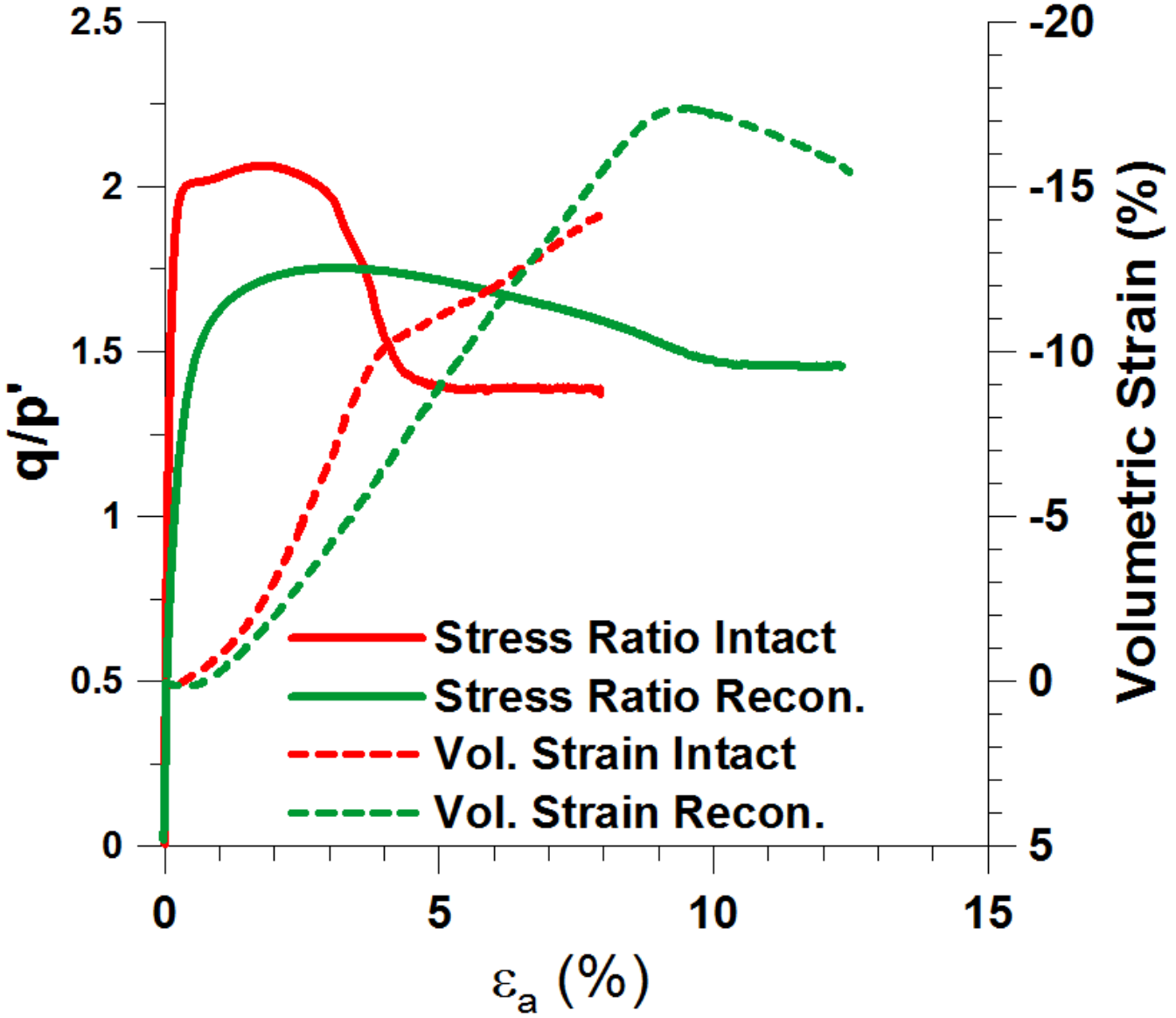

Intact
e_0=0.48

Reconstituted
e_0=0.49

Cell pressure
300 kPa

Fonseca et al. (2013)
Géotechnique

μCT Imaging Points

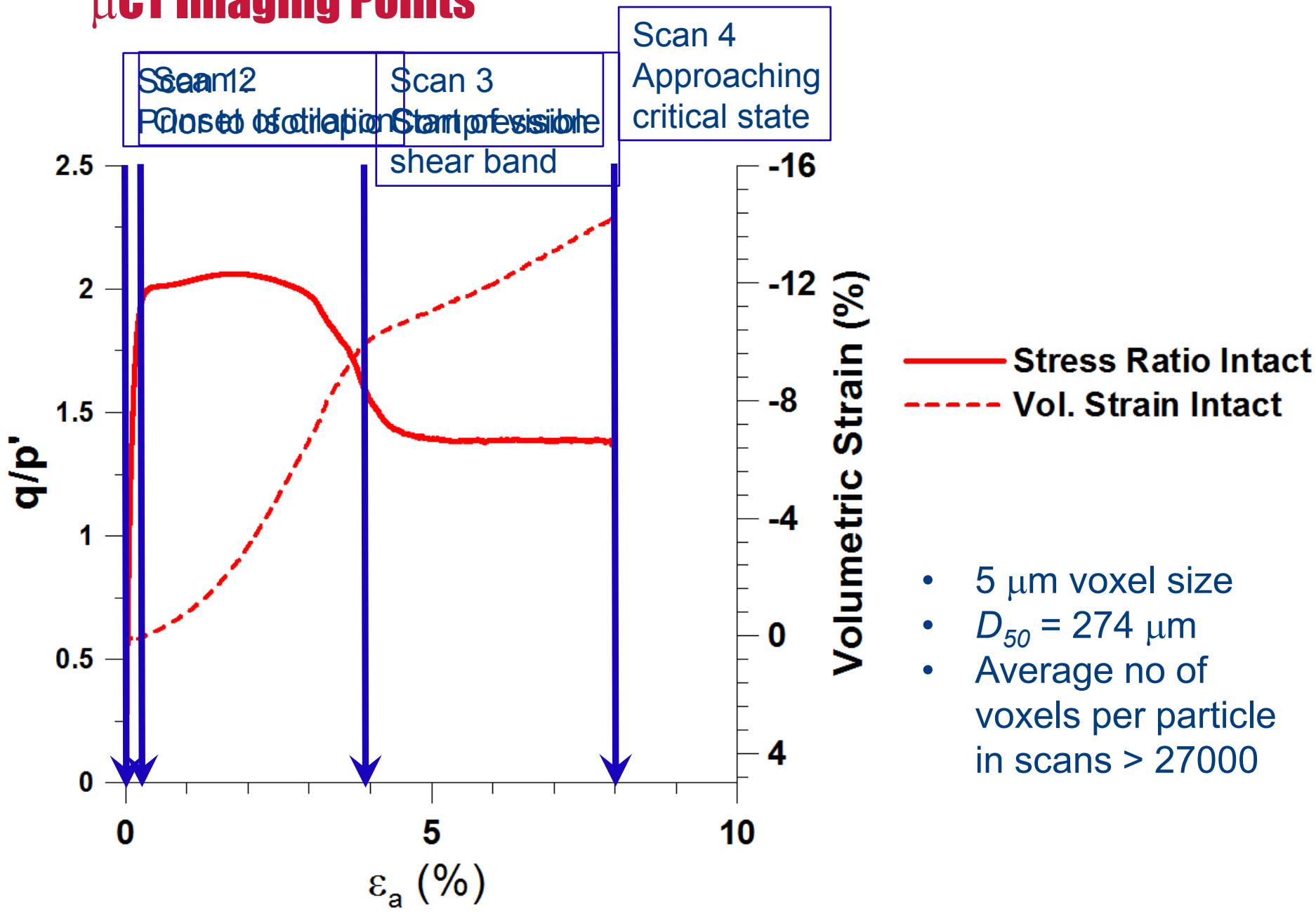

- 5 μm voxel size
- D_{50} = 274 μm
- Average no of voxels per particle in scans > 27000

MicroCT Images

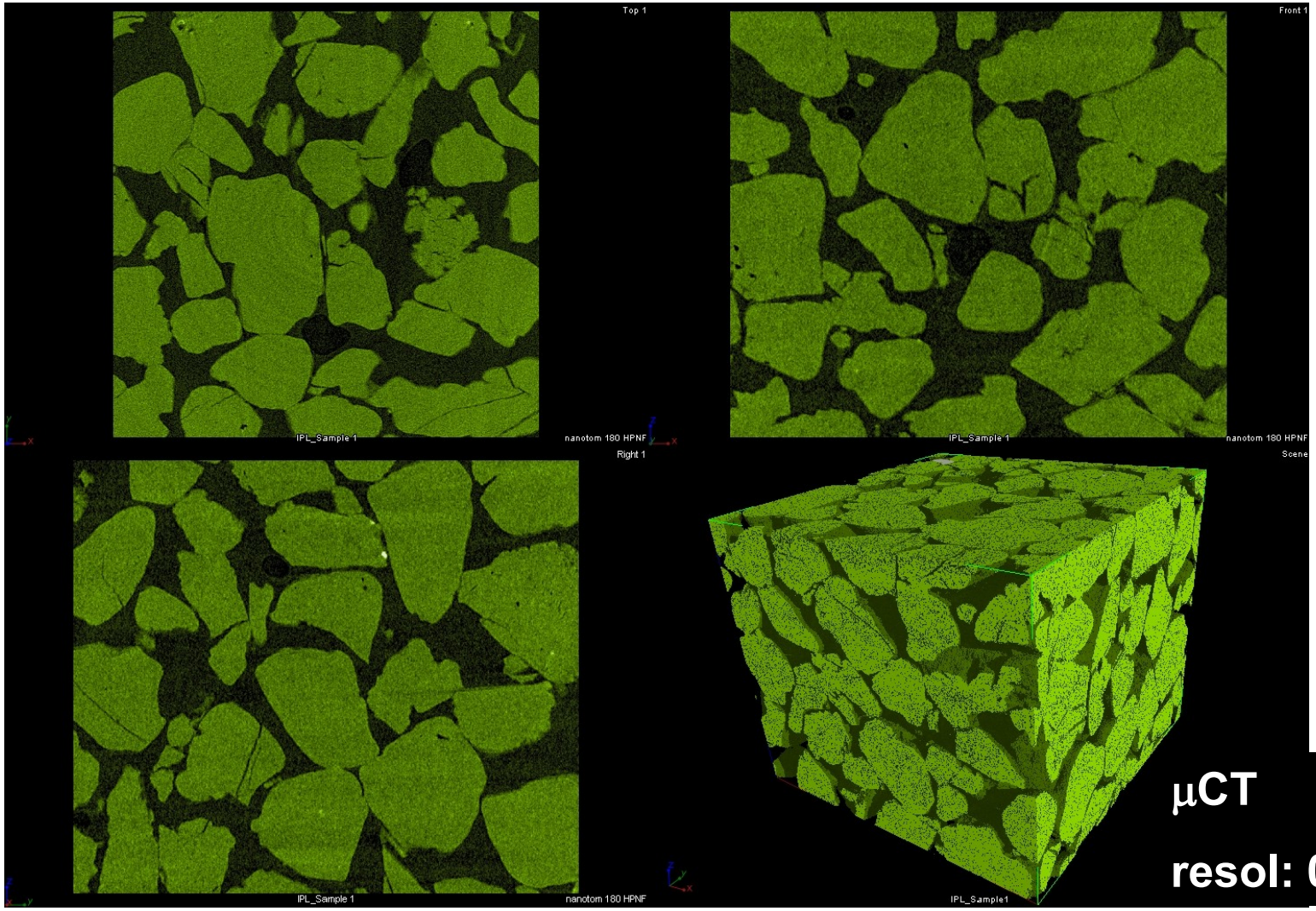

Particle Size Distributions from microCT

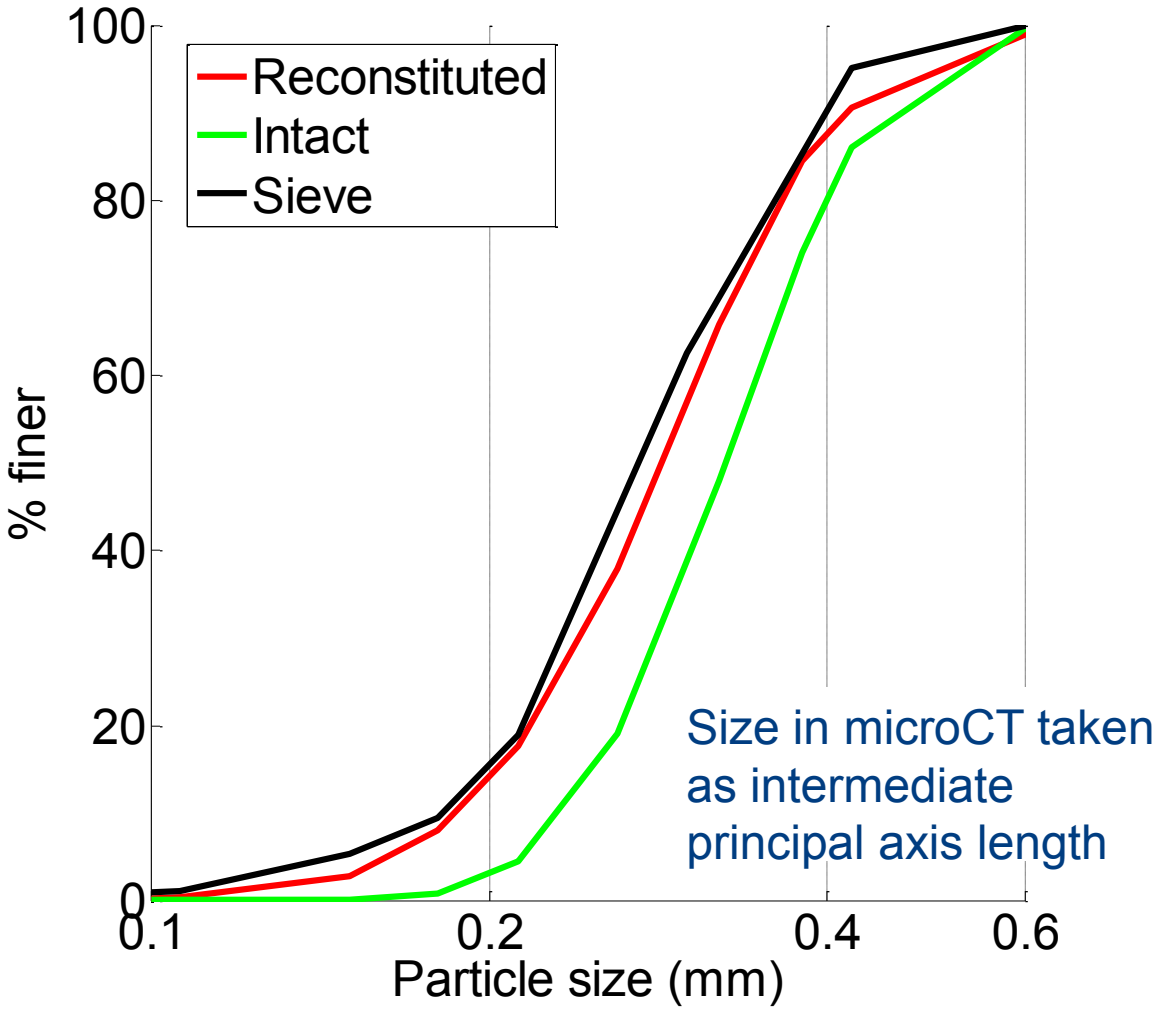

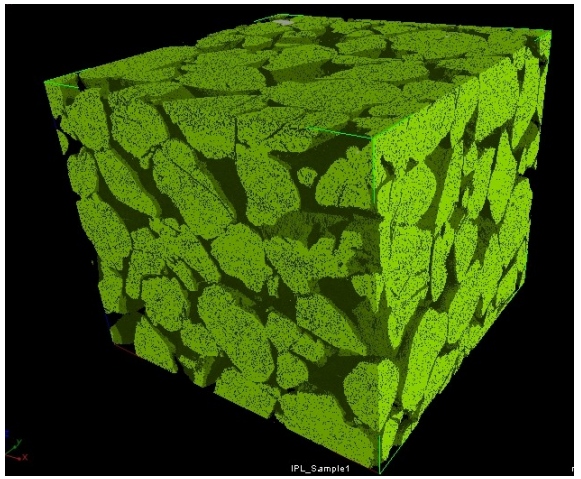

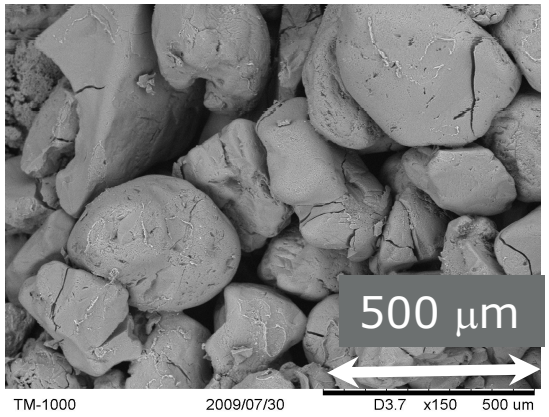

Fonseca et al. (2013) Soils and Foundations

Scalar Fabric Description – Contact Density

Coordination Number (N_c):
Number of contacts per particle

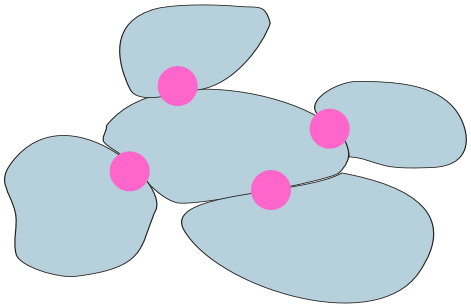

Contact Index:

$$\frac{\text{Contact area}}{\text{Particle surface area}}$$

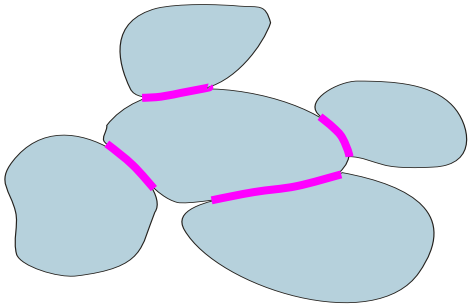

Representative Particle

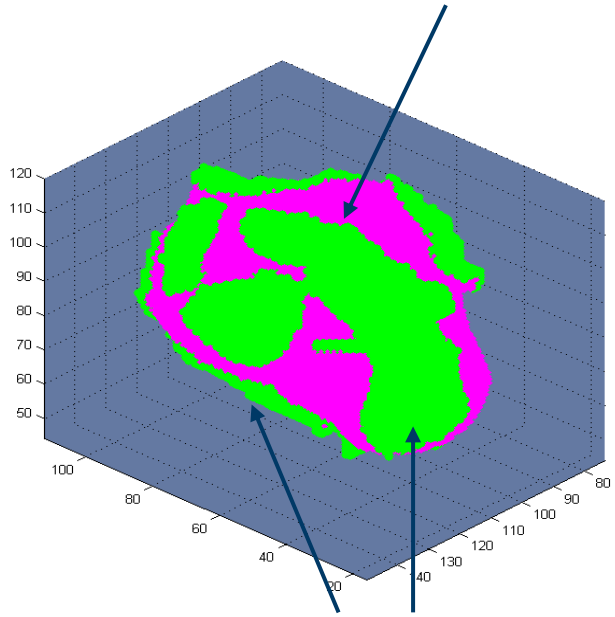

Contacts

Coordination Number Distribution

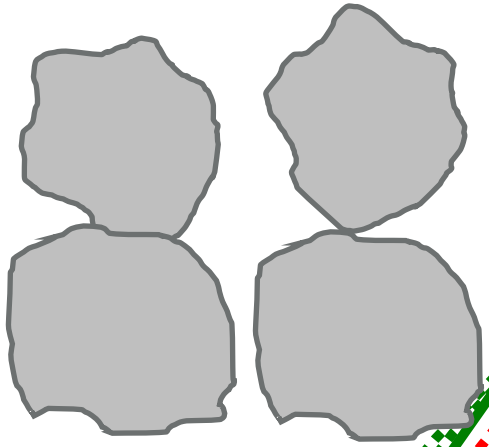

Contact index distribution

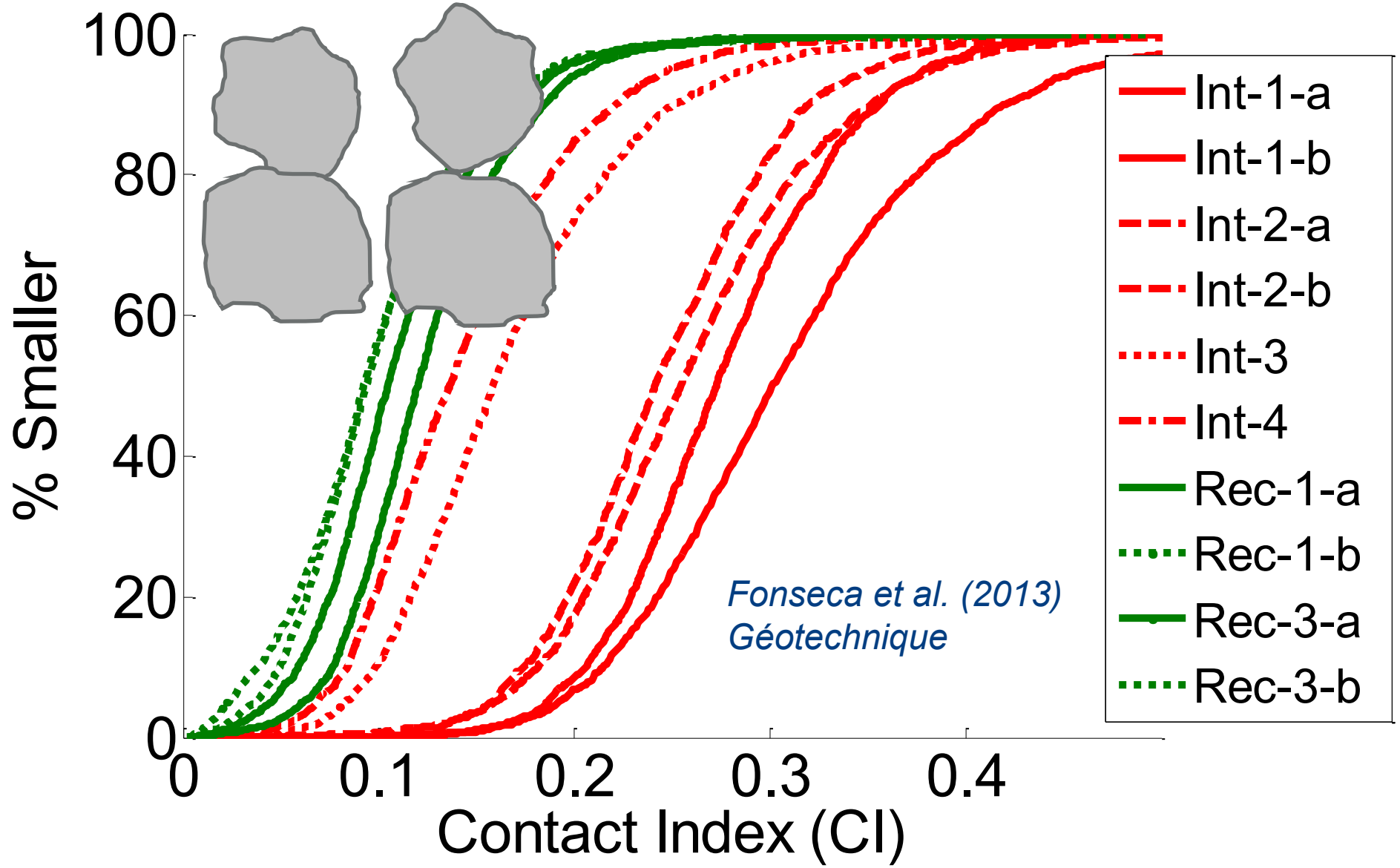

Influence of Contact Area on ϕ'_p

- Force chains more stable when contact area is greater

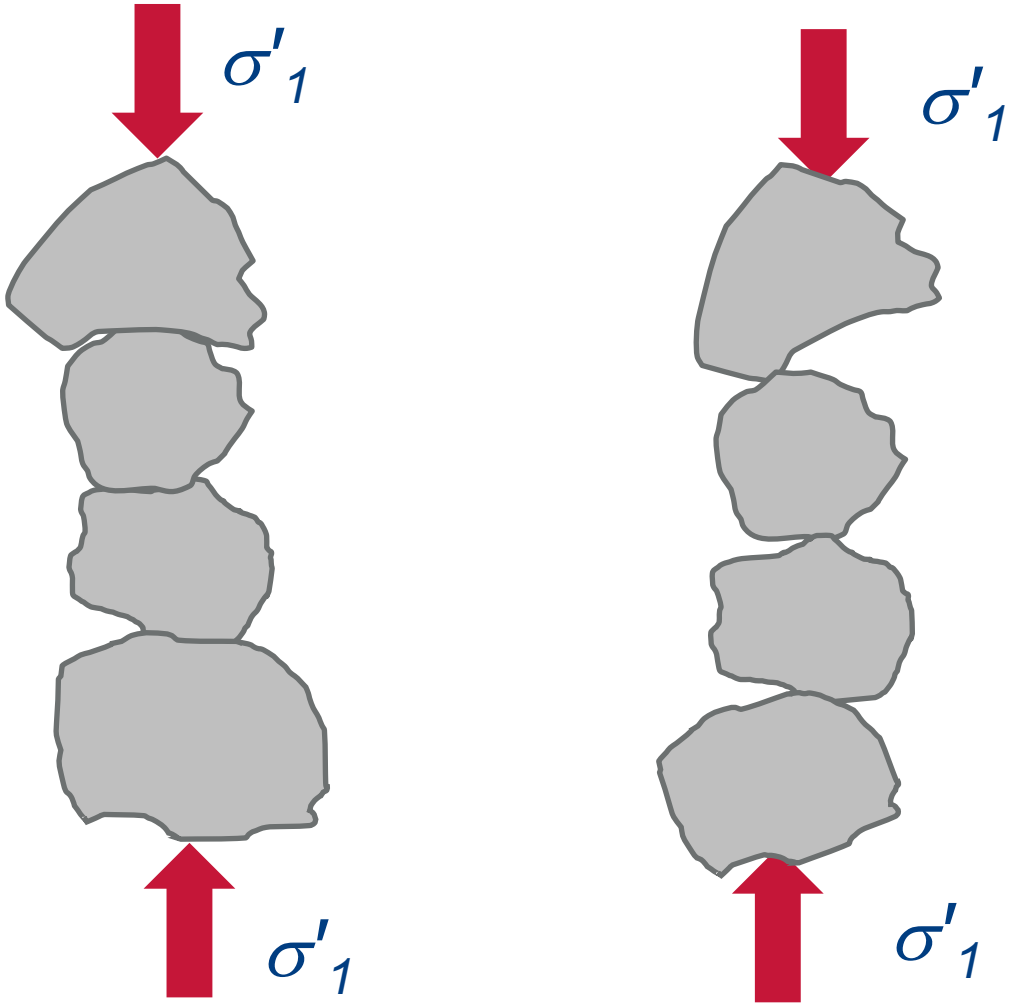

Particle Scale Analyses of Locked Sand

- Triaxial test data confirmed difference in response of intact and reconstituted materials tested at same void ratio
- Micro CT data revealed a difference between particle size distributions
- At the same void ratio the intact material had a higher coordination number and contact index than reconstituted material
- Contact index better discriminates two materials

Tools of Particulate Soil Mechanics

DEM

- Model with inherent idealizations - simplified geometries and contact models

- Information on contact forces and kinematics

microCT

- Can observe topology of real materials

- No information on contact forces or particle velocities

Internal Stability of Dam Filters

- WAC Bennett Dam
- British Columbia, Canada
- 183 m high
- Zoned earthfill dam
- Constructed 1968

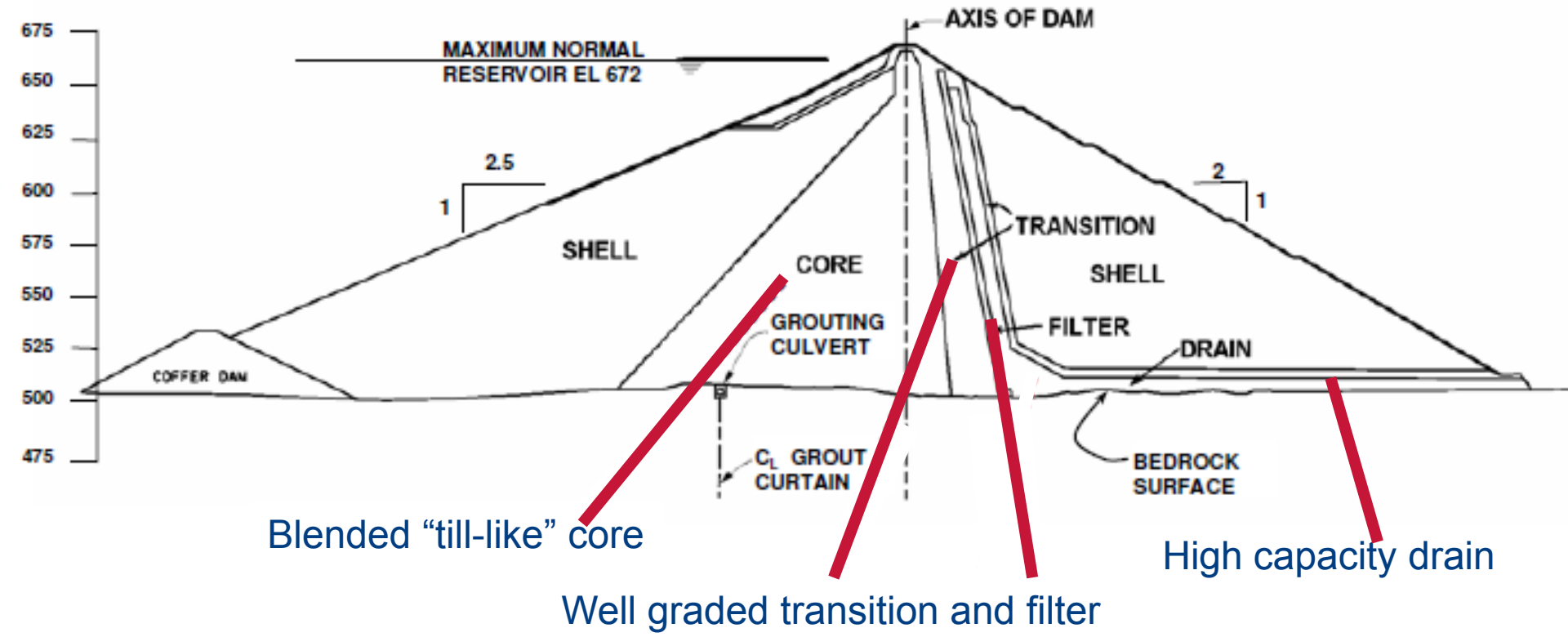

BC Hydro as cited by Muir Wood (2007)

Internal Instability

- Internal instability occurs where "sand can migrate within the interstices of a framework or primary fabric formed predominantly of the gravel particles"

- "Sandy gravels having a bimodal (gap-graded) grain-size distribution with less than about 25% of sand exhibit internal instability"

- "Such materials can present serious problems where piping is possible, notably in dams and barrages."

Quotes from *Skempton and Brogan (1994) Géotechnique*

Internal Instability

- Internal instability occurs where "sand can migrate within the interstices of a framework or primary fabric formed predominantly of the gravel particles"
- "Sandy gravels having a bimodal (gap-graded) grain-size distribution with less than about 25% of sand exhibit internal instability"
- "Such materials can present serious problems where piping is possible, notably in dams and barrages."

Quotes from *Skempton and Brogan (1994) Géotechnique*

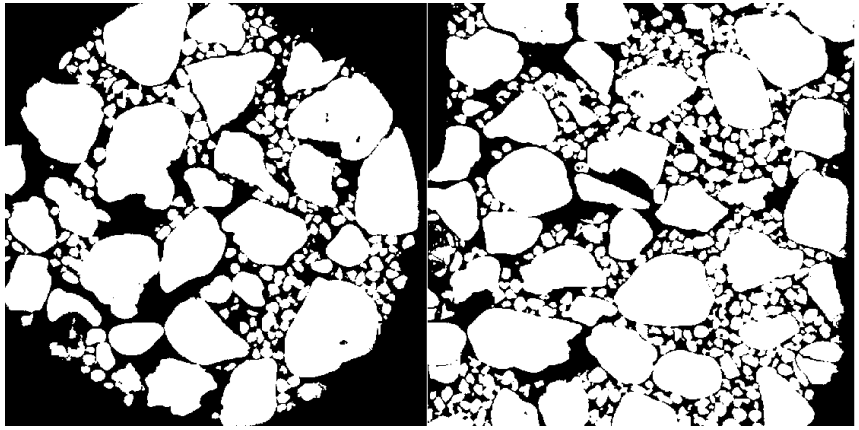

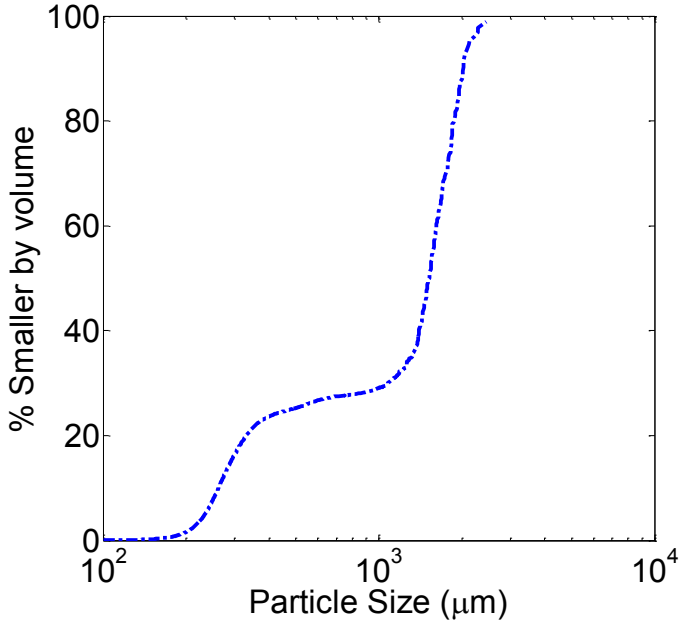

Fonseca et al. (2014) Géotechnique

Internal Instability

- Internal instability occurs where "sand can migrate within the interstices of a framework or primary fabric formed predominantly of the gravel particles"
- "Sandy gravels having a bimodal (gap-graded) grain-size distribution with less than about 25% of sand exhibit internal instability"
- "Such materials can present serious problems where piping is possible, notably in dams and barrages."

Quotes from *Skempton and Brogan (1994) Géotechnique*

1996 Sinkhole at WAC Bennett Dam *(BC Hydro as cited by Muir Wood, 2007)*

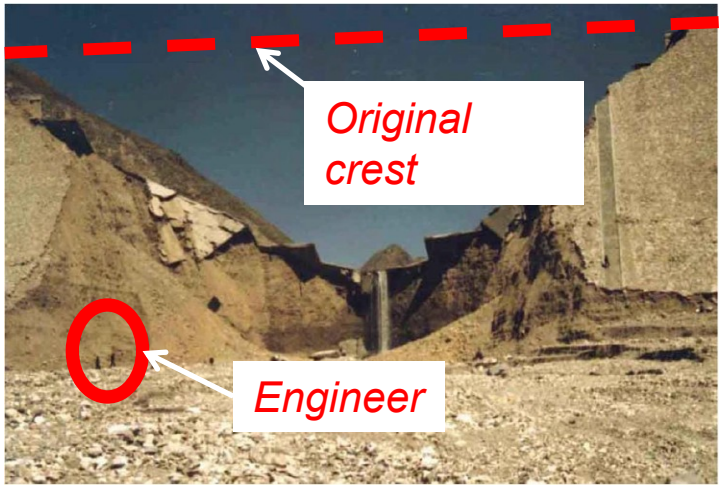

Gouhou Dam, China (1993)
71m High; 300 Deaths
(Chang, 2011)

Empirical Filter Criteria: Kézdi (1979)

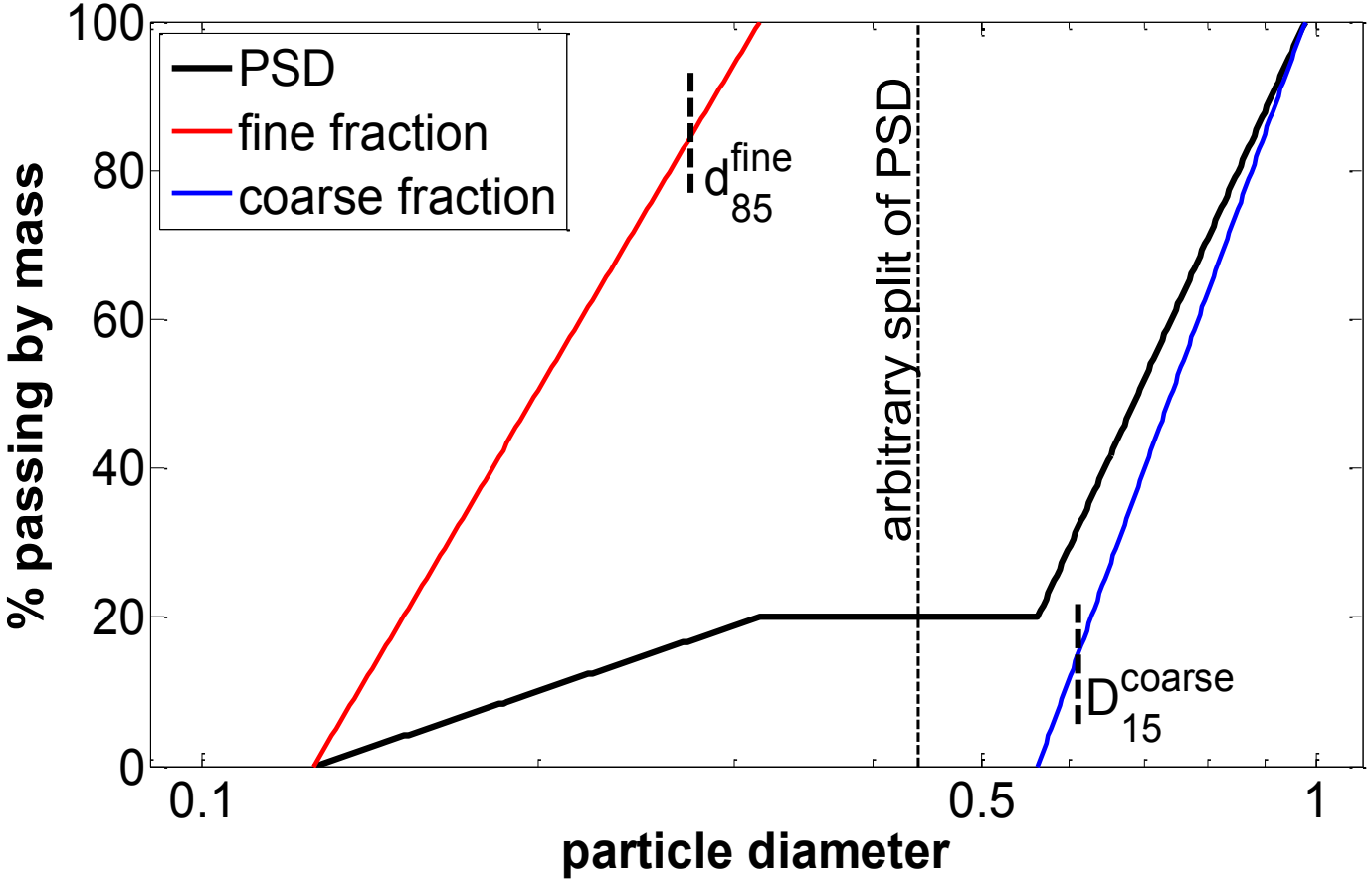

Relates to Terzaghi filter rule

Split PSD into coarse and fine "PSDs"

Stable if: $d_{85}^{fine} > (D_{15}^{coarse} / 4)$

i.e. if

$D_{15}^{coarse} / d_{85}^{fine} < 4$

Particle-Scale Basis for Kézdi Criterion

Samples K_0 consolidated to p'=300kPa
Voxel size 10 mm
($0.005d_{50}$-$0.01d_{50}$)

Increasing Kézdi no.

Decreasing stability

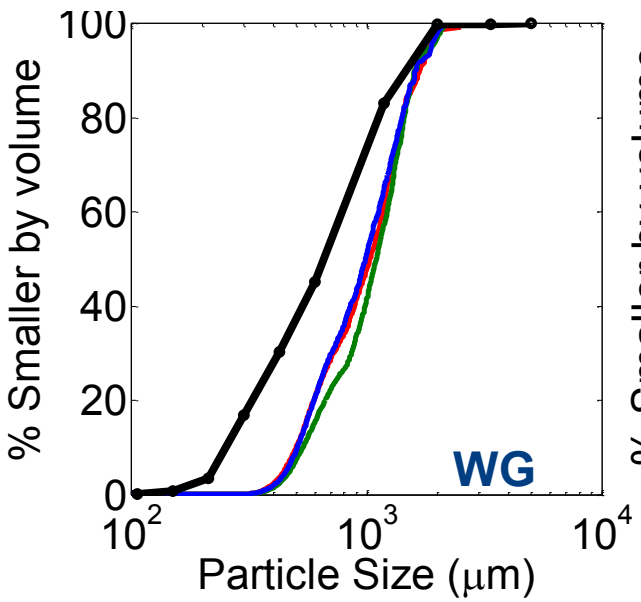

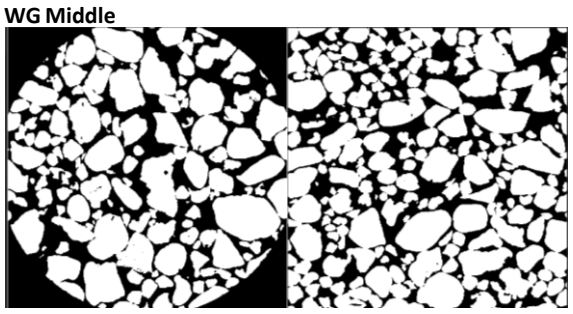

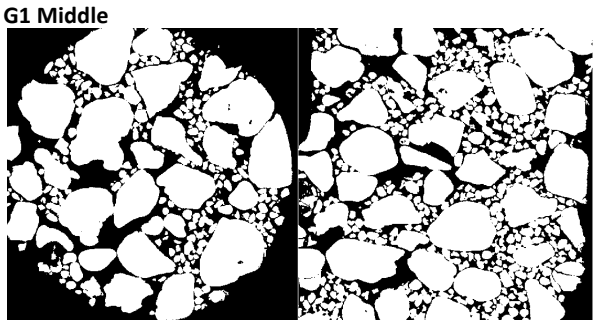

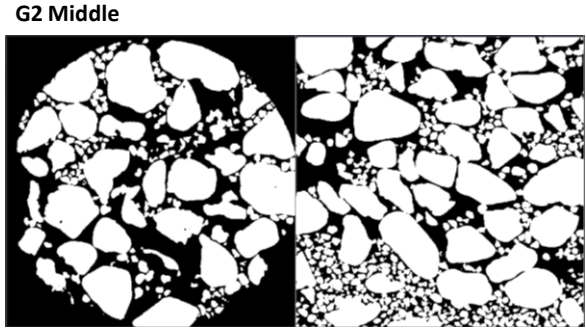

Fonseca et al. (2014) Géotechnique

Variation in Coordination Number with Kézdi Ratio

Increasing Kézdi no.

Decreasing stability

N_c = Coordination number

No of contacts per particle

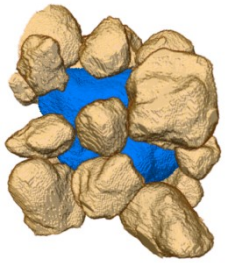

Leighton Buzzard Sand
Blue particle
20 contacts

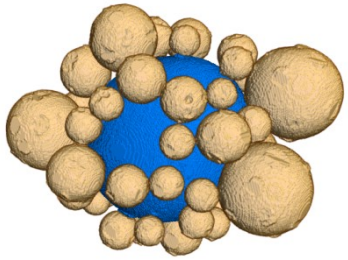

Glass beads
Blue particle
50 contacts

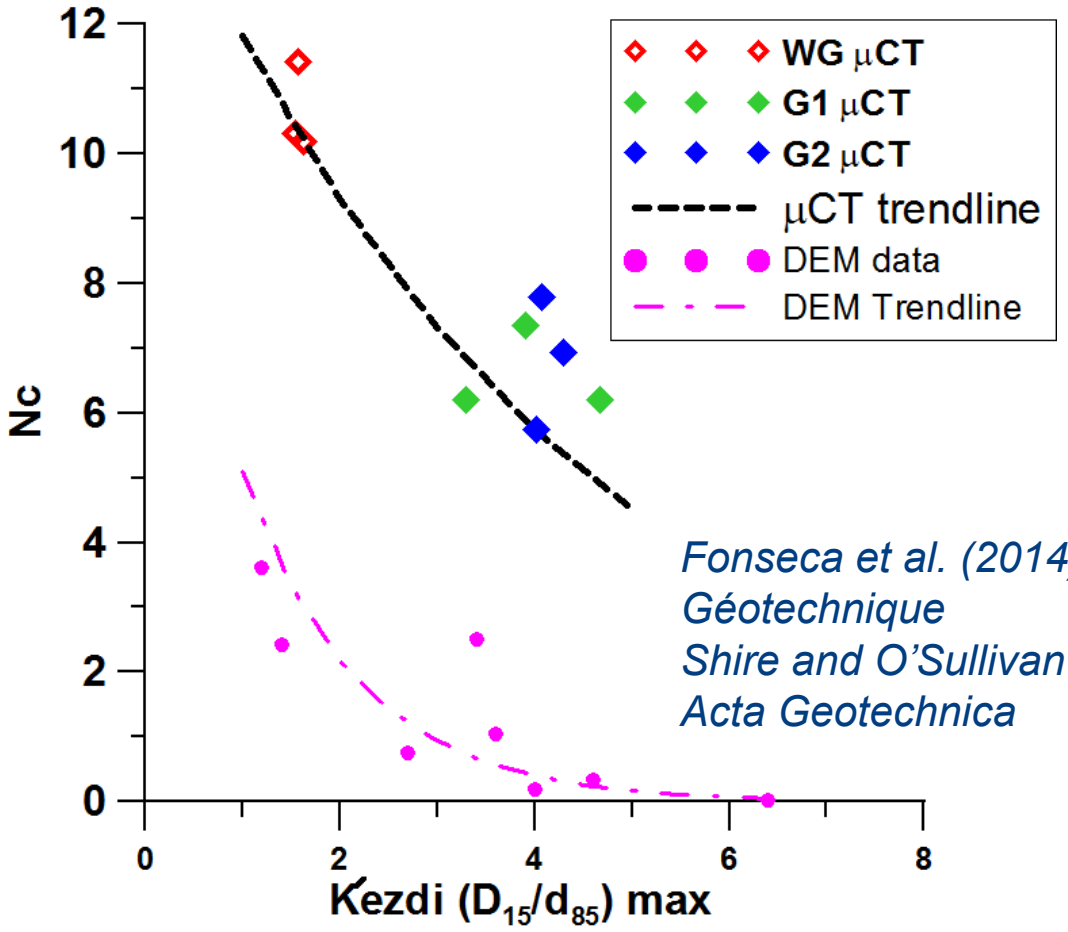

Fonseca et al. (2014)
Géotechnique
Shire and O'Sullivan (2013)
Acta Geotechnica

Images from H. Taylor

Skempton and Brogan Permeameter Experiments

Skempton and Brogan (1994)
Géotechnique

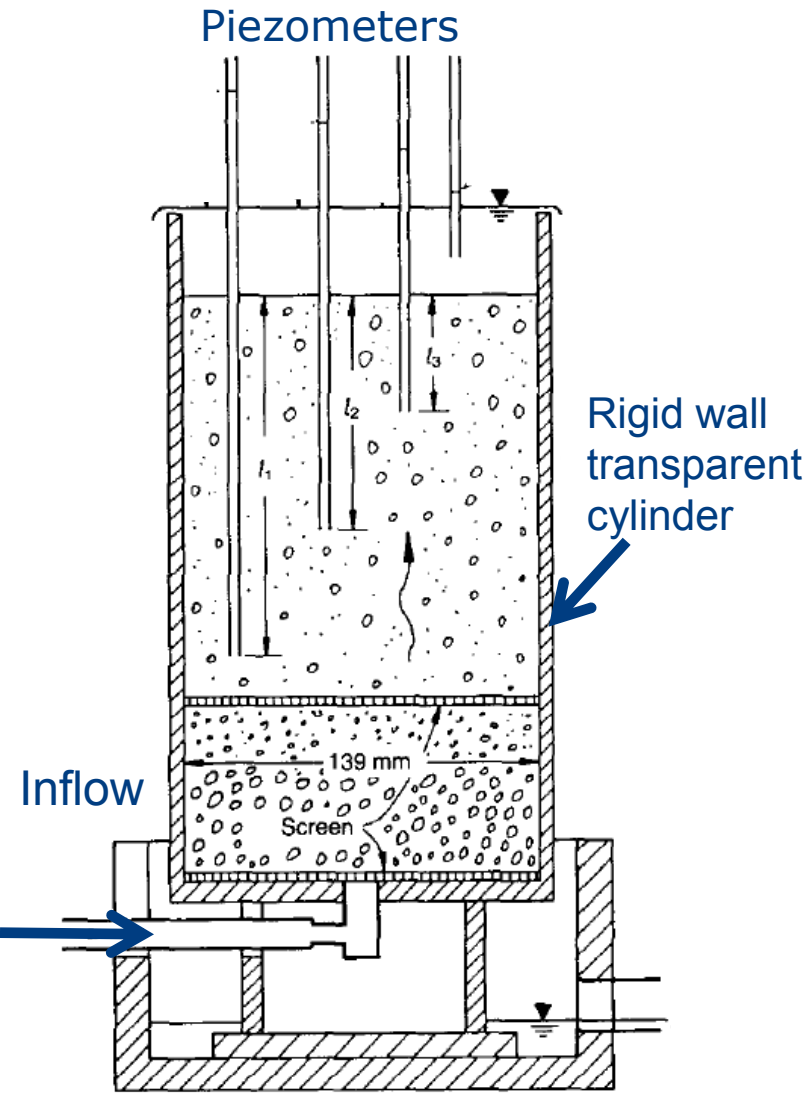

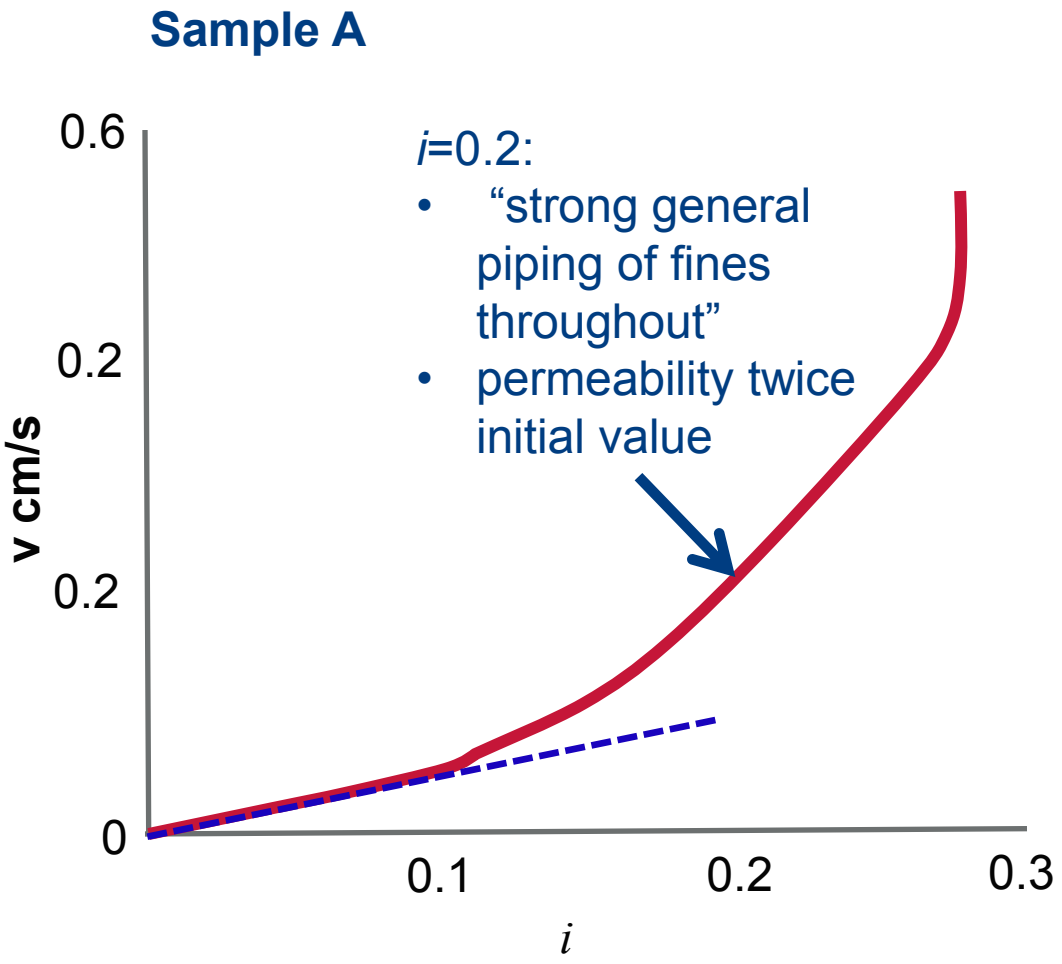

Stress Partition - α

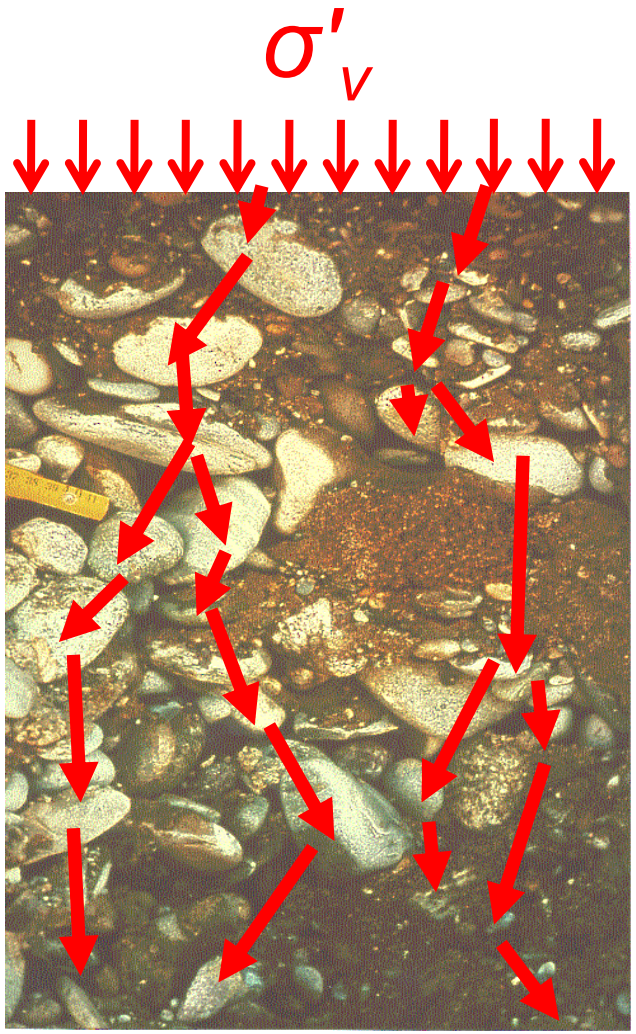

Micromechanical hypothesis to explain i_{crit}<-1:

- Coarse matrix transfers overburden
- Fines carry reduced effective stress:
  - $\alpha = i_{crit} / i_{crit(heave)}$
  - $\sigma'_{fines} = \alpha \times \sigma'$

Skempton and Brogan (1994)
Géotechnique

DEM Simulations to Investigate Instability

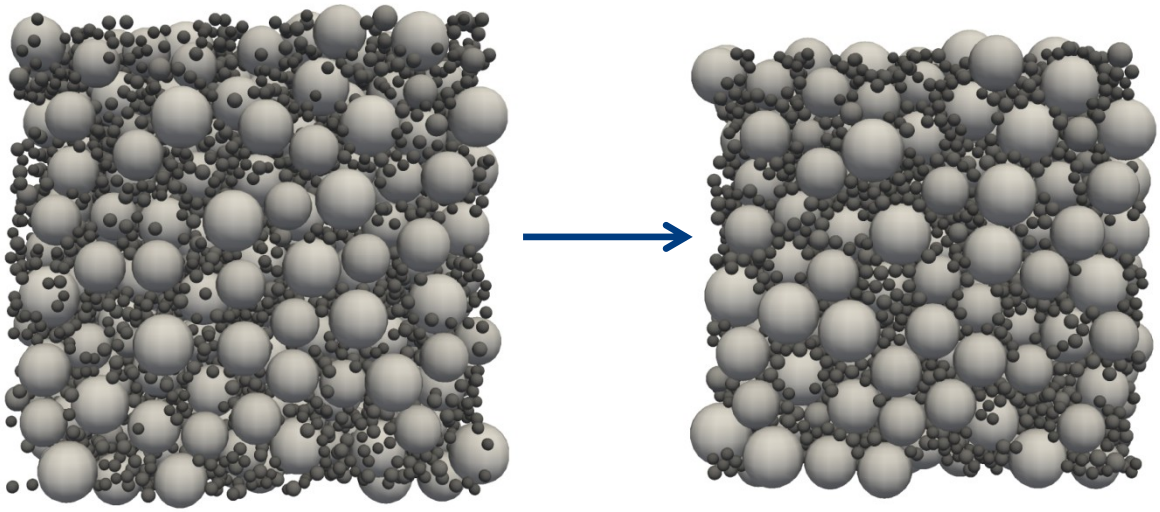

- DEM code granular LAMMPS with periodic boundaries
- Isotropic compression at to p' = 50kPa
- Sample density controlled using interparticle friction (μ):

  μ = 0.0 (Dense)
  μ = 0.1 (Medium dense)
  μ = 0.3 (Loose)

Shire et al. (2014) ASCE JGGE

α – DEM Calculations

$$\alpha = \frac{p'_{fine}}{p'}$$

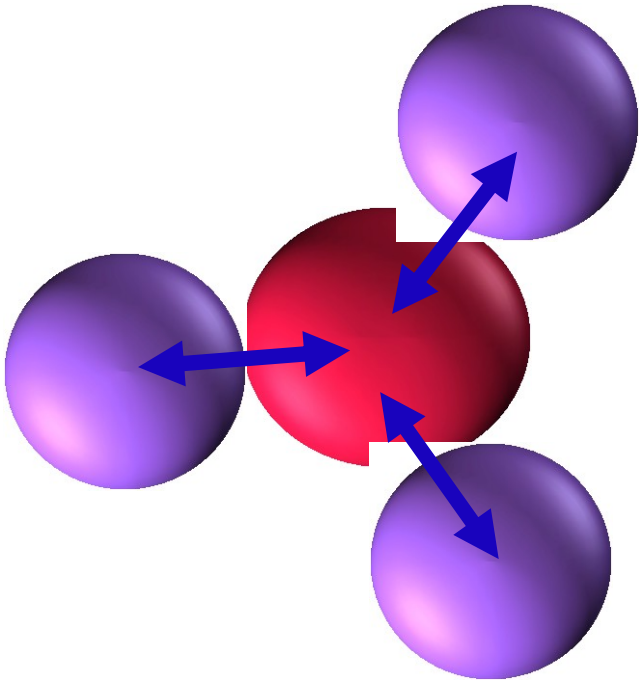

- p'=overall mean effective stress
- p'_{fine}=mean effective stress in finer fraction
- p' and p'_{fine} can be directly obtained from a summation of contact forces in DEM

Skempton and Brogan Sample A: Comparison of α Values

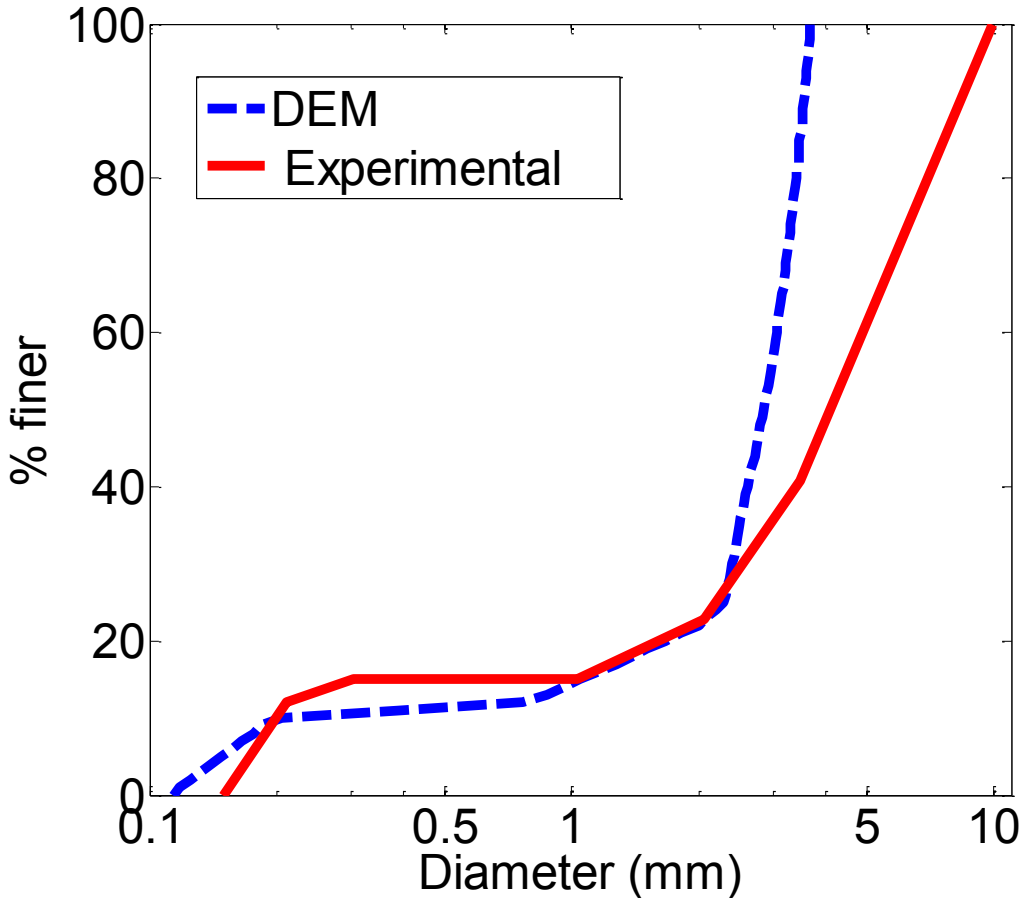

Density	α_{DEM}
Loose	0.15
Medium	0.06
Dense	0.04

$\alpha_{experiment}$=0.18

Experimental sample placed moist with no densification

Shire et al. (2014) ASCE JGGE

Parametric Study on Effect of Gap Width and Fines Content

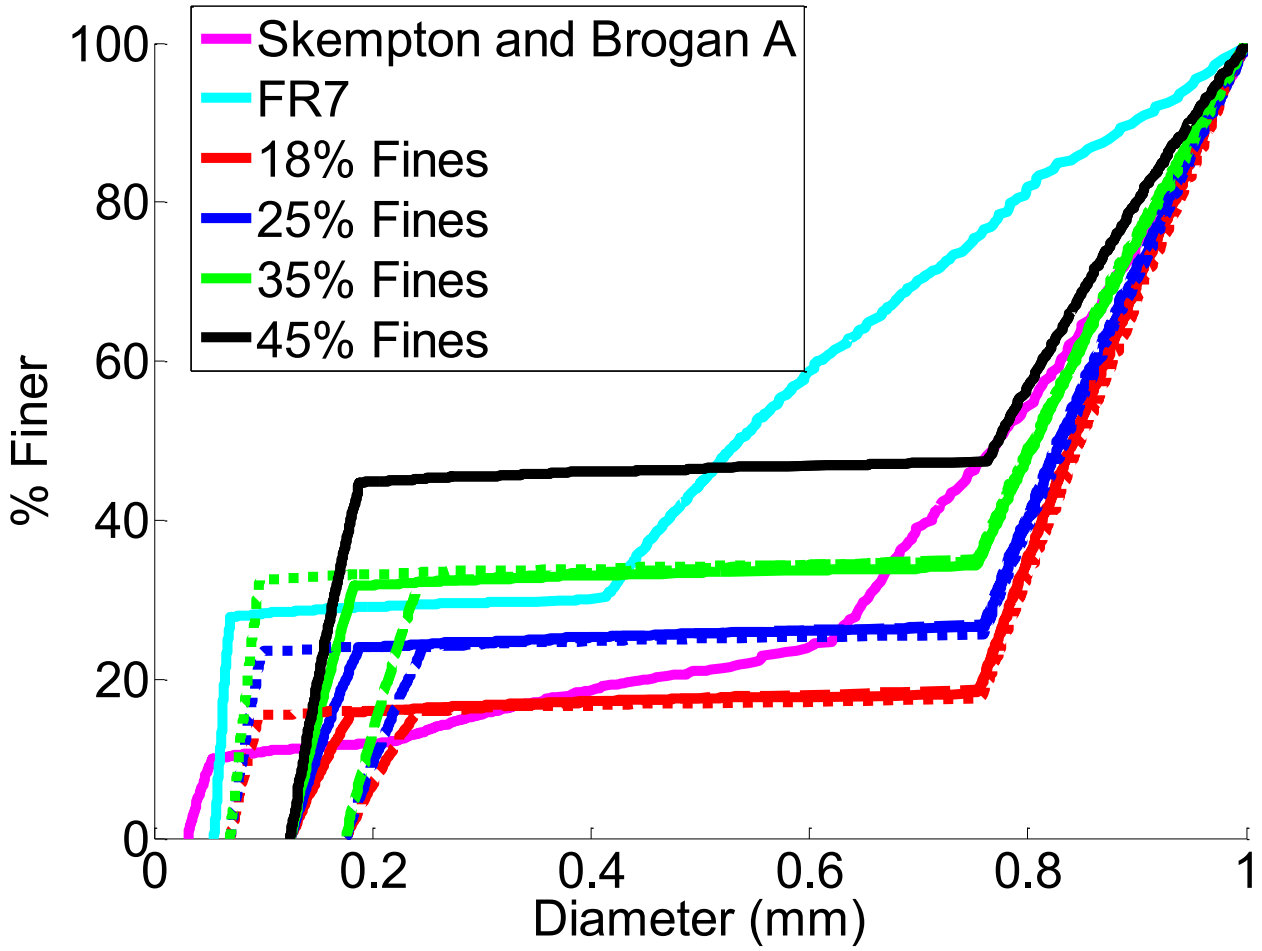

Gap width varied to vary Kézdi ratio (D_{15}/d_{85}) from 3.4 to 11.5

D_{15}/d_{85} =3.4 “stable”

D_{15}/d_{85} =11.5 “unstable”

Density varied for all samples

Up to 304,205 particles

Shire et al. (2014) ASCE JGGE

Variation in α with Fines Content (F_{fine})

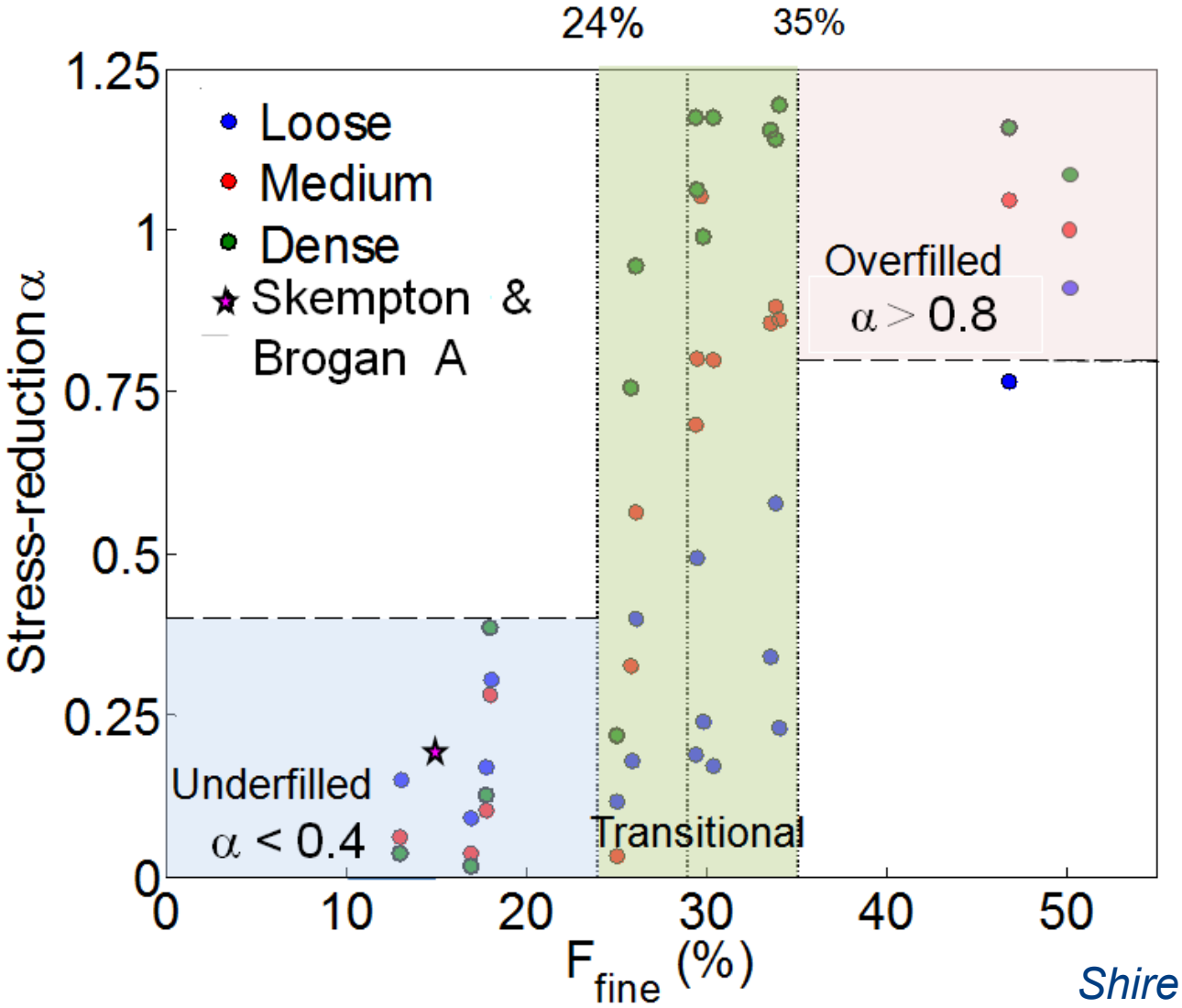

Skempton and Brogan(1994):

Critical fines content where fines just fill voids: F_{fine}=24-29%

Finer fraction separates coarse fraction particles: F_{fine}=35%

Shire et al. (2014) ASCE JGGE

Variation in α with Fines Content (F_{fine})

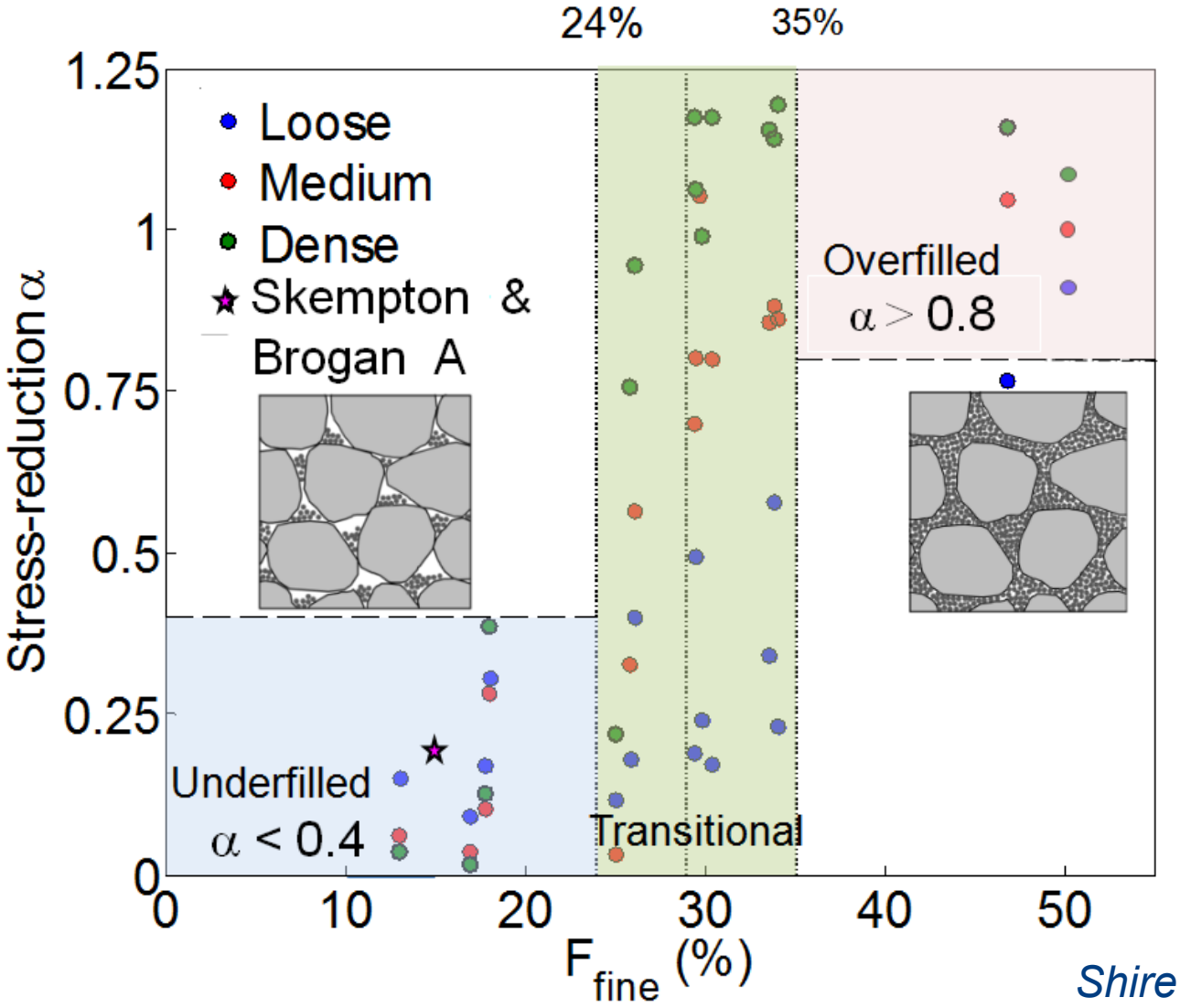

Skempton and Brogan(1994):

Critical fines content where fines just fill voids: F_{fine}=24-29%

Finer fraction separates coarse fraction particles: F_{fine}=35%

Shire et al. (2014) ASCE JGGE

Visualization of Particle Stresses

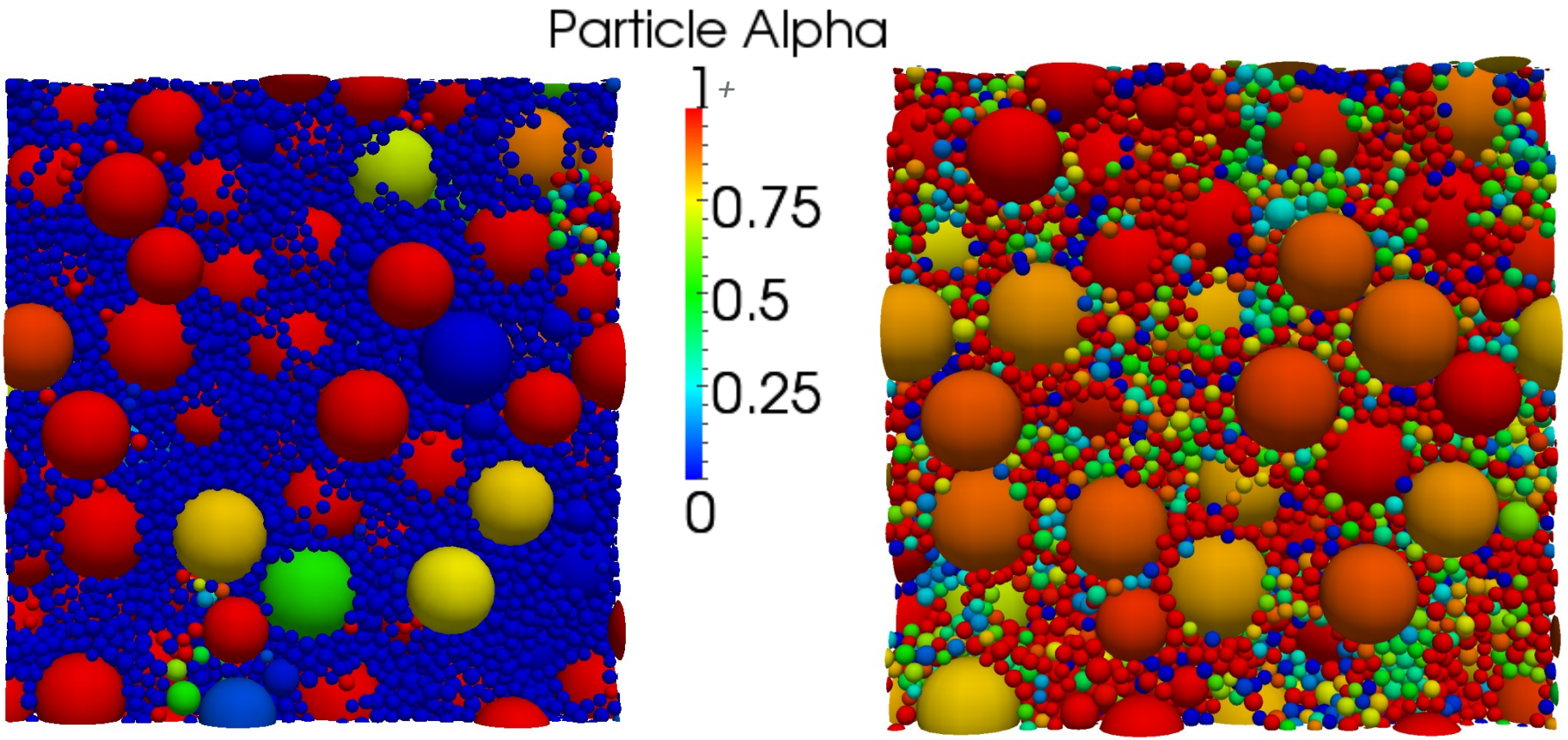

30% Fines - Loose

Relative density increase

30% Fines - Dense

Particle-Scale Analysis of Internal Instability

- Particle scale analyses (microCT and DEM) link between the Kézdi criterion and fabric
- DEM analyses confirm Skempton and Brogan's α hypothesis
- DEM analyses confirm Skempton and Brogan's delineation of underfilled and overfilled fabrics
- DEM analyses highlight the sensitivity of transitional materials to relative density

A Particulate Perspective on Soil Mechanics Can…

- Reveal soil behaviour under stress states that cannot be attained in experiments
- Explain perplexing soil behaviour
- Provide scientific rationale for empirical results used in design

Tools:

Discrete Element Method (DEM)

Micro Computed Tomography

Acknowledgements

Co-authors:
Dr. Daniel Barreto, Edinburgh Napier
Prof. John Burland, Imperial College
Dr. Liang Cui, University of Surrey
Dr. Ignazio Cavarretta, University of Surrey
Prof. Matthew Coop, City University Hong Kong
Dr. Shane Donoghue, Queens, Belfast
Dr. Joana Fonseca, City University
Dr. K. Hanley, University of Edinburgh
Dr. X. Huang, Tongji University
Dr. Erdin Ibraim, University of Bristol
Dr. Fiona Kwok, University of Hong Kong
Prof. Peter Lee, University of Manchester
Dr. Mike Long, University College Dublin
Dr. George Marketos, Utrecht University
Mr. Masahide Otsubo, Imperial College
Dr. Tom Shire, Imperial College
Dr. Way Way Sim, Imperial College
Prof. Ahmer Wadee, Imperial College

Sponsors:
EPSRC
IRCSET (Ireland)
Royal Commission for the Exhibition of 1851
Institution of Civil Engineers R+D Fund

Additional microCT images provided by Howard Taylor, Imperial College

Prof. J. Fannin, University of British Columbia collaborated on internal erosion research

Géotechnique Contributions

Cui, L. and O'Sullivan, C. (2006) "Exploring the macro- and micro-scale response characteristics of an idealized granular material in the direct shear apparatus" *Géotechnique* Vol. 56, 455-468

Cui, L. O'Sullivan, C. and O'Neill, S. (2007) "An analysis of the triaxial apparatus using a mixed boundary three-dimensional discrete element model" *Géotechnique* Vol. 57, No. 10, p 831-844.

Donohue, S., O'Sullivan, C. and Long, M. (2009) "Particle breakage during cyclic triaxial loading of a carbonate sand" *Géotechnique* Vol: 59, Pages: 477 - 482,

Cavarretta, I. , Coop, M. , O'Sullivan, C. (2010) "The Influence of Particle Characteristics on the Behaviour of Coarse Grained Soils" *Géotechnique* 60, pp 413-423

Cavarretta, I. and O'Sullivan, C. (2012) "The mechanics of rigid irregular particles subject to uniaxial compression" *Géotechnique*, 62, pp 681-692

Géotechnique Contributions

Fonseca, J., O'Sullivan, C., Coop, M.R., Lee, P.D. (2012) "Quantifying the Evolution of Soil Fabric during Shearing using Directional Parameters" *Géotechnique, Volume 63, Issue 6, October 2012 pages 487 –499* 10.1680/geot.12.P.003

Shire, T., O'Sullivan, C., Barreto, D., Gaudray, G. (2012) "Quantifying Stress Induced Anisotropy using Inter-Void Constrictions" GEOTECHNIQUE, 2013, Vol:63, Pages:85-91, ISSN:0016-8505(doi)

Bym, T., Marketos, G., Burland, J.B. and O'Sullivan, C. (2013) "Use of a two-dimensional discrete element model to gain insight into tunnelling-induced deformations" *Géotechnique* Vol: 63, Pages: 791-795

Fonseca, J., O'Sullivan, C., Coop, M.R., Lee, P.D. (2013) "Quantifying the Evolution of Soil Fabric during Shearing using Scalar Parameters" *Géotechnique* Vol: 63, Pages: 818-829,

O'Sullivan, C., Wadee, M. A., Hanley, K. J. and Barreto, D. (2013) "Use of DEM and elastic stability analysis to explain the influence of the intermediate principal stress on soil strength" *Géotechnique* Vol: 63, Pages: 1298-1309

Géotechnique Contributions

Fonseca, J., Sim, W. W., Shire, T., and O'Sullivan, C. (2014) "Micro-structural analysis of sands with varying degrees of internal stability" *Geotechnique* Vol: 64, Pages: 405-411

Huang, X., O'Sullivan, C., Hanley, K. J., Kwok, C.Y. (2014) "DEM Analysis of the State Parameter", *Géotechnique* 64(12) 954-965

Otsubo, M., O'Sullivan, C., Sim, W. W., Ibraim, E. (2015) "Quantitative assessment of the influence of surface roughness on soil stiffness" Vol: 65, Pages: 694-700

Additional References

Been, K. & Jefferies, M. G. (1985). A state parameter for sands. *Géotechnique* 35, No. 2, 99–112

Cheng YP,Nakata Y,Bolton MD (2003) Discrete element simulation of crushable soil. *Géotechnique*, 53(7), 633 – 641

Cresswell, A. and W. Powrie (2004). Triaxial tests on an unbonded locked sand. *Géotechnique* 54(2), 107-115.

Cundall, P.A. & Strack, O.D.L. (1979) A discrete numerical model for granular assemblies. *Géotechnique*. 29 (1), 47–65

Dusseault, M. B. and N. R. Morgensten (1979).Locked sands.*Q. J. Engng Geol.* 12, 117-131.

Fonseca J, O'Sullivan C, Coop MR, Lee PD, 2012, Non-invasive characterization of particle morphology of natural sands, *Soils and Foundations*, Vol: 52, Pages: 712-722

Hanley KJ, O'Sullivan C, Byrne EP, Cronin K, 2012, Discrete element modelling of the quasi-static uniaxial compression of individual infant formula agglomerates, *Particuology*, Vol: 10, Pages: 523-531

Hight D.W. (1983), *Laboratory investigation of sea-bed clays*, PhD thesis, Imperial College London.

Additional References

Jefferies, M.G. & Been, K. (2006) *Soil liquefaction: a critical state approach. Taylor and Francis.*

Muir Wood, D. (2007). The magic of sands - The 20th Bjerrum Lecture presented in Oslo, 25 November 2005. *Canadian Geotechnical Journal, 44(11)*

Shire T, O'Sullivan C, 2013, Micromechanical assessment of an internal stability criterion, *Acta Geotechnica*, Vol: 8, Pages: 81-90

Shire, T.; O'Sullivan, C. ; Fannin, R.J.; Hanley, K. (2014) "Fabric and effective stress distribution in internally unstable soils" *ASCE Journal of Geotechnical and Geoenvironmental Engineering*, 140(12)

Skempton AW, Brogan J (1994) Experiments on piping in sandy

gravels. *Géotechnique* 44(3):449–460

Taylor HF, O'Sullivan C, Sim WW, 2015, A new method to identify void constrictions in micro-CT images of sand, *Computers and Geotechnics*, Vol: 69, Pages: 279-290

Thornton, C. (1979) The conditions for failure of a face-centered cubic array of uniform rigid spheres. *Géotechnique*. 29 (4), 441–459.

Additional References

Verdugo, R. (1992) The critical state of sands-discussion *Géotechnique*. 42 (4), 655–663.

Yuan L, O'Sullivan C, Gourlay CM, 2012, Exploring dendrite coherency with the discrete element method, Acta Materiala, Vol: 60, Pages: 1334-1345